INFORMATION TO USERS

This manuscript has been reproduced from the microfilm master. UMI films the text directly from the original or copy submitted. Thus, some thesis and dissertation copies are in typewriter face, while others may be from any type of computer printer.

The quality of this reproduction is dependent upon the quality of the copy submitted. Broken or indistinct print, colored or poor quality illustrations and photographs, print bleedthrough, substandard margins, and improper alignment can adversely affect reproduction.

In the unlikely event that the author did not send UMI a complete manuscript and there are missing pages, these will be noted. Also, if unauthorized copyright material had to be removed, a note will indicate the deletion.

Oversize materials (e.g., maps, drawings, charts) are reproduced by sectioning the original, beginning at the upper left-hand corner and continuing from left to right in equal sections with small overlaps. Each original is also photographed in one exposure and is included in reduced form at the back of the book.

Photographs included in the original manuscript have been reproduced xerographically in this copy. Higher quality 6" x 9" black and white photographic prints are available for any photographs or illustrations appearing in this copy for an additional charge. Contact UMI directly to order.

UMI

A Bell & Howell Information Company
300 North Zeeb Road, Ann Arbor MI 48106-1346 USA
313/761-4700 800/521-0600

THE STABLE HYDROGEN ISOTOPIC COMPOSITION OF METHANE EMITTED FROM BIOMASS BURNING AND REMOVED BY OXIC SOILS: APPLICATION TO THE ATMOSPHERIC METHANE BUDGET

by

Amy Katherine Snover

A dissertation submitted in partial
fulfillment of the requirements for the
degree of

Doctor of Philosophy

University of Washington

1998

Approved by _____
Co-chairperson of Supervisory Committee

_____
Co-chairperson of Supervisory Committee

Program Authorized
to Offer Degree Department of Chemistry

Date December 16, 1998

Doctoral Dissertation

In presenting this dissertation in partial fulfillment of the requirements for the Doctoral degree at the University of Washington, I agree that the Library shall make its copies freely available for inspection. I further agree that extensive copying of this dissertation is allowable only for scholarly purposes, consistent with "fair use" as prescribed in the U.S. Copyright Law. Requests for copying or reproduction of this dissertation may be referred to University Microfilms, 1490 Eisenhower Place, P.O. Box 975, Ann Arbor, MI 48106, to whom the author has granted "the right to reproduce and sell (a) copies of the manuscript in microform and/or (b) printed copies of the manuscript made from microform."

Signature 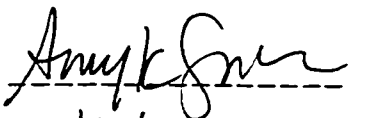

Date 12/16/98

University of Washington

Abstract

THE STABLE HYDROGEN ISOTOPIC COMPOSITION OF METHANE EMITTED FROM BIOMASS BURNING AND REMOVED BY OXIC SOILS: APPLICATION TO THE ATMOSPHERIC METHANE BUDGET

by Amy Katherine Snover

Co-chairperson of the Supervisory Committee:
Professor Paul D. Quay
School of Oceanography

Co-chairperson of the Supervisory Committee:
Professor Richard H. Gammon
Department of Chemistry
School of Oceanography

The stable hydrogen isotopic composition (δD) of CH_4 was developed for use as a constraint for the atmospheric CH_4 budget by characterizing the δD of CH_4 emitted from biomass burning and removed by oxic soils and the δD of atmospheric CH_4 in tropospheric background air. These measurements were combined with literature values for the strength and δD of the other CH_4 sources and sinks to develop regional, hemispheric and global CH_4 - δD budgets.

The hydrogen kinetic isotope effect (KIE) during soil uptake of atmospheric methane was $\alpha^{D}_{soil} = k(CH_4)/k(CH_3D) = 1.099 \pm 0.030$ and 1.067 ± 0.007 for a native grassland and a temperate forest, respectively. This is

significantly less than the KIEs associated with the other CH_4 sinks. The interhemispheric asymmetry in the soil sink strength suggests a ~5‰ difference between the overall KIEs during atmospheric CH_4 loss in the two hemispheres.

The δD of methane emitted from biomass burning ($\delta D_{CH4(bb)}$) measured in large-scale laboratory combustion experiments and the Brazilian Amazon was -233±2‰ and -210±16‰, respectively. These measurements suggest that $\delta D_{CH4(bb)}$ may have a relatively narrow δD range globally. Measurements of the fuel biomass δD content indicated a significant hydrogen KIE, of -130‰ to -180‰, during combustion.

The mean δD of atmospheric CH_4 at Cheeka Peak, Washington (48°N) was -92.6±0.5‰ with a seasonal cycle of amplitude 8.6±2.9‰ between 1991 and 1996. The seasonal cycle was controlled by the balance between CH_4 emissions from bogs and removal by OH. The mean δD's for the northern and southern hemispheres were -93.0±1.9‰ and -83.3±1.5‰, respectively, determined from air samples collected at ~150°W between 55°N and 65°S during 1989 to 1995. The southward δD increase resulted from the higher strength and δD of CH_4 loss compared to the CH_4 source in the southern hemisphere. The δD of the global CH_4 source derived from the atmospheric measurements and the total KIE during CH_4 loss was -280±37‰, in good agreement with -279±6‰ estimated from the strength and δD of the individual CH_4 sources. This indicates that current understanding of the CH_4 - δD budget, including the determinations of $\delta D_{CH4(bb)}$ and α^D_{soil} presented here, is robust.

TABLE OF CONTENTS

LIST OF FIGURES

LIST OF TABLES

ACKNOWLEDGMENTS

I am indepted to many people whose generosity made this work possible. Kent Keller (WSU) provided the field site and logistical support for the grassland study of soil uptake and a wonderful welcome to Pullman. Chris Pfeiffer facilitated my work in the Washington Park Arboretum. Shiway Wang was the most cheerful field assistant in the history of the universe, despite our long days and various mishaps together. Sherry Wilhelm taught me how to use the GC. Wei Min Hao (USFS) welcomed me into his lab for my combustion experiments and made it possible for me to join his research group in Brazil. Pat Boyd assisted with the laboratory combustion experiments. Steve Baker cheerfully analyzed the trace gas contents of the smoke samples. Ron Babbitt and Bento Barros made the Brazilian field work a success, with their experience and ability to keep cool, despite the heat. Tad Anderson and David Covert provided expert advice and cannister shuttling services to help keep the Cheeka Peak time series measurements going. Many thanks to David Wilbur, the Stable Isotope Lab's mass-spec guru extraordinaire. My advisor, Paul Quay, provided thoughtful and constructive criticism on all drafts of my dissertation. My advisor, Richard Gammon, has inspired and encouraged the application of my research to climate change issues. Most importantly, *thanks* to Rolf Sonnerup and Steve Gerst for everything, lo these many years. I couldn't have done it without you.

I have been blessed with an extensive support group and cheering section off campus. The confidence of my parents has carried me far. My spirits have never failed to be buoyed by the cheers, and cheer, of my brother. And many, many thanks to Chip.

The research was performed under appointment to the U.S. Department of Energy, Graduate Fellowships for Global Change Program, administered by Oak Ridge Institute for Science and Education.

CHAPTER 1: INTRODUCTION

Methane (CH_4) is a radiatively and chemically important trace gas constituent of the atmosphere. After carbon dioxide, CH_4 is the second most important anthropogenically emitted greenhouse gas. It has contributed ~20% of the total increase in radiative forcing that has resulted from changes in the atmospheric concentrations of anthropogenic greenhouse gases since pre-industrial times (Schimel *et al.*, 1996). Methane is a major regulator of tropospheric hydroxyl radicals (OH), the oxidant responsible for removing almost all reactive trace gases from the troposphere (Crutzen, 1995). Methane is a major source of tropospheric CO and a source of O_3 in polluted (high NO_x) areas (Wayne, 1993). It is also an important source of water vapor to the stratosphere (Jones *et al.*, 1986) which, in turn, can enhance both HO_x-catalyzed and heterogeneous chemical loss of stratospheric O_3. Methane reaction with stratospheric chlorine radicals, however, provides a termination step for chlorine-catalyzed stratospheric O_3 loss (Wayne, 1993; Crutzen, 1995; Prather *et al.*, 1995).

The concentration of atmospheric CH_4 has changed significantly over time. Measurements of air bubbles enclosed in polar ice cores have shown that atmospheric CH_4 levels doubled from ~350 parts per billion by volume (ppb) during glacial times to ~650 ppb during interglacial periods (Raynaud *et al.*, 1988; Khalil and Rasmussen, 1989a; Chappellaz *et al.*, 1990). Atmospheric CH_4 levels have more than doubled again since pre-industrial times to a current atmospheric mixing ratio of ~1715 ppb (Blunier *et al.*, 1993;

Dlugokencky *et al.*, 1998). This increase has not occurred at a constant rate. Initially, the increase in atmospheric CH_4 was linked to the growth in world population. Most (50-70%) of the CH_4 increase since pre-industrial times resulted from increases in the human-controlled CH_4 sources of ruminants and rice agriculture (Khalil and Rasmussen, 1985, 1993b; Blunier *et al.*, 1993). During the late 1970s and early 1980s, CH_4 was increasing at ~1% yr^{-1} (Blake and Rowland, 1988) but the rate of increase was no longer tied to population growth (Khalil and Rasmussen, 1993a). In 1992, the CH_4 growth rate dramatically slowed to almost zero (Dlugokencky *et al.*, 1994a). Methane increases have again been observed since 1992, although with a lower growth rate of ~ 6 ppb yr^{-1}, perhaps indicating stabilization of CH_4 emissions (Dlugokencky *et al.*, 1998).

The atmospheric CH_4 budget is best constrained by knowledge of its lifetime with respect to removal by CH_4 sinks. The primary CH_4 sink is oxidation by OH. Global atmospheric OH levels are determined indirectly, via atmospheric photochemical models that calculate OH production based on variations in sunlight, NO_x, CO, CH_4 and non-methane hydrocarbons (Spivakovsky *et al.*, 1990a,b; Krol *et al.*, 1998). These OH fields are tested using observations of atmospheric mixing ratios of methyl chloroform (CH_3CCl_3), a trace gas of exclusively industrial origin with well-known atmospheric release rates (Prinn *et al.*, 1995) whose dominant atmospheric sink is reaction with OH. The temperature-dependent rate constant for CH_4 removal by OH has been determined in laboratory studies, most recently as $k = 1.59 \cdot 10^{-20} \cdot T^{2.84} \cdot e^{(-978/T)}$ cm^3 $mole^{-1}$ s^{-1} by Vaghjiani and Ravishankara (1991).

Combined with current estimates of atmospheric OH levels, this yields an lifetime for atmospheric CH_4 with respect to removal by OH of 8.0 ± 0.5 years (Prinn *et al.*, 1995).

The lifetime of atmospheric CH_4 also depends on the rates of its removal by the secondary CH_4 sinks: uptake by oxic soils and chemical loss in the stratosphere. The global amount of CH_4 oxidation by soils has been estimated at 29 (9-56) Tg yr^{-1} from observations of a relationship between soil texture and CH_4 consumption rates (Dörr *et al.*, 1993). The amount of CH_4 removed by photolysis and oxidation by OH, Cl and $O(^1D)$ in the stratosphere has been estimated at 40 (32-38) Tg yr^{-1} (Schimel *et al.*, 1996).

The lifetime of atmospheric CH_4 with respect to OH oxidation, soil uptake and stratospheric loss has been estimated at 8.6 ± 1.6 years (Schimel *et al.*, 1996). Combined with the current atmospheric CH_4 burden of ~4850 Tg (1 Tg = 10^{12} g) (Schimel *et al.*, 1996), and the observed atmospheric increase of ~13 ppb yr^{-1} during the 1980s (Dlugokencky *et al.*, 1998), this implies an annual CH_4 source of ~600 Tg. The estimated uncertainty in the CH_4 lifetime reflects mainly the uncertainty in the tropospheric turnover time of CH_3CCl_3 (± 12%) and in the rate constants for reaction of CH_3CCl_3 and CH_4 with OH (Schimel *et al.*, 1996). However, a rigorous derivation of this uncertainty is lacking.

The natural sources of atmospheric CH_4 are wetlands, termites, and oceans. Human-controlled, *i.e.*, anthropogenic, sources of CH_4 are ruminants, rice paddies, natural gas leakage and venting, coal mining, biomass burning, landfills, and domestic sewage (Schimel *et al.*, 1996). Methane production in wetlands, the largest single source of CH_4 and the only significant natural

source, occurs via acetate fermentation and CO_2 reduction by anaerobic methanogenic bacteria (Whiticar *et al.*, 1986; Schoell, 1988). Bacterial production of CH_4 also occurs in rice paddies, landfills and ruminants, with the latter predominantly cows and sheep. Approximately 20% of CH_4 associated with natural gas reservoirs is of bacterial origin (Rice and Claypool, 1981). Non-bacterial CH_4 is produced by thermal degradation of buried organic matter, *i.e.*, CH_4 associated with coal mining and ~80% of natural gas CH_4, and via incomplete combustion such as during biomass burning.

Recent budget compilations (*e.g.*, Prather *et al.*, 1995) indicate that approximately two-thirds of the global CH_4 source results from bacterial production in wetlands, rice paddies, ruminants and landfills (Table 1.1). Methane emissions associated with fossil fuels constitute ~20% of the total source and biomass burning contributes ~10%. Estimating the contribution of individual CH_4 sources to the global CH_4 budget generally relies on extrapolation of local flux measurements, which vary significantly both spatially and temporally, to the global scale, resulting in large, *i.e.*, $\pm$ 20 - 75%, uncertainties in the individual source terms (Table 1.1) (Prather *et al.*, 1995). The global CH_4 source strength, estimated to be ~535 Tg yr^{-1}, is therefore quite uncertain, with a range of estimates of 410 to 660 Tg yr^{-1} (Table 1.1).

Thus, the total CH_4 source strength estimated from the strengths of the individual CH_4 sources (410 - 610 Tg) is in agreement with the total CH_4 source strength derived from the CH_4 sinks and observed atmospheric increase (~600 Tg). The uncertainties in the strengths of the individual CH_4 sources and sinks are large enough, however, that it is difficult to attribute the recently

Table 1.1 Sources and sinks of atmospheric methane.

Source[a]	Strength (range) ($Tg\ CH_4\ yr^{-1}$)	
Wetlands	115	(55-150)
Ruminants	85	(65-100)
Rice Paddies	60	(20-100)
Fossil Fuel		
Natural Gas	40	(25-50)
Coal Mines	30	(15-45)
Petroleum Industry	15	(5-30)
Biomass Burning	40	(20-80)
Landfills	40	(20-70)
Animal Waste	25	(20-30)
Domestic Sewage	25	(15-80)
Termites	20	(10-50)
Oceans	10	(5-50)
Total Identified Sources	535	(410-660)

Sink[b]	Strength (range) ($Tg\ CH_4\ yr^{-1}$)	
Oxidation by OH	490	(405-575)
Stratospheric Loss	40	(32-48)
Soil Uptake	30	(15-45)
Atmospheric Increase	37	(35-40)
Total Sinks + Atmospheric Increase	597	(495-700)

[a] Prather *et al.* (1995)
[b] Schimel *et al.* (1996)

observed changes in atmospheric CH_4 levels to changes in specific CH_4 sources or sinks (Bekki *et al.*, 1994; Dlugokencky *et al.*, 1994a; Hogan and Harriss, 1994; Schauffler and Daniel, 1994).

The constraint of mass balance for the atmospheric CH_4 budget can be expressed as follows:

$$\frac{dC}{dt} = \sum_{i=1}^{j} S_i - \sum_{i=1}^{k} M_i \qquad (1)$$

where C represents atmospheric CH_4 concentration and S and M represent the strength of each of the j sources and k sinks, respectively. With a constraint of mass balance alone, however, the atmospheric CH_4 budget is underdetermined.

The isotopic composition of atmospheric CH_4 provides additional information about the CH_4 budget. The global isotopic mass balance can be expressed as follows:

$$C \cdot \frac{d(\delta_{atm})}{dt} + \delta_{atm} \cdot \frac{dC}{dt} = \sum_{i=1}^{j} S_i \delta_{src(i)} - \sum_{i=1}^{k} M_i \delta_{sink(i)} \qquad (2)$$

where C, S and M are as defined above. δ is the isotopic composition of CH_4, expressed in parts per thousand,[Ψ] where the subscripts *atm*, *src* and *sink* refer

---

[Ψ] Isotopic compositions are expressed in parts per thousand using customary δ notation: $\delta(‰) = \left(\frac{R_{sample}}{R_{standard}} - 1 \right) \cdot 1000$, where R = $^{13}C/^{12}C$, or D/H. For $\delta^{13}C$, the reference standard is a marine carbonate, Pee Dee Belemnite (PDB). For δD, the reference standard is "standard mean ocean water" (SMOW). In δ notation, negative numbers denote samples depleted in the heavy isotope, *i.e.*, samples containing less of the heavier isotope than the standard.

to the isotopic composition of atmospheric CH_4 and its sources and sinks, respectively. Three isotopic species of CH_4 have been applied to studies of atmospheric CH_4, *i.e.*, $^{13}CH_4$, $^{14}CH_4$, and CH_3D. Each isotopic tracer (if it is independent) adds a constraint to the global CH_4 budget.

Each CH_4 sink involves a characteristic kinetic isotope effect (KIE), preferentially removing CH_4 depleted in the heavy isotope with respect to atmospheric CH_4. The KIE associated with loss of atmospheric CH_4 results from the different loss rates for CH_4 and $^{13}CH_4$ and is represented by

$$\alpha = {}^{k}\!/_{*k} \tag{3}$$

where k/*k = the ratio of the rate constants for loss of isotopically light (CH_4) and heavy ($^{13}CH_4$, $^{14}CH_4$, or CH_3D) methane. The KIE can be expressed in parts per thousand, *i.e.*,

$$\varepsilon(‰) = \left({}^{1}\!/_{\alpha} - 1\right) \cdot 1000 \tag{4}$$

to indicate the approximate isotopic content of the CH_4 removed (δ_{sink}) since

$$\delta_{sink}(‰) \approx \delta_{atm} + \varepsilon. \tag{5}$$

This is an approximation of the exact expression for the isotopic composition of the CH_4 removed, *i.e.*,

$$\delta_{sink}(‰) = \left[\alpha \cdot \left(\frac{\delta_{atm}}{1000} + 1\right) - 1\right] \cdot 1000. \tag{6}$$

Thus, the isotopic composition of atmospheric CH_4 reflects the flux-weighted sum of the individual CH_4 sources, after correction for the isotope effects associated with CH_4 loss (and any time rates of change observed for the

concentration and isotopic composition of atmospheric CH_4) (equation (2)). The isotopic composition of atmospheric CH_4 can therefore be used to constrain the CH_4 source budget. Use of isotopic information to constrain the atmospheric CH_4 budget requires knowledge of the isotopic signatures of the individual CH_4 sources and sinks, as well as the isotopic composition of atmospheric CH_4 in clean, *i.e.*, "background" air.

The $^{13}C/^{12}C$ content of CH_4 is the best developed stable isotopic tracer of atmospheric CH_4 (*e.g.*, Stevens and Engelkemeir, 1988; Stevens, 1988; Wahlen *et al.*, 1989; Quay *et al.*, 1988, 1991, in press; Tyler, 1992; Lowe *et al.*, 1991, 1994; Lassey *et al.*, 1993; Thom *et al.*, 1993; Gupta *et al.*, 1996). Systematic measurements of the $\delta^{13}C$ of atmospheric CH_4 were begun in 1978 by Stevens and Rust (1982; Stevens, 1995). Subsequent time series measurements have been made at ~ 8 sites worldwide (Quay *et al.*, 1991, in press; Lassey *et al.*, 1993; Lowe *et al.*, 1994; Gupta *et al.*, 1996). The mean $\delta^{13}C$ of atmospheric CH_4 is currently ~-47.3‰ (Quay *et al.*, in press).

Many measurements have been made of the $^{13}C/^{12}C$ of the CH_4 sources (*e.g.*, review in Quay *et al.*, 1991). Methane sources are generally categorized by $^{13}C/^{12}C$ content, with bacterial sources most depleted in ^{13}C, at ~-60‰, and biomass burning emissions most enriched, at ~-24‰. Fossil sources emit CH_4 with intermediate $^{13}C/^{12}C$, at ~-40‰. The $\delta^{13}C$ of atmospheric CH_4 is sensitive to the biomass burning source of CH_4, due to the significant ^{13}C enrichment in CH_4 emitted from this source (*e.g.*, Lassey *et al.*, 1993; Quay *et al.*, 1991).

The carbon isotope effects during CH_4 loss to each of the sinks have also been determined. Reaction with OH removes CH_4 with a $\delta^{13}C$ that is ~-5.4‰

lower than ambient (Cantrell *et al.*, 1990) and stratospheric loss removes CH_4 depleted by ~12.4‰ (Brennikmeijer *et al.*, 1995; Sugawara *et al.*, 1997). In contrast, the $\delta^{13}C$ of CH_4 removed by soil uptake is ~23‰ depleted versus ambient (King *et al.*, 1989; Tyler *et al.*, 1994a; Reeburgh *et al.*, 1997). The average KIE occurring during CH_4 loss is the average of the individual KIEs weighted by the sink strengths, *i.e.*, ~-6.8‰. The $\delta^{13}C$ of CH_4 removed from the atmosphere is equal to the $\delta^{13}C$ of CH_4 inputs at steady state (equation (2)). As a result of the isotopic fractionations occurring during CH_4 loss, therefore, atmospheric CH_4 would be ~6.8‰ more enriched in ^{13}C than the total CH_4 source at steady state. Given the non-steady state situation for CH_4 concentration (Dlugokencky *et al.*, 1988) and $\delta^{13}C$ (Quay *et al.*, in press), this balance is only approximately held.

Knowledge of the $\delta^{13}C$ content of CH_4 sources and sinks have been combined with measurements of the $\delta^{13}C$ of atmospheric CH_4 to examine regional, hemispheric and global budgets of atmospheric CH_4. Seasonal variations in the $^{13}C/^{12}C$ of atmospheric CH_4 have been used to elucidate the relative importance of CH_4 source and sink processes at the regional level, providing information additional to that inherent in observations of atmospheric CH_4 concentrations alone (Quay *et al.*, in press; Lassey *et al.*, 1993). The latitudinal gradient in $^{13}C/^{12}C$ has been used to constrain the isotopic composition of the bulk southern hemisphere CH_4 source and the proportion of that source contributed by biomass burning (Quay *et al.*, in press). Lowe *et al.* (1994) attributed part of the observed 1992 decrease in the atmospheric CH_4 growth rate to a reduction in the southern hemisphere

biomass burning source, as a result of their observations of increasingly ^{13}C-depleted southern hemisphere atmospheric CH_4 during this time. Thom *et al.* (1993) used measurements of the $\delta^{13}C$ content of atmospheric CH_4 in Heidelberg to show that the CH_4 budget for the Heidelberg region was typical of central Europe. Measurements of $\delta^{13}C$ on CH_4 in air bubbles trapped in polar ice cores have shown that the $\delta^{13}C$ of atmospheric CH_4 was ~2‰ lighter 350 years ago and that much of the modern ^{13}C enrichment in atmospheric CH_4 resulted from an increase in human-controlled biomass burning (Craig *et al.*, 1988).

The ^{14}C composition of CH_4 sources reflects the age of the carbon contained in the CH_4 emitted from each source (Wahlen *et al.*, 1989) and is therefore sensitive to fossil fuel-associated CH_4, *i.e.*, the only CH_4 source containing no ^{14}C. The ^{14}C content of atmospheric CH_4 is also sensitive, however, to the significant production of $^{14}CH_4$ by pressurized light-water nuclear reactors (25-30% of the total $^{14}CH_4$ burden) (Wahlen *et al.*, 1989; Quay *et al.*, 1991). ^{14}C has been used to constrain the relative strength of the fossil source of atmospheric CH_4 to 18 ± 9% (Quay *et al.*, in press). Many recent CH_4 budget compilations have relied on ^{14}C-based constraints of the fossil source (*e.g.*, Fung *et al.*, 1991; Prather *et al.*, 1995; Crutzen, 1995).

The D/H content of CH_4 is a potentially useful tracer of the atmospheric CH_4 budget (Ehhalt, 1973; Wahlen *et al.*, 1990; Wahlen, 1993; Thom *et al.*, 1993; Bergamaschi *et al.*, 1998a; Quay *et al.*, in press) but is less well developed than $^{13}C/^{12}C$. There are fewer determinations of the D/H composition of atmospheric CH_4 in background air, of the D/H composition of the CH_4

sources, and of the hydrogen KIEs associated with the CH_4 sinks. There have been only a few published measurements of the D/H content of atmospheric CH_4 in clean air and none since the late 1980s. Ehhalt (1973) reported δD of -86 and -94‰ for two air samples. Wahlen *et al.* (1990) reported average δD's for the northern and southern hemispheres of -87 ± 5‰ and -77 ± 2‰, respectively, during 1986 to 1987. There are no published time series observations of the D/H of atmospheric CH_4.

CH_4 sources are generally categorized by D/H content, as by $^{13}C/^{12}C$ content, with bacterially-produced CH_4 significantly more depleted, at δD ≈ -310‰, than fossil fuel-associated CH_4, with δD = -215 to -150‰ (Table 1.2). Methane emitted from landfills has an intermediate D/H content, *i.e.*, δD ≈ -290‰. The D/H content of CH_4 emitted from biomass burning has been estimated to be -10 to -50‰ (Wahlen, 1993) and -90‰ (Whiticar, 1993), but has not been carefully quantified. The lack of measurements of the δD of CH_4 emitted from biomass burning prevents an estimation of the δD content of the global CH_4 source.

The hydrogen isotope fractionation occurring during CH_4 reaction with OH at 298K has been determined experimentally to be -140‰ (DeMore, 1993) and -200‰ (Gierczak *et al.*, 1997) and calculated theoretically as -250‰ (Xiao *et al.*, 1993) (Table 1.3). The KIE during loss in the stratosphere was measured at -160‰ (Irion *et al.*, 1996). No published values exist of the hydrogen isotope fractionation associated with soil uptake of atmospheric CH_4. The lack of measurements of the hydrogen KIE associated with soil uptake prevents an estimation of the δD content of the global CH_4 sink. Without measurements

Table 1.2 The δD content of atmospheric CH_4 sources.

Source	δD ± 1σ (‰ vs. SMOW)	n	Reference
Wetlands			
Amazon floodplain (3° S)	-339 ± 11	13	Wassman et al. (1992)
Amazon floodplain (3° S)	-294 ± 18	3	Lansdown (1992)
African lakes (5° N)	-269 ± 6	8	Kling et al. (1991)
Florida Everglades (26°N)	-293 ± 14	50	Burke et al. (1988)
Florida lakes (28° N)	-306 ± 16	127	Burke et al. (1992)
SE USA lakes (32° N)	-300 ± 24	50	Burke and Sackett (1986)
West Virginia peat bogs (39° N)	-300 ± --[a]	--[a]	Wahlen et al. (1989)*
New York wetlands (43° N)	-322 ± --[a]	--[a]	Wahlen et al. (1989)*
Minnesota peat bogs (47°N)	-339 ± 10	7	Lansdown (1992)
Washington peat bog (48° N)	-308 ± 11	10	Lansdown (1992)
German swamp (50° N)	-310 ± 9	7	Levin et al. (1993)
Ontario fen, bog (50° N)	-353 ± --[a]	--[a]	Wahlen et al. (1989)*
German lakes (53° N)	-322 ± 10	53	Woltemate et al. (1984)
Manitoba tundra (59° N)	-357 ± --[a]	--[a]	Wahlen et al. (1989,1991)*
Yukon Delta (61° N)	-342 ± 18	21	Martens et al. (1992)
Alaskan tundra (68° N)	-391 ± 8	7	Lansdown (1992)
Rice Paddies			
Italy	-332 ± 9	7	Levin et al. (1993)
Louisiana	-302 ± 13	8	Wahlen et al. (1989, 1990)*
China	-336 ± 10	19	Bergamaschi (1997)
Ruminants			
Cows (unspecified diet)	-308 ± 30	6	Wahlen et al. (1989, 1990)*
Cows (C3 diet)	-301 ± 10	13	Levin et al. (1993)
Cows (60-80% C4 diet)	-295 ± 10	4	Levin et al. (1993)
Cows (C3 diet; barn air)	-390 ± 10	1	Lansdown (1992)
Landfills[b]			
Massachusetts	-282 ± 21	9	Liptay et al. (1998)
Massachusetts	-278 ± 7	1	Liptay et al. (1998)
Massachusetts	-271 ± 26	10	Liptay et al. (1998)
Massachusetts	-301 ± 21	2	Liptay et al. (1998)
New Hampshire	-259 ± 53	11	Liptay et al. (1998)
New Hampshire	-298 ± 6	4	Liptay et al. (1998)
Germany/Holland (covered landfills)	-269 ± 42	30	Bergamaschi et al. (1998)
Germany/Holland (uncovered waste)	-328 ± 6	13	Bergamaschi et al. (1998)
Germany (gas collection system)	-302 ± 12	24	Bergamaschi et al. (1998)
Germany (gas collection system)	-299 ± 10	4	Bergamaschi et al. (1998)
Germany (gas collection system)	-310 ± 5	5	Bergamaschi et al. (1998)
Holland (gas collection system)	-308 ± 6	13	Bergamaschi et al. (1998)
Germany (gas collection system)	-302 ± 12	23	Bergamaschi and Harris (1995)
Germany (anoxic landfill air)	-312 ± 8	8	Levin et al. (1993)
Fossil fuel-associated			
Natural gas (Heidelberg, Germany)	-185 ± 29	7	Levin et al. (1993)
Natural gas	-188 ± 17	--[a]	Ehhalt (1973)
Biogenic natural gas	-214 ± 23	35	Schoell (1980)
Thermogenic natural gas	-197 ± 36	38	Schoell (1980)
Coal-associated gas	-146 ± 8	8	Schoell (1980)

a. Not reported.
b. Each mean δD listed is for a separate landfill.
* personal communication (in Lansdown, 1992).

Table 1.3 The hydrogen kinetic isotope effects associated with removal of atmospheric methane.

Removal pathway	α [a] ($k(CH_4)/k(CH_3D)$)	ε (‰)[a] ($1/\alpha - 1)\cdot 1000$	**Reference**
Tropospheric OH[b]	1.16 ± 0.03	-138 ± 22	DeMore (1993)
	1.32 to 1.35	-242 to -259	Xiao *et al.* (1993)
	1.25 ± 0.07	-200 ± 45	Gierczak *et al.* (1997)
Stratospheric loss	1.19 ± 0.02	-160 ± 14	Irion *et al.* (1996)

[a] Uncertainties are $\pm 1\sigma$.

[b] All values correspond to 298K.

of the δD of CH_4 released from biomass burning and removed by soils, therefore, δD cannot be used as a tracer for the global atmospheric CH_4 budget.

The goal of the research presented in this dissertation was to develop δD as a tracer for atmospheric CH_4. This was accomplished by first filling the remaining knowledge gaps, *i.e.*, determining the δD signature of CH_4 removed by soils and emitted by biomass burning, as well as the δD content of atmospheric CH_4 and its spatial and temporal variability. These measurements were then applied to analyses of regional, hemispheric and global CH_4 - δD budgets in order to evaluate current understanding of controls on the δD content of atmospheric CH_4. Finally, the potential for δD as a tracer for atmospheric CH_4 was evaluated.

The dissertation is organized as follows. In Chapter Two, the first field measurements of the hydrogen kinetic isotope effect (KIE) occurring during soil uptake of atmospheric CH_4 are presented. Concurrent determinations of the carbon KIE facilitate comparison of findings to earlier studies. The relative contributions of microbial oxidation and molecular diffusion to the observed KIEs are determined. In Chapter Three, the first detailed measurements of the δD of CH_4 emitted from biomass burning are presented, determined from both laboratory combustion studies and tropical biomass fires in the Brazilian Amazon. The apparent hydrogen KIE occurring during combustion of biomass is quantified. In Chapter Four, the latitudinal trend in the δD content of atmospheric CH_4 and the seasonal variation in δD at a temperate northern hemisphere clean air monitoring site are presented in order to quantify the δD content of atmospheric CH_4 and its spatial and

temporal variations. These data, combined with the signatures of the biomass burning source and soil sink presented in Chapters Two and Three, are used to evaluate current understanding of controls on the δD content of atmospheric CH_4. Controls on the latitudinal trend in δD and the seasonal cycle of δD at 48°N are determined. Conclusions and suggested directions for future research are summarized in Chapter Five.

CHAPTER 2: HYDROGEN AND CARBON KINETIC ISOTOPE EFFECTS DURING SOIL UPTAKE OF ATMOSPHERIC METHANE

INTRODUCTION

Oxidation of atmospheric methane (CH_4) has been observed to occur in most types of oxic soils, *e.g.*, tundra (Whalen and Reeburgh, 1990), boreal, temperate and deciduous forests (Whalen *et al.*, 1991; Castro *et al.*, 1995; Crill, 1991), grasslands (Torn and Harte, 1996; Mosier *et al.*, 1996; Heipieper and deBont, 1997), agricultural lands (Mosier *et al.*, 1991; Keller *et al.*, 1990), tropical soils (Seiler *et al.*, 1984; Mosier and Delgado, 1997), and some deserts (Striegl *et al.*, 1992; Dörr *et al.*, 1993). Soil oxidation of CH_4 is mediated by a diverse group of unidentified aerobic methanotrophic bacteria (Davidson and Schimel, 1995; Conrad 1996). Microbial oxidation of CH_4 occurs over a soil texture-dependent moisture range; extremely dry conditions inhibit microbial activity while increased soil moisture can limit diffusional supply of CH_4 (Torn and Harte, 1996; Mosier *et al.*, 1996; Striegl, 1993; Davidson and Schimel, 1995; Reeburgh *et al.*, 1993). During some times of year, temperature imparts a secondary control on CH_4 consumption rates (Crill, 1991; Castro *et al.*, 1995). Addition of nitrogen fertilizer has been found to significantly inhibit CH_4 oxidation for decades or longer in some soils (Mosier *et al.*, 1996; Steudler *et al.*, 1989; Willison *et al.*, 1995). Dörr *et al.* (1993) used observations of a relationship between soil texture class and CH_4 consumption rates to estimate the global amount of atmospheric CH_4 oxidized by soils to be 29 (9-56) Tg yr^{-1}.

This amount corresponds to ~5% of the total annual sink for atmospheric CH_4. Oxidation of atmospheric CH_4 by hydroxyl radicals (OH) comprises about 87% of the total sink (490 Tg yr^{-1}) and the remaining 7% is removed in the stratosphere (Houghton *et al.*, 1996).

Uptake of atmospheric CH_4 by soils is accompanied by a kinetic isotope effect (KIE) which represents the different rates of uptake of $^{12}CH_4$ and either CH_3D or $^{13}CH_4$. The KIE is represented by $\alpha_{soil} = k/\hat{k}$, where $k/\hat{k}$ is the ratio of the rate constants for uptake of isotopically light (CH_4) and heavy (CH_3D or $^{13}CH_4$) methane. Previous determinations of the carbon KIE have been made in Alaskan tundra, where $\alpha^C_{soil} = 1.016$ and 1.027 (King *et al.*, 1989), a mixed deciduous hardwood forested soil, where $\alpha^C_{soil} = 1.023 \pm 0.004$ (Tyler *et al.*, 1994), and in boreal forest soils, where $\alpha^C_{soil} = 1.023$ and 1.026 (Reeburgh *et al.*, 1997). Both King *et al.* (1989) and Tyler *et al.* (1994) utilized *in situ* static flux chambers to sample air depleted in CH_4 concentration and enriched in ^{13}C by CH_4-consuming soils. Reeburgh *et al.* (1997) measured *in situ* steady state profiles of soil air CH_4 concentration and $^{13}C/^{12}C$ to determine α^C_{soil}.

The KIE occurring during soil uptake of atmospheric CH_4 depends on the isotopic fractionations associated with two processes: diffusion of CH_4 into the soil (α_{diff}) and microbial oxidation of CH_4 (α_{ox}). The latter was determined *in situ* by Reeburgh *et al.* (1997), using soil air CH_4 concentration and $\delta^{13}C$ profiles, at $\alpha^C_{ox} = 1.022$-1.025, and by Coleman *et al.* (1981) in laboratory cultures of methanotrophic bacteria at $\alpha^C_{ox} = 1.013$-1.025. For both the hydrogen and carbon isotopes of CH_4, $\alpha_{diff} = 1.0195$, *i.e.*, the square root of the ratio of the reduced masses of $^{13}CH_4$ or CH_3D and CH_4 in air. However, an

understanding of the relative importance of α_{ox} and α_{diff} in determining the overall KIE (α^{C}_{soil}) has not been applied to previous studies of uptake of atmospheric CH_4 by soils.

The relatively large carbon isotopic fractionation effect associated with soil uptake of CH_4 enhances the importance of this sink in the global isotopic budget of atmospheric CH_4. To make this comparison, it is useful to express the KIE associated with the CH_4 sinks as a deviation from unity in parts per thousand (‰), *i.e.*, $\varepsilon = (1/\alpha - 1)\cdot 1000$, since $\delta_{sink} \approx \delta_{atm} + \varepsilon$. During soil uptake of CH_4, based on the estimates of α^{C}_{soil} discussed above, the $\delta^{13}C$ of the CH_4 removed is ~23‰ lower than that of ambient CH_4. In contrast, reaction with OH removes CH_4 with a $\delta^{13}C$ that is ~5.4‰ lower than ambient (Cantrell *et al.*, 1990) and stratospheric loss processes remove CH_4 depleted by ~12.4‰ (Brennikmeijer *et al.*, 1995; Sugawara *et al.*, 1997). Inclusion of the KIE associated with soil uptake in a stable isotopic budget of atmospheric CH_4 therefore increases the overall fractionation due to CH_4 sinks to -6.8‰ from -5.6‰. A recent recalculation of the KIE associated with oxidation by OH indicates that this fractionation may be as large as 10‰ (Gupta *et al.*, 1997). In either case, the greater KIE for CH_4 loss resulting from soil uptake implies, at steady state, a correspondingly lower $\delta^{13}C$ of the global CH_4 source.

The importance of soil oxidation as a sink for atmospheric CH_4 may change in the future. For example, changes in precipitation patterns could shift soils from being net sources (flooded anoxic soils) to net sinks (aerated and oxic). A shift of this type could potentially impact the mass distribution and isotopic composition of atmospheric CH_4. Thus there is a need to

quantify the isotopic effects of soil uptake in order to help interpret interannual trends in the isotopic compositions and concentrations of this trace gas.

The D/H content of atmospheric CH_4 is a potentially useful isotopic tracer of the global CH_4 budget but is less well developed than $^{13}C/^{12}C$ (Wahlen *et al.*, 1990; Quay *et al.*, in press; Snover *et al.*, in preparation). The hydrogen fractionation occurring during CH_4 reaction with OH has been determined experimentally at $\alpha^D_{OH} = 1.25 \pm 0.07$ (Gierczak *et al.*, 1997) and $\alpha^D_{OH} = 1.16 \pm 0.03$ (DeMore, 1993) and calculated theoretically at $\alpha^D_{OH} = 1.32\text{-}1.35$ (Xiao *et al.*, 1993); all values correspond to 298 K. During stratospheric loss, $\alpha^D_{STRAT} = 1.19 \pm 0.02$ (Irion *et al.*, 1996). No published values exist of the hydrogen isotope fractionation associated with soil uptake. The lack of measurements of α^D_{soil} limits the use of δD as tracer for atmospheric CH_4.

This work presents the results of the first field measurements of α^D_{soil}. Concurrent determinations of α^C_{soil} facilitate comparison of these findings to earlier studies. The relative contributions of α_{ox} and α_{diff} to α_{soil} are determined. The apparent α_{ox} observed at these study sites is reported.

METHODS

FIELD SITES

Chamber flux studies of CH_4 uptake by soils were performed at two contrasting sites in Washington State: a native grassland and a forested arboretum. The grassland site, located approximately 1.5 km east of the city of

Pullman, Washington (46.8° N, 117.2° W), is managed by Washington State University (WSU). Quaternary loess (silt loam) is deposited in dunelike hills which are more than 10 meters thick at the site. The soil is a Mollisol and the vegetation is native grasses (Wood *et al.*, 1993). The site has been undisturbed for ~20 years and shows no evidence of current contamination by fertilizer-nitrogen from nearby cultivated fields (Severson *et al.*, 1992). Subsurface CO_2 production rates at this site have been determined by Wood *et al.* (1993); total organic carbon content and nutrient concentrations were measured by Severson *et al.* (1992). Precipitation in the Pullman area averages 544 mm yr^{-1} with 75% falling between October and April; the mean annual temperature is 8.3°C (Western Regional Climate Center, 1998). Flux chamber experiments were performed at the WSU site during September, 1998 when temperatures averaged 17.4°C and precipitation was negligible (National Climatic Data Center, 1998). Experiments were performed at two different locations, separated by ~5 m, to determine the within-ecosystem variability of α_{soil}.

The forested field site was located at the Washington Park Arboretum (47.7° N, 122.3° W) in the city of Seattle, Washington. The specific site used for chamber flux studies at the Arboretum (ARB) was located in well-drained Indianola series soil, under 70-80 year-old second growth coniferous forest vegetation. The general soil profile has a thin layer of forest duff above slightly acid to neutral moderately coarse textured mineral soils (loam and loamy fine sand) that formed in glacial outwash sand (Emery, 1977; Gessel, 1966). The mean annual temperature of this area is 11.6°C. Precipitation averages 908 mm yr^{-1}, with 81% falling between October and April. (Western

Regional Climate Center, 1998). Flux chamber experiments were performed at ARB in August 1998, when the average temperature was 21.3°C and precipitation was negligible (National Climatic Data Center, 1998).

Sample Collections

Rigid static flux chambers have been widely used to measure rates of emission and uptake of trace gases by soils, as well as for determinations of the KIEs associated with these processes (*e.g.*, review by Mosier, 1989; King *et al.*, 1989; Tyler *et al.*, 1994). During collection of large volume samples from a rigid chamber, the pressure within the chamber is generally maintained by admission of ambient air in order to minimize the withdrawal of air from soil pore spaces during sampling. In order to avoid significant dilution of the large volume air samples required for analysis of δD - CH_4, (~200 L), a collapsible chamber was developed for use in this study.

A stainless steel collar (150 cm x 150 cm x 25 cm) was inserted into the ground to a depth of 8-10 cm several days before a chamber flux experiment and left in place for all replicate experiments at a single study location. The collar was equipped with 1/4" septum fittings for syringe sample collection and 1/2" fittings (Swagelok Co., Solon, OH) for large volume sample collection. The chamber enclosure was made by sealing a 5-sided bag of flexible laminate material (Scotchpak #20, Pollution Prevention Inc., Chicago, IL) to the collar with electrical tape. The total volume of air enclosed was ~1400 L. The laminate material was shown to have no effect on enclosed air CH_4 concentration for enclosure times up to 4 weeks. The chamber enclosure

was supported by an external PVC frame and protected from buffeting by wind gusts by a large wind block. Two internally-mounted battery-operated fans (flow rate ~550 L min^{-1}) were run continuously to ensure that the air in the chamber headspace was well-mixed.

Near the beginning of each chamber flux experiment, a sample of ambient air was collected for isotopic analysis. Large volume air samples for isotopic analysis were collected through 1/2" OD tubing (Dekoron type 1300, Furon, Laguna Niguel, CA) and a glass drying tube containing silica gel. Samples were compressed into 30 L high pressure Spectra Seal aluminum cylinders (Airco, City of Industry, CA) to ~ 400 psig using a gas-powered scuba compressor (Rix model, with charcoal scrubber removed, Bauer Compressors, Inc., Norfolk, VA). Neither sample drying nor compression have been found to alter the δD of sample CH_4, *i.e.*, the measured δD of dried and compressed air samples was within 4‰ of samples collected simultaneously using an aluminum/neoprene diaphragm pump and no drying agent (n=3).

During a chamber flux experiment, the concentration of CH_4 in the chamber was monitored by analyzing air samples collected from the chamber headspace using 10 ml gas-tight syringes (Alltech Associates Inc., Deerfield, IL) with a gas chromatograph (GC) on site (WSU) or nearby (ARB). Samples were found to be stable in syringes for at least 3.5 hours and were analyzed within 1-2 hours of collection. After the CH_4 concentration dropped to 25-55% of the initial level in the chamber, a large volume sample was collected from the chamber headspace for isotopic analysis. The flexible chamber enclosure was detached from its supporting frame and allowed to gently collapse during

sample collection. Collection of the final sample took ~10 minutes, during which time 275-350 L were removed from the ~1400 L chamber enclosure. The experiment duration ranged from 1 to 16 hours depending on the CH_4 oxidation rate at the site. At the WSU site, replicate flux chamber experiments were performed at two locations. Four flux experiments were performed using the same collar installation in a single location at the ARB site.

Soil probes were installed at both sites for measurement of the profile of CH_4 concentration in soil air. The probes were made from 3/8" OD stainless steel tubing surrounding a removable driving rod that protruded ~4 cm below the bottom of the tubing. The probes were equipped with Swagelok fittings with rubber septa, providing an air-tight seal and enabling syringe sampling. Soil gas samples were collected for CH_4 concentration analysis in air-tight 10 ml glass syringes after removal of 3x the probe volume with a large syringe. An array of 5-6 probes were installed at different depths (5-85 cm) inside the collar footprint at both WSU sampling locations. This set-up allowed the determination of both the steady state CH_4 concentration profile before a flux experiment and the perturbed CH_4 concentration soil profile at the end of an experiment. At the Arboretum site, probes were installed adjacent to the chamber to determine only the steady state CH_4 concentration profile.

An inert tracer, CCl_2F_2 (CFC-12) was added to the chamber to quantify the volume of air enclosed within the chamber headspace, enabling determinations of CH_4 uptake rates. The initial concentration of CCl_2F_2 in the

chamber was calculated from the average of 3 syringe samples collected within a few minutes after tracer injection, *i.e.*, before significant diffusion into the soil could occur.

Air and soil temperatures were measured during each experiment (Table 2.1). Soil samples were collected for moisture content and bulk density analysis by coring at the soil surface at WSU. Soil moisture content was determined by weight difference after drying to a constant mass at 105°C. Soil bulk density was determined from the dry mass of a known field volume of soil. At WSU, the soil moisture content (g H_2O/g soil) was 13.5% and bulk density was 1.3 g/cm^3. At ARB, the soil bulk density was 1 g/cm^3 (M. Atkinson, personal communication).

Gas Concentration Measurements

Measurements of CH_4 and CCl_2F_2 concentrations in syringe and cylinder samples were performed using a gas chromatograph equipped with a flame ionization detector (FID) (GC Mini-2, Shimadzu Scientific Instruments, Columbia, MD) and a Porapak Q column (100/120 mesh; 1/8"x6', Alltech) at 80°C. The flow rate of carrier gas helium was 40 ml/min. Precision ($\pm 1\sigma$) of gas concentration analysis was 0.5% for CH_4 and 2.2% for CCl_2F_2, based on 50 and 35 sets of replicate analyses, respectively. Binary standards known to an accuracy of ± 2% were prepared by dilution of calibrated volumes of 100% CH_4 and 100% CCl_2F_2 with hydrocarbon-free ultrapure air (Scott Marrin Inc., Riverside, CA). The standards had CH_4 and CCl_2F_2 concentrations ranging from 0.74 to 2.10 parts per million (ppm) and from 11.1 to 51.0 ppm,

respectively. For CH_4, a four-point standard calibration curve had $r^2 \geq 0.9991$, verifying the linearity of the FID response to CH_4 and of the standard synthesis procedure. The FID response was non-linear for CCl_2F_2, requiring a second-order polynomial fit for the standard curve. The drift in the GC response to CH_4 that occurred during long (10-16 hour) chamber deployments was $\leq 3.5\%$ and corrected for by repeated standard analysis.

Stable Isotope Measurements

The sample preparation procedure for $^{13}C/^{12}C$ and D/H analysis of CH_4 in air used a high vacuum extraction system with cryogenic collection of CO_2 and H_2O from combusted CH_4, following the standard method described by Stevens and Rust (1982). The concentration procedures necessary for D/H determinations were described by Wahlen *et al.*, (1989) and Alei *et al.*, (1987). The air sample was pulled through a 'Russian doll' trap at -196°C on a vacuum extraction line to remove CO_2, H_2O, N_2O and some nonmethane hydrocarbons (Brenninkmeijer, 1991), and then through 100 g charcoal (SK-4 Carbon, 40/60 mesh, Alltech Associates, Inc., Deerfield, IL) at -196°C to concentrate the CH_4. Pressure was maintained at 1/3 atmosphere or less to minimize condensation of O_2. The charcoal trap was warmed to -80°C using a dry ice/isopropanol slush while pumping to remove trapped gases such as N_2 and O_2, while retaining the CH_4. The charcoal trap was then transferred to a second high vacuum extraction line where it was heated to 100°C and purged with hydrocarbon-free ultrapure air (Scott Marrin) to liberate the CH_4. The emitted gas flowed through a series of three traps at -196°C to freeze out any

CO_2 and H_2O in the carrier gas and through a bed of Schütze reagent (LECO Chemical, St. Joseph, MI), quantitatively oxidizing CO to CO_2 (Smiley, 1949) which, along with the resultant H_2O, was trapped at -196°C. The CH_4 in the gas stream was then oxidized to CO_2 and H_2O, by flowing over platinized quartz wool (high sensitivity total carbon catalyst, Shimadzu Scientific Instruments, Inc., Columbia, MD) at ~730°C, and the resultant gases trapped at -196°C. The resultant CO_2 was cryogenically distilled from the H_2O at -80°C using a dry-ice/isopropanol slush transfer, and measured manometrically before mass spectrometer analysis. The H_2O was transferred at 100°C to a Pyrex ampoule containing 40 ± 1 mg zinc reagent turnings previously activated at 350°C for 5 minutes under vacuum (Biogeochemical Laboratories, Indiana University). The ampoule containing the water sample was then flame-sealed and heated at 500°C for 30 minutes to reduce H_2O to H_2 for mass spectrometric analysis. The H_2 was manometrically measured at the inlet to the mass spectrometer.

Measurements of $^{13}C/^{12}C$ and D/H were made on a Finnigan MAT 251 isotope-ratio mass spectrometer and the results reported in customary δ notation: δ (‰) = $(R_{sample}/R_{standard} - 1)\cdot 1000$, where R = $^{13}C/^{12}C$ or D/H. Gas standards for $\delta^{13}C$ are calibrated against NBS-19 with $\delta^{13}C$ = +1.95‰ vs. V-PDB. δD measurements are scale-corrected such that H_2 derived from H_2O standards V-SMOW and SLAP yield δD values of 0‰ and -428‰, respectively. All $\delta^{13}C$ and δD measurements reported here are referenced to V-PDB and V-SMOW, respectively.

The δD analysis of CH_4 requires about 100 liters of air containing CH_4 at ambient concentrations, yielding ~400 µl H_2O and ~200 µl CO_2. Extraction yields were 102 ± 2% for H_2O and 102 ± 1% for CO_2 (n=20). Typical extraction blanks were ~14 µl H_2O and ~0.07 µl CO_2 (n=15). The precision of this method was ± 2.7‰ for δD (n=19) and ± 0.16‰ for $\delta^{13}C$ (n=20) from replicates of 3 laboratory standards analyzed during this study. The accuracy of the method has been tested by comparing the δD and $\delta^{13}C$ of pure CH_4 combusted in sealed tubes to standard dilutions of this CH_4 extracted using the procedure described above. The sealed tube method yielded -137.8 ± 4.0‰ δD (n=4) and -31.74 ± 0.13‰ $\delta^{13}C$ (n=10) and the air sample extraction method yielded δD = -135.0 ± 2.7‰ (n=19) and $\delta^{13}C$ = -31.88 ± 0.16‰ (n=20); uncertainties are ± 1σ.

RESULTS AND DISCUSSION

Nine static flux chamber experiments were performed at a total of three locations (WSU-site 1, WSU-site 2 and ARB) in two ecosystems. During the course of a static flux chamber experiment, the CH_4 concentration in the chamber headspace typically decreased by ~45% (Figure 2.1). Methane concentration and isotopic composition were determined from the large volume cylinder samples for initial (background air) and final (chamber headspace) conditions for each flux experiment (Table 2.1). At WSU-site 1, when CH_4 concentration decreased by ~41%, the δD and $\delta^{13}C$ of CH_4 in the chamber headspace increased by ~38‰ and ~7.5‰, respectively. At WSU-site 2, when CH_4 concentration decreased by ~44%, δD and $\delta^{13}C$ increased by ~61‰ and ~9.5‰, respectively. At ARB, when CH_4 concentration decreased by

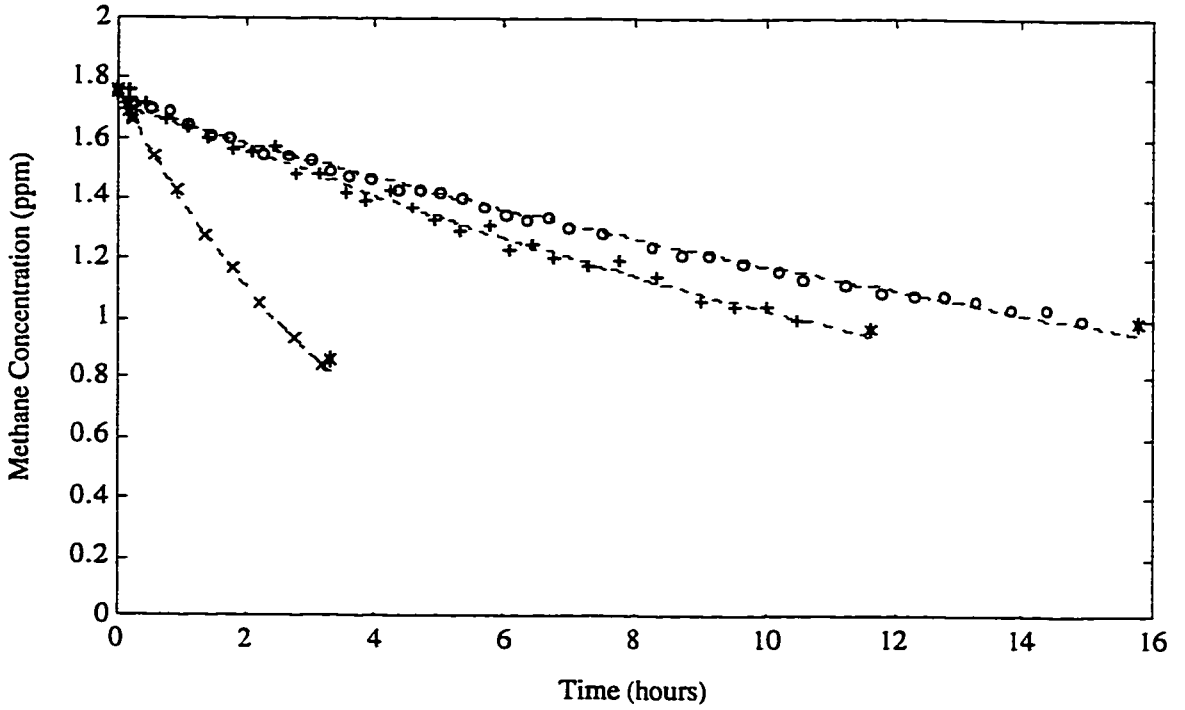

Figure 2.1 Time rate of change of methane concentration observed in the headspace of the static flux chamber for a representative experiment at each study site.
CH_4 concentration is shown for syringe samples (WSU-site 1, expt. #2 (o); WSU-site 2, expt. #4 (+); ARB, expt. #3 (x)) and final large volume cylinder samples (*). Measurement uncertainty is ± 0.5% (*i.e.*, smaller than symbol size). The lines shown are an exponential fit to the syringe sample data for each experiment.

Table 2.1 Changes in methane concentration and stable isotopic composition measured in static flux chambers in a native grassland (WSU) and a forested arboretum (ARB) in Washington State.

Study site	Expt. #	Expt. duration (hours)	Tair (°C)	Tsoil[a] (°C)	Tsoil[b] (°C)	$[CH_4]_i$[c] (ppm)	$[CH_4]_f$[c] (ppm)	$\frac{[CH_4]_f}{[CH_4]_i}$	δD_i[c] (‰)	δD_f[c] (‰)	$\delta^{13}C_i$[c] (‰)	$\delta^{13}C_f$[c] (‰)	Enclosure dilution (%)[d]	CH_4 uptake rate[e] ($\mu g\ m^{-2}\ hr^{-1}$)
WSU-site 1	1	13.6	15.6	14.7	14.6	1.739	1.054	0.61	-90.5	-53.3	-47.34	-40.33	5.8	--[f]
"	2	15.8	19.5	15.4	14.6	1.758	0.992	0.56	-90.3	-50.7	-47.37	-39.29	5.3	43
"	3	7.1	18.2	15.7	15.4	1.733	1.306	0.75	-88.9	-66.7	-47.14	-42.26	0	33
WSU-site 2	4	11.6	24.0	19.1	17.1	1.750	0.965	0.55	-85.1	-21.6	-47.23	-37.63	0	39
"	5	11.8	20.8	17.4	15.3	1.729	0.977	0.57	-88.2	-30.3	-47.61	-38.21	0	37
ARB	1	3.1	21.7	16.8	--[f]	1.732	0.779	0.45	-89.7	-42.2	-47.23	-34.18	3.9	145
"	2	2.6	25.3	17.5	17.9	1.745	0.884	0.51	-92.6	-48.0	-47.47	-36.18	0	--[f]
"	3	3.3	18.7	17.2	16.4	1.754	0.864	0.49	-94.0	-50.9	-47.50	-35.95	4.8	182
"	4	1.1	20.0	--[f]	15.9	1.828	1.413	0.77	-93.5	-80.5	-47.61	-43.18	0	--[f]

a. Measured at 0.1 m depth.

b. Measured at 0.2 m depth.

c. Initial and final concentration, δD and $\delta^{13}C$ of CH_4 were determined in the laboratory from large volume cylinder samples.

d. Enclosure dilution is reported as percent ambient air in final sample as determined by comparison of measured $[CH_4]_f$ with $[CH_4]$ predicted for the time of sample collection by the time rate of change measured by the syringe samples throughout the chamber experiment. An enclosure dilution of 0% is reported when the measured $[CH_4]_f$ is within $\pm 2\sigma$ of the predicted $[CH_4]$.

e. CH_4 uptake rates were determined from linear fit to ambient and syringe samples during first 2 hours (WSU) or first hour (ARB) of chamber flux experiment.

f. Not measured.

~52%, δD and $\delta^{13}C$ increased by ~45‰ and ~12‰, respectively. At WSU-site 1 and ARB, shorter chamber flux experiments were also performed. For a CH_4 concentration decrease of ~24% at each site, δD and $\delta^{13}C$ increased by ~22‰ and ~5‰, respectively, at WSU-site 1 and ~13‰ and ~4‰, respectively, at ARB. For five of the nine chamber experiments, the CH_4 concentration measured in the large volume cylinder sample collected from the headspace at the end of the chamber experiment was within $\pm 2\sigma$ of the CH_4 concentration predicted for the time of sample collection by the time rate of change measured by the syringe samples throughout the chamber experiment (*e.g.*, Figure 2.1 - WSU-site 2, experiment #4). For these experiments, the large volume samples were representative of air in the chamber headspace at the time of sample collection and were not significantly diluted by ambient or soil air during sample collection. For four chamber experiments, the CH_4 concentration measured in the final cylinder sample was higher than the $\pm 2\sigma$ range of the predicted CH_4 concentration, indicating an average dilution of 5% of these chamber headspace samples with ambient air during collection (Table 2.1).

Methane uptake rates were calculated from a linear regression of the observed decrease in CH_4 concentration with time using the chamber volume determined from the measured initial CCl_2F_2 concentration. Because the chamber experiments were long enough to perturb the steady state CH_4 concentration soil gradients, slowing the rate of CH_4 uptake, only samples from the first one (ARB) or two (WSU) hours of a chamber flux experiment were used for the regression. Calculation of CH_4 uptake rates during the

period when $d[CH_4]/dt$ was linear allows comparison of the rate of CH_4 uptake measured for the soils in this study to determinations of CH_4 uptake rates in other locations. Methane uptake rates were 33 and 43 μg CH_4 m^{-2} hr^{-1} (WSU-site 1), 37 and 39 μg CH_4 m^{-2} hr^{-1} (WSU-site 2), and 145 and 182 μg CH_4 m^{-2} hr^{-1} (ARB) (Table 2.1). These uptake rates are within the range reported for similar ecosystems, *e.g.*, up to ~55 μg CH_4 m^{-2} hr^{-1} in a Colorado grassland (Mosier *et al.*, 1996) and up to ~200 μg CH_4 m^{-2} hr^{-1} in temperate forests (Tyler *et al.*, 1994; Crill, 1991). Because the KIE occurring during soil uptake depends on the *relative* rates of uptake of isotopically light and heavy CH_4, it will be shown to be relatively insensitive to the decreasing rate of CH_4 uptake observed during a chamber flux experiment.

The steady state concentration of CH_4 in the soil air decreased approximately exponentially from ambient atmospheric concentrations (~1.74 ppm) at the surface to 0.1 to 0.3 ppm at 80 cm depth (Figure 2.2). The soil air profiles of CH_4 concentration show no evidence of a below-ground CH_4 source at any of the sites, within the depth range and resolution sampled. The non-zero CH_4 concentration observed below 0.5 m at WSU was verified by comparison with air samples collected at 0.4 and 0.9 m from permanently-installed gas monitoring probes (Wood *et al.*, 1993) at the study site and indicated no significant contamination of deeper soil samples by ambient air. Profiles of CH_4 concentration in soil air measured upon completion of flux chamber experiments at WSU (Figure 2.3) indicated the substantial decrease of soil air CH_4 concentration and the soil air CH_4 concentration gradient that occurred above ~ 0.4 m during a flux chamber experiment.

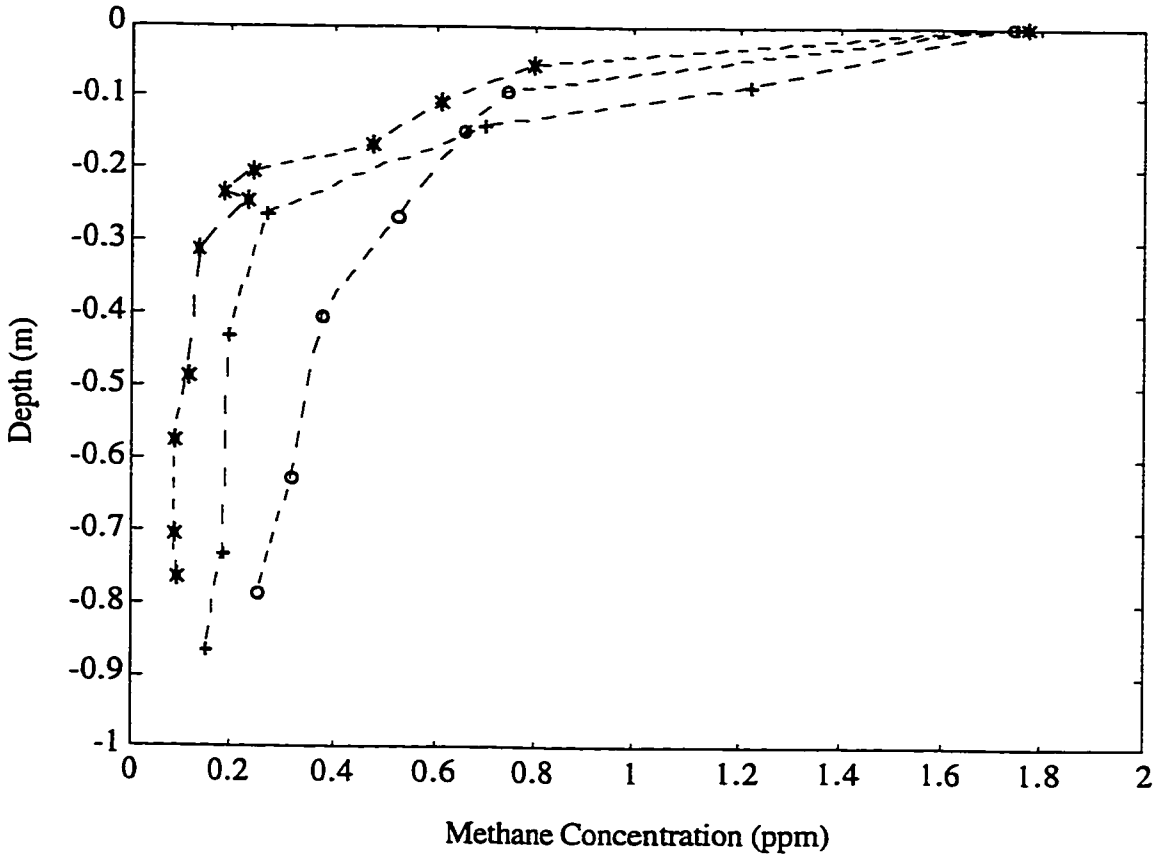

Figure 2.2 Steady state soil air profiles of CH_4 concentration measured at each experimental site.
Symbols denote WSU-site 1 (+), WSU-site 2 (o) and ARB (*). Profiles shown for WSU represent averages of replicate profile determinations, with an average CH_4 concentration reproducibility at each depth of ± 0.042 ppm (WSU-site 1, n=5) and ± 0.025 ppm (WSU-site 2, n=2). At ARB, the profile is comprised of a single measurement at each depth shown. The different profile shapes indicate different ratios of the rates of CH_4 oxidation and diffusion at the three sites.

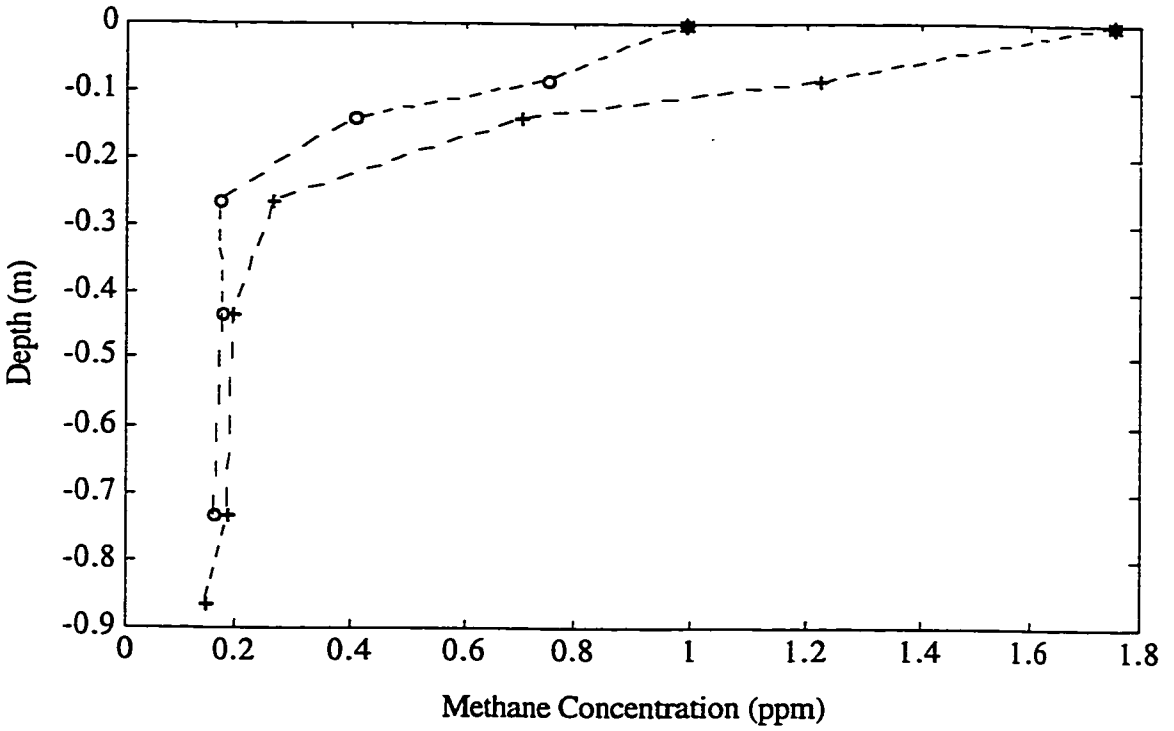

Figure 2.3 Profiles of methane concentration in soil air measured before and after a flux chamber experiment.
CH_4 concentration in soil air measured from syringe samples collected before (+) and after (o) a flux chamber experiment at WSU-site 1 (expt. #2) illustrate the substantial depletion of soil air CH_4 concentration and the decrease of the soil CH_4 concentration gradient that occur during an experiment. Samples at depth = 0 m (*) are cylinder samples collected either at height = +1 m (steady state profile) or from the chamber headspace at the end of the flux-chamber experiment (post-flux experiment profile).

CALCULATION OF α_{SOIL}

The hydrogen and carbon kinetic isotope fractionations occurring during soil uptake of atmospheric CH_4 (α_{soil}) were calculated from the experimental data, summarized in Table 2.1, using a Rayleigh distillation approach. This method, which assumes a closed system, allows calculation of the fractionation factor that best explains the relationship between the measured changes in CH_4 concentration and isotopic composition in the chamber, using the following expression:

$$\frac{1}{\alpha_{soil}} = \frac{\ln\left(\frac{\delta_t + 1000}{\delta_o + 1000}\right)}{\ln\left(\frac{C_t}{C_o}\right)} + 1. \qquad (1)$$

Here α_{soil} equals the kinetic isotope effect ($\alpha^D_{soil} = k(CH_4)/k(CH_3D)$; $\alpha^C_{soil} = k(CH_4)/k(^{13}CH_4)$), δ_o and δ_t are the measured isotopic compositions of the initial CH_4 and the CH_4 remaining at time t, respectively, and C_o and C_t are the measured concentrations of CH_4 initially and at time t, respectively. For experiments in which substantial dilution of the final cylinder sample occurred during sampling, δ_t and C_t represent the dilution-corrected CH_4 isotopic composition and concentration at time t. The average hydrogen KIEs for the three sites were 1.088 ± 0.007, 1.124 ± 0.006 and 1.069 ± 0.007 for WSU-site 1, WSU-site 2, and ARB, respectively. The average carbon KIEs were 1.0163 ± 0.0018, 1.0173 ± 0.0004 and 1.0179 ± 0.0003, for the same sites (Table 2.2). The correction for dilution of the chamber headspace with ambient air

Table 2.2 Hydrogen and carbon KIEs for soil uptake of atmospheric CH_4 (α^D_{soil} and α^C_{soil}), calculated using the Rayleigh distillation approach, and for microbial oxidation of CH_4 (α^D_{ox} and α^C_{ox}).

Study site	Expt. #	α^D_{soil}[a]	$\pm 1\sigma$[b]	α^D_{ox}[c]	$\pm 1\sigma$[d]	α^C_{soil}[a]	$\pm 1\sigma$[b]	α^C_{ox}	$\pm 1\sigma$[d]
WSU-site 1	1	1.089	0.010	1.159	0.020	1.0152	0.0005	1.0111	0.0010
"	2	1.082	0.009	1.145	0.018	1.0153	0.0005	1.0114	0.0010
"	3	1.093	0.018	1.167	0.035	1.0184	0.0010	1.0174	0.0020
WSU-site 2	4	1.127	0.009	1.229	0.018	1.0171	0.0005	1.0150	0.0009
"	5	1.121	0.009	1.217	0.018	1.0175	0.0005	1.0158	0.0009
ARB	1	1.070	0.006	1.122	0.013	1.0178	0.0004	1.0162	0.0008
"	2	1.076	0.007	1.134	0.015	1.0176	0.0004	1.0158	0.0008
"	3	1.072	0.007	1.126	0.015	1.0178	0.0004	1.0162	0.0008
"	4	1.059	0.018	1.098	0.035	1.0184	0.0011	1.0172	0.0021

a. Uses final CH_4 concentration and isotopic composition corrected, when necessary, for dilution by ambient air during sample collection, see text.

b. Uncertainty in α_{soil} is $\pm 1\sigma$ calculated using a bootstrap analysis to account for the analytical uncertainty in the measurements of CH_4 concentration and isotopic composition and the uncertainty in the percentage dilution for experiments in which the final sample was diluted with ambient air.

c. KIEs for microbial oxidation of CH_4 (α^D_{ox} and α^C_{ox}) were calculated from α^D_{soil} and α^C_{soil} and the relative rates of CH_4 oxidation and diffusion, derived from the observed steady-state [CH_4] soil depth profiles, see text.

d. Uncertainty in α_{ox} is $\pm 1\sigma$, calculated using a boot-strap analysis from the $\pm 1\sigma$ uncertainty in α_{soil}.

during sample collection resulted in adjustments to α^{D}_{soil} of ≤ 0.0021 and α^{C}_{soil} of ≤ 0.0005.

The uncertainty in the individual determinations of α_{soil} was calculated using a Monte Carlo-based bootstrap analysis (*e.g.*, Efron, 1991) and accounts for the analytical uncertainty in the measurements of CH_4 concentration and isotopic composition, with the latter contributing most of the error (> 95% for δD; > 80% for $\delta^{13}C$). For the experiments in which the final cylinder was diluted, this uncertainty analysis also included the uncertainty in the amount of dilution. The uncertainties reported for the average KIEs for each site are $\pm 1\sigma$ and represent the larger of the uncertainties resulting from the analytical uncertainty in determining α_{soil} and the observed variability in replicate determinations of α_{soil} at a single site ($\pm 1\sigma$ for $n \geq 3$, $\pm$ range for $n = 2$). These two uncertainties were generally of the same magnitude.

Calculation of α_{ox}

The overall kinetic isotope effect during soil uptake of atmospheric CH_4 results from a combination of the KIEs occurring during CH_4 diffusion through soil air (α_{diff}) and during microbial oxidation of CH_4 (α_{ox}). The relationship between α_{soil}, α_{ox}, and α_{diff} can be derived from knowledge of the shape of the steady state soil profile of CH_4 concentration, given certain assumptions about CH_4 oxidation and diffusion within the soil column.

If diffusion and microbial oxidation are the only processes affecting CH_4 in the soil, and the oxidation of CH_4 is first-order, the time rate of change of CH_4 concentration in the soil is described by:

$$\frac{dC}{dt} = K \cdot \frac{d^2C}{dz^2} - L \cdot C \qquad (2)$$

where C is CH_4 concentration; K is the effective diffusivity of CH_4 in soil (m^2/sec), which includes the effects of soil properties (*i.e.*, tortuosity and porosity) on molecular diffusion in the soil; L is the first-order loss rate constant for microbial oxidation of CH_4 (1/sec); t is time; and z is depth in the soil, zero at the surface and positive numbers with depth.

At steady state, if C goes to zero at infinite depth, and L and K are constant with depth, the solution to equation (2) is:

$$C_z = C_0 e^{-z\sqrt{L/K}} \qquad (3)$$

where C_o is the CH_4 concentration at z=0 and is equal to atmospheric CH_4 concentration. Equation (3) shows that the relative rates of CH_4 oxidation and diffusion determine the shape of the soil distribution of CH_4 concentration. Similar expressions can be written for CH_3D and $^{13}CH_4$, utilizing the relationships $[^*CH_4]=R\cdot[CH_4]$, $L(^*CH_4)=L(CH_4)/\alpha_{ox}$ and $K(^*CH_4)=K(CH_4)/\alpha_{diff}$ where $^*CH_4$ is isotopically-heavy CH_4, R is the CH_4 D/H or $^{13}C/^{12}C$ ratio, and α_{ox} is the appropriate KIE of oxidation (α^D_{ox} or α^C_{ox}).

Bender (1990) showed that when the flux of a trace gas is described by Fick's law (Flux = -K·dC/dz) and the trace gas concentration decreases exponentially with depth (equation (3)),

$$\alpha_{soil} = \sqrt{\alpha_{ox} \cdot \alpha_{diff}}. \qquad (4)$$

Thus, α_{ox} can be calculated from knowledge of α_{soil} at steady state conditions.

Although the eventual sink for soil CH_4 is microbial oxidation, equation (4) shows that the KIE expressed during this process is somewhat obscured in the overall KIE (α_{soil}) by the fractionation effect associated with diffusion. However, because α_{diff} is independent of temperature and specific soil characteristics, variations in α_{soil} will derive from variations in α_{ox}. Spatial and temporal variability in α_{ox} may result from substrate limitation or the different reaction kinetics of different soil bacteria populations. This variability, however, is attenuated in α_{soil} by its square-root dependence on α_{ox}.

Since CH_4 concentration was not observed to reach zero at depth at the sites in this study, equation (2) was solved by imposing a zero flux constraint at depth z_o. This is equivalent to the condition that L=0 at z= z_o and below and results in the following solution at steady state:

$$C_z = \frac{C_0}{1+e^{-2z_0\omega}} \cdot \left(e^{(z\omega-2z_0\omega)} + e^{-z\omega}\right) \qquad \text{for } z < z_o \qquad (5a)$$

$$C_z = C_{z_0} \qquad \text{for } z \geq z_o \qquad (5b)$$

where $\omega = \sqrt{L/K}$. Similar expressions can again be written for $[CH_3D]$ and $[^{13}CH_4]$, as before. Following Bender (1990), it can be shown that

$$\alpha_{soil} = \sqrt{\alpha_{ox} \cdot \alpha_{diff}} \cdot \Omega \qquad (6)$$

$$\text{where } \Omega = \frac{\left(1+e^{-2z_0\omega\sqrt{\alpha_{diff}/\alpha_{ox}}}\right)\cdot\left(1-e^{-2z_0\omega}\right)}{\left(1+e^{-2z_0\omega}\right)\cdot\left(1-e^{-2z_0\omega\sqrt{\alpha_{diff}/\alpha_{ox}}}\right)}.$$

In this case, α_{soil} varies not only as a result of variations in α_{ox}, as described by equation (4), but also as a result of variations in L/K, *i.e.*, the relative rates of

CH_4 oxidation and diffusion in the soil column. For $^{13}C/^{12}C$, because $\alpha_{ox} \approx \alpha_{diff}$, $\Omega \approx 1$ and equation (6) reduces approximately to equation (4).

Under steady state conditions, α_{ox} can be calculated iteratively from equation (6). Values of α^D_{ox} and α^C_{ox} were calculated for each chamber flux experiment, using the Rayleigh-determined α^D_{soil} and α^C_{soil} and values for z_o and L/K determined by fitting, using equations (5), the observed steady state CH_4 concentration profile at each site. This calculation therefore assumes that the Rayleigh-determined values for α_{soil} were representative of steady state conditions. The error introduced by this assumption is discussed in the following section. The average hydrogen KIEs for microbial oxidation for the three sites were 1.157 ± 0.015, 1.223 ± 0.013 and 1.120 ± 0.015 for WSU-site 1, WSU-site 2 and ARB, respectively. The average carbon KIEs for the same sites were 1.0133 ± 0.0035, 1.0154 ± 0.0008 and 1.0164 ± 0.0006 (Table 2.2). The uncertainty in the individual determinations of α_{ox} was calculated using a bootstrap analysis and accounts for the uncertainty in α_{soil} (Table 2.2).

The Effect of Non-steady State Conditions on α_{soil} and α_{ox}

Because a static flux chamber perturbs steady state conditions, by altering the gradients of CH_4, CH_3D, and $^{13}CH_4$ concentrations in the soil, the value of α_{soil} determined from a chamber flux experiment is not necessarily the same as the steady state value for α_{soil}. The effect of non-steady state conditions on α_{soil} was examined using a one-dimensional diffusion-oxidation model coupled to a finite reservoir at the soil surface to simulate

the changing concentrations of the three CH_4 species within both the chamber headspace and soil column.

The model was initialized with the observed initial concentration, δD and $\delta^{13}C$ of CH_4 in the chamber headspace and the initial, assumed steady state, soil air concentrations of CH_4, CH_3D and $^{13}CH_4$. The steady state profile of soil air CH_4 concentration was described by the best fit of equations (5) to the observed steady state CH_4 concentration profile (*e.g.*, Figure 2.4b, dotted line), obtained using the fitting parameters shown in Table 2.3. Steady state profiles of soil air CH_3D and $^{13}CH_4$ concentrations were simulated using equations (5) modified for these isotopic species, with $\alpha_{diff} = 1.0195$ and values for α^D_{ox} and α^C_{ox} derived from the Rayleigh-determined α^D_{soil} and α^C_{soil} (Table 2.2), assuming, for the moment, that these values for α_{soil} and α_{ox} were representative of steady state conditions.

As the model was stepped forward in time, the fluxes of CH_4, CH_3D and $^{13}CH_4$ into the soil were calculated using Fick's law and the concentration of each isotopic species of CH_4 in the chamber headspace recalculated to reflect this diffusive loss. Changes to the soil air concentrations of CH_4, CH_3D and $^{13}CH_4$ resulting from diffusion and oxidation within the soil were described by equation (2), using a finite-difference approach and the Dufort-Frankel scheme (Fletcher, 1988) for parameterizing diffusion. The ratio of CH_4 oxidation to diffusion (L/K) was obtained from the steady state CH_4 concentration profile (Table 2.3). The CH_4 oxidative loss rate constant (L) was chosen in the model to best reproduce the observed time rate of change of CH_4 in the chamber headspace (Figure 2.4a, Table 2.3). L was assumed to be

Table 2.3 Fitting parameters for the observed, assumed steady state, soil air CH_4 concentration profiles and the CH_4 loss rate constants used in the diffusion-oxidation model.

Study Site	$\omega (=\sqrt{L/K})^a$ (m^{-1})	z_o^a (m)	$L(CH_4)^b$ (sec^{-1})
WSU-site 1	7.0	0.44	6.29e-5
WSU-site 2	7.5	0.35	7.16e-5
ARB	10.1	0.36	5.20e-4

a. Determined from the best fit of equations (5) to the observed, assumed steady state CH_4 concentration profiles (Figure 2.2).

b. Chosen to best reproduce the observed time rate of change of CH_4 in the chamber headspace (*e.g.*, Figures 2.1 and 2.4).

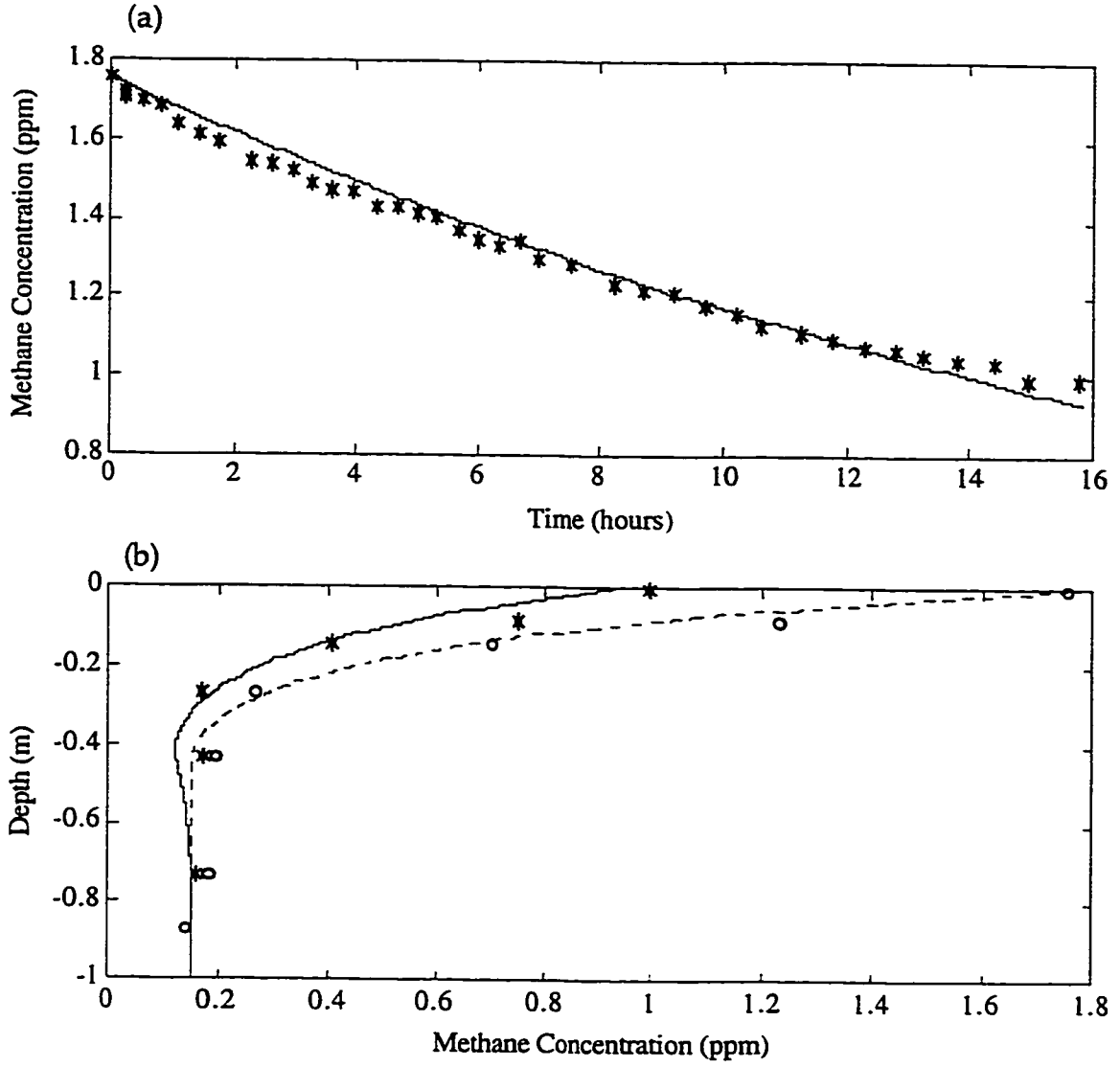

Figure 2.4 Comparison of model predictions to observations for flux chamber experiment #2 at WSU-site 1.

Model predictions are from a one-dimensional diffusion/oxidation model simulating the changing concentration of CH_4 within both the headspace of a static flux chamber and the soil column during a chamber flux experiment.

(a) Observed (*) and predicted (—) time rate of change of CH_4 concentration in the chamber headspace.

(b) Observed (*) and predicted (—) post-chamber soil CH_4 concentration profile, with the steady state CH_4 concentration profile used to initialize the model (- -) and the observed steady state CH_4 concentration profile (o) shown for comparison.

unperturbed by the chamber experiment, *i.e.*, L(chamber) = L(steady state). Model predictions of soil air CH_4 concentration profiles for the end of a chamber experiment generally compared well to observations (*e.g.*, Figure 2.4b, solid line).

The KIEs associated with soil uptake of CH_4 were calculated from the model-predicted isotopic composition of CH_4 in the chamber headspace using the Rayleigh distillation equation (equation (1)). The difference between these non-steady state KIEs, $\alpha^D_{soil(non\text{-}ss)}$ and $\alpha^C_{soil(non\text{-}ss)}$, and the values of α^D_{soil} and α^C_{soil} used to initialize the model indicates the degree to which the KIE determined from a chamber flux experiment is perturbed from steady state. The deviation ($\Delta\alpha_{soil(chamb)}$ or $\Delta\varepsilon_{soil(chamb)}$ in units of ‰) of the model-predicted $\alpha_{soil(non\text{-}ss)}$ from the initial α_{soil} was determined for a representative experiment at each study site (Figure 2.5). As the modeled chamber experiment progressed, the deviation of the predicted $\alpha_{soil(non\text{-}ss)}$ from its initial value generally increased. This perturbation was in the direction of α_{ox}, indicating that the KIE associated with microbial oxidation, *i.e.*, the actual sink of CH_4, becomes increasingly important to the overall KIE in the non-steady state conditions inherent to a flux chamber experiment. As the chamber experiment progresses, the system approaches total CH_4 loss which is driven only by oxidation (α_{ox}), not diffusion (α_{diff}). This is illustrated by the fact that the perturbations to α^D_{soil} and α^C_{soil} are of opposite sign. For δD, because α^D_{ox} (1.098-1.229, Table 2.2) is much larger than α_{diff} (1.0195), the perturbed KIE is larger than the steady state KIE and $\Delta\varepsilon^D_{soil(chamb)}$ is positive. (Figure 2.5a). The size of this perturbation depends on the magnitude of α^D_{ox}. For $\delta^{13}C$, in contrast,

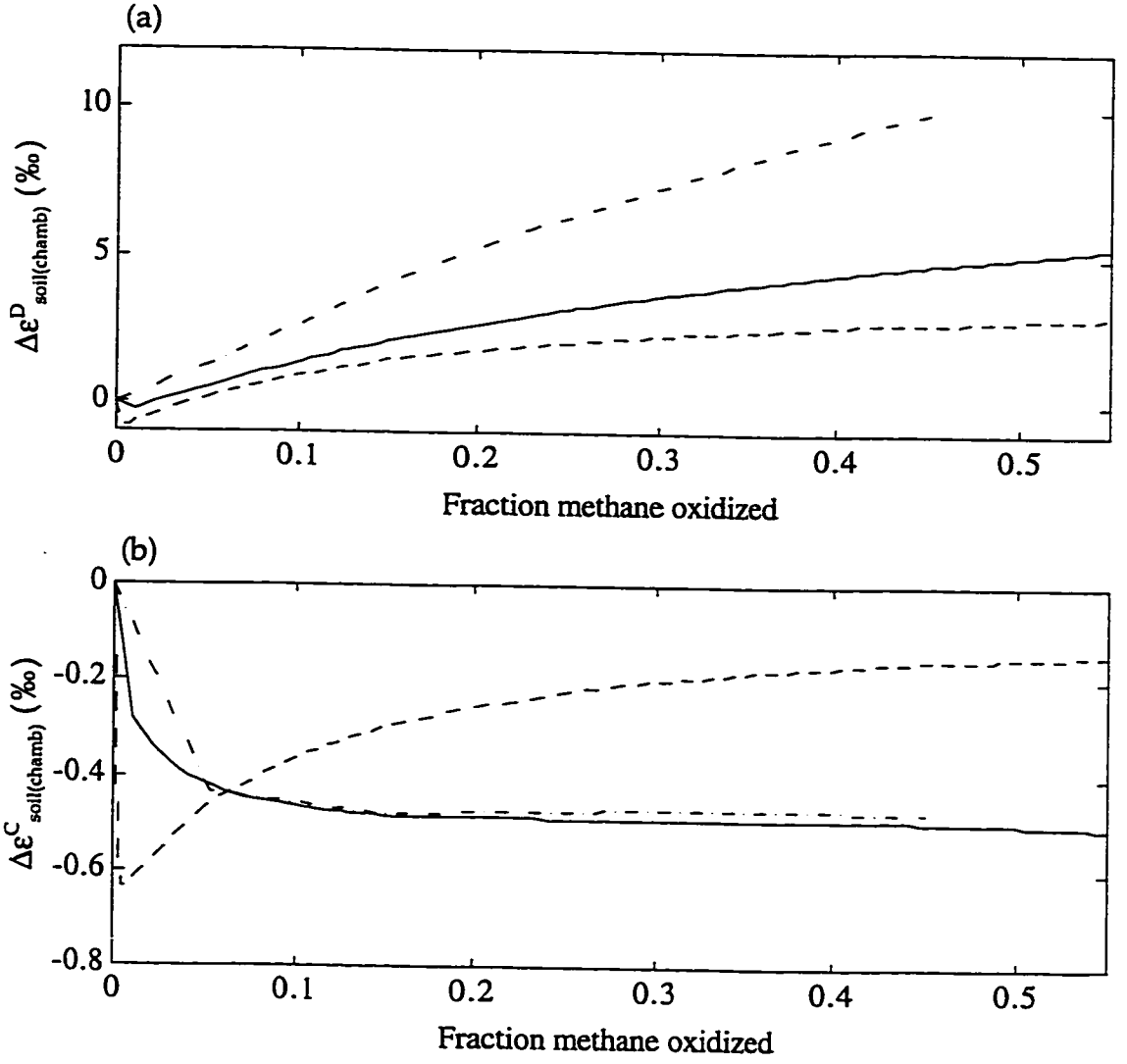

Figure 2.5 Effect of a chamber flux experiment on the hydrogen and carbon KIEs associated with soil uptake of atmospheric CH_4.
The perturbations of the KIEs by the non-steady state conditions resulting from a chamber flux experiment are plotted as $\Delta\varepsilon_{soil(chamb)}$, where $\Delta\varepsilon_{soil(chamb)}$ (‰) = $(\alpha_{soil(non\text{-}ss)} - \alpha_{soil})\cdot 1000$, *i.e.*, the deviation of the model-predicted $\alpha_{soil(non\text{-}ss)}$ from the initial steady state value of α_{soil}. Diffusion/oxidation model predictions are shown for a representative experiment at each study site (WSU-site 1, expt. #2 (—); WSU-site 2, expt. #4 (--); ARB, expt. #3 (–)). The sign and magnitude of the perturbation generally depends on the relative sizes of α_{ox}, α_{diff} and $\alpha_{soil(ss)}$. In general, $\alpha_{soil(chamb)}$ is perturbed in the direction of α_{ox} as the experiment proceeds. For δD, (a), because $\alpha^D_{ox} > \alpha^D_{soil}$, $\Delta\varepsilon^D_{soil(chamb)}$ is positive. For $\delta^{13}C$, (b), because $\alpha^C_{ox} < \alpha_{soil}$, $\Delta\varepsilon^C_{soil(chamb)}$ is negative.

because α^{C}_{ox} (1.0111-1.0174, Table 2.2) is less than α_{diff} (1.0195), $\alpha^{C}_{soil(non\text{-}ss)}$ is smaller than the steady state KIE and $\Delta\varepsilon^{C}_{soil(chamb)}$ is therefore negative (Figure 2.5b).

Because α^{C}_{ox} and α_{diff} are similar in magnitude, the magnitude of the perturbation to α^{C}_{soil} depends on the relative rates of CH_4 oxidation and diffusion in the soil (L/K). This ratio determines the degree to which α^{C}_{ox}, *i.e.*, the actual CH_4 sink, is expressed in α^{C}_{soil} during the experimental time scale. The initial perturbation of $\alpha^{C}_{soil(non\text{-}ss)}$ depends on the rate of CH_4 oxidation (relative to diffusion) near the soil surface and is larger for a higher relative rate of oxidation. As the experiment proceeds, $\alpha^{C}_{soil(non\text{-}ss)}$ is affected by the balance between CH_4 oxidation and diffusion throughout the soil column. In general, $\Delta\varepsilon^{C}_{soil(chamb)}$ is inversely proportional to L/K. A higher rate of CH_4 diffusion decreases the isotopic importance of diffusion by increasing the "communication" between the soil microbia and the chamber headspace, thereby increasing the overall importance of α^{C}_{ox} to $\alpha^{C}_{soil(non\text{-}ss)}$.

Notably, the perturbations resulting from the non-steady state conditions of a chamber experiment were relatively small, *i.e.*, < 10‰ for $\Delta\varepsilon^{D}_{soil(chamb)}$ and < -0.5‰ for $\Delta\varepsilon^{C}_{soil(chamb)}$, and were on the order of the analytical uncertainty in the Rayleigh-derived ε_{soil} (Table 2.2). This indicates that the KIE during soil uptake is well-determined from a static flux chamber experiment and, even after substantial CH_4 uptake, is affected little by the presence of the flux chamber. The model-predicted values for $\Delta\varepsilon_{soil(chamb)}$ were relatively insensitive to uncertainty in the model input parameters, *i.e.*, the assumed shape of the steady state soil air CH_4 concentration profile and the assumed steady state values for α_{ox} and L. For example, varying $\alpha_{ox} \pm 1\sigma$,

$L(CH_4) \pm 5\%$ and allowing the concentration of CH_4 to go to zero at depth, instead of asymptoting to a non-zero value, resulted in an uncertainty in the model-predicted $\Delta\varepsilon_{soil(chamb)}$ of $\pm 0.7‰$ for δD and $\pm 0.05‰$ for $\delta^{13}C$ for experiment #2 at WSU-site 1.

The Rayleigh-distillation calculated values of α^{D}_{soil} and α^{C}_{soil} (Table 2.2) were corrected for the perturbation caused by a flux chamber experiment using the relationship between $\Delta\alpha_{soil(chamb)}$ and fraction CH_4 oxidized determined for each study site (Figure 2.5). The calculated steady state values of α^{D}_{soil} are 1.084 ± 0.007, 1.114 ± 0.006 and 1.067 ± 0.007 for WSU-site 1, WSU-site 2 and ARB, respectively. For α^{C}_{soil}, the steady state values are 1.0168 ± 0.0018, 1.0178 ± 0.0004 and 1.0181 ± 0.0004 for the same sites (Table 2.4). The uncertainties in the individual determinations of $\alpha_{soil(ss)}$ at WSU-site 1 (Table 2.4) were calculated by accounting for both the analytical uncertainty in the Rayleigh-derived value for α_{soil} (Table 2.2) and the uncertainty in the model-derived correction for the non-steady state perturbation described above. Because analytical uncertainty dominated the total uncertainty in $\alpha_{soil(ss)}$ at this site, the overall uncertainty in $\alpha_{soil(ss)}$ was assumed to equal the analytical uncertainty at WSU-site 2 and ARB (Table 2.4).

The determination of $\alpha_{soil(ss)}$ allows calculation of the apparent steady state α_{ox} using equation (6). The average $\alpha^{D}_{ox(ss)}$ was 1.149 ± 0.015, 1.204 ± 0.013 and 1.115 ± 0.014 for WSU-site 1, WSU-site 2, and ARB, respectively. The average $\alpha^{C}_{ox(ss)}$ was 1.0142 ± 0.0035, 1.0163 ± 0.0007, and 1.0167 ± 0.0007, for the same sites (Table 2.4). The uncertainty in the individual determinations of

Table 2.4 Steady-state hydrogen and carbon KIEs for uptake of atmospheric CH_4 ($\alpha_{soil(ss)}$) and for microbial oxidation of CH_4 in soil ($\alpha_{ox(ss)}$). These values have been adjusted from the KIEs in Table 2.2 to account for the perturbation of soil air steady-state CH_4 concentration gradients by the static flux chamber experiment, see text.

Study Site	Expt. #	$\alpha^D_{soil(ss)}$	$\pm 1\sigma^a$	$\alpha^D_{ox(ss)}$	$\pm 1\sigma^b$	$\alpha^C_{soil(ss)}$	$\pm 1\sigma^a$	$\alpha^C_{ox(ss)}$	$\pm 1\sigma^b$
WSU-site 1	1	1.084	0.010	1.150	0.020	1.0157	0.0005	1.0121	0.0009
"	2	1.078	0.009	1.136	0.017	1.0158	0.0005	1.0124	0.0010
"	3	1.090	0.018	1.160	0.037	1.0189	0.0010	1.0183	0.0019
WSU-site 2	4	1.117	0.009	1.209	0.017	1.0176	0.0005	1.0159	0.0009
"	5	1.111	0.009	1.198	0.018	1.0180	0.0005	1.0166	0.0009
ARB	1	1.067	0.006	1.116	0.012	1.0180	0.0004	1.0165	0.0008
"	2	1.073	0.007	1.128	0.015	1.0178	0.0004	1.0161	0.0008
"	3	1.069	0.007	1.120	0.014	1.0180	0.0004	1.0165	0.0008
"	4	1.057	0.018	1.094	0.036	1.0186	0.0011	1.0177	0.0022

a. Uncertainty in $\alpha_{soil(ss)}$ at WSU site 1 is $\pm 1\sigma$ uncertainty propagated from analytical and model error. Because analytical error dominates the overall uncertainty at WSU site 1, the overall uncertainty was taken to equal the analytical uncertainty for WSU site 2 and ARB.

b. Uncertainty in α_{ox} is $\pm 1\sigma$, calculated, using a boot-strap analysis, from the $\pm 1\sigma$ uncertainty in $\alpha_{soil(ss)}$.

$\alpha_{ox(ss)}$ resulting from the uncertainty in $\alpha_{soil(ss)}$ was calculated using a bootstrap analysis. The adjustment to steady state conditions yields slightly different KIEs for microbial oxidation (Table 2.4) than were originally derived from the Rayleigh-distillation calculated values of α_{soil} (Table 2.2). Because these changes were generally less than the uncertainty in α_{ox}, *i.e.*, -4 to -20‰ for ε^{D}_{ox} and 0.3 to 1‰ for ε^{C}_{ox}, they do not significantly affect the calculation of $\alpha_{soil(ss)}$.

Previous studies of biologically-mediated isotopic fractionations have shown that the magnitude of KIE expressed can depend on substrate concentration. When substrate is plentiful, the KIE expressed is generally larger than when less substrate is available (*e.g.*, Park and Epstein, 1960). To test whether the decrease in soil air CH_4 concentration resulting from a chamber flux experiment affected the fractionation expressed during microbial oxidation of CH_4, short chamber flux experiments were performed at both WSU-site 1 (expt. #3) and ARB (expt. #5). There was no detectable difference between the values of $\alpha^{D}_{soil(ss)}$ at both sites and $\alpha^{C}_{soil(ss)}$ at ARB obtained from short (~25% CH_4 oxidized) versus long (45-55% CH_4 oxidized) experiments (Table 2.4). These results suggest that the α_{ox} expressed by the microbia at these sites was not significantly affected by changes in CH_4 availability. At WSU-site 1, however, the carbon KIE was smaller for long, versus short, experiments.

VARIABILITY IN α_{SOIL}

Replicate determinations of α^{D}_{soil} and α^{C}_{soil} in each experimental location agreed well, indicating that α_{soil} could be precisely measured. For

both α^{D}_{soil} and α^{C}_{soil}, the within-ecosystem (WSU-sites 1 and 2) and between-ecosystem (WSU and ARB) variabilities were comparable. The hydrogen KIE was distinctly different at the three study sites and more variable than the carbon KIE (Table 2.4).

Differences in α_{soil} between experimental locations may reflect real variations in α_{ox}. Alternatively, the variability in α_{soil} between locations could reflect a constant α_{ox} and variations in the relative rates of CH_4 oxidation and diffusion (L/K) within the soil columns at the different sites. If, for example, cracks in the soil surface at one site exposed methanotrophic bacteria directly to the atmosphere, the KIE associated with microbial oxidation would be expressed more strongly there than at a different location where the bacteria "communicated" to the atmosphere, and the expression of α_{ox} was tempered, via diffusion.

Previous investigators (Tyler *et al.*, 1994), noting the similarity between α^{C}_{soil} and α_{diff}, have suggested that soil uptake of atmospheric CH_4 was diffusion-limited in the environments they studied. It has been shown here, however, that α^{C}_{soil} can resemble α_{diff} when oxidation and diffusion both affect the rate of CH_4 uptake in soils. When the rates of CH_4 oxidation and diffusion are evenly distributed throughout the soil column, $\alpha_{soil} \approx \sqrt{\alpha_{ox} \cdot \alpha_{diff}}$. Because $\alpha^{C}_{ox} \approx \alpha_{diff}$, determination of α_{soil} cannot distinguish between diffusion- and oxidation-limited CH_4 uptake. For hydrogen, since $\alpha^{D}_{ox} >> \alpha_{diff}$, determinations of α^{D}_{soil} are much more sensitive to diffusion- versus oxidation-limited CH_4 uptake. The results of α^{D}_{soil} of 1.057 to 1.117 presented

here are significantly larger than $\alpha_{diff} = 1.0195$ and indicate that CH_4 uptake in soils at the sites in this study was not limited by diffusion.

The greater sensitivity of α^D_{soil} to controls on the rate of CH_4 uptake suggests that α^D_{soil} will exhibit much more variability than α^C_{soil}. This conclusion is supported by the observation of a ~60‰ range in the results for α^D_{soil} reported here, as compared to a ~10‰ range observed for α^C_{soil} in a variety of different ecosystems and seasons (this study; King *et al.*, 1989; Tyler *et al.*, 1994; Reeburgh *et al.*, 1997). Estimating an accurate average value for α^D_{soil} for application to the global atmospheric CH_4 - δD budget will therefore require additional measurements elucidating the magnitude of spatial and seasonal variability in α^D_{soil}.

Comparison to Previous Determinations of α_{soil} and α_{ox}

The determinations presented here for α^D_{soil} are the first measurements of the hydrogen KIE associated with soil uptake of atmospheric CH_4. The average value for α^D_{soil} determined at the three experimental locations in this study was $\alpha^D_{soil} = 1.088 \pm 0.024$. The values of the hydrogen KIE for microbial oxidation of CH_4 derived from these observations of α^D_{soil} range from $\alpha^D_{ox} = 1.094$ to 1.209 and are the first field measurement based determinations of the KIE expressed by aerobic soil microbia oxidizing CH_4 at or below atmospheric concentrations. The magnitude is in general agreement with previous laboratory culture measurements. Coleman *et al.*'s (1981) measurements of the KIE exhibited by methane-oxidizing bacteria cultures, grown in an atmosphere of 18-30% CH_4, ranged from $\alpha^D_{ox} = 1.103 \pm 0.006$ to 1.311 ± 0.014.

Bergamaschi *et al.* (1998) found $\alpha^{D}_{ox} = 1.039 \pm 0.026$ in landfill cover soils where CH_4 supply was from below ground and there was net emission of CH_4 to the atmosphere.

The determinations presented here of $\alpha^{C}_{soil} = 1.0173 \pm 0.0010$ for a native grassland and 1.0181 ± 0.0004 for a forested site in Washington state fall within the range of previously reported values measured in other ecosystems. In Alaskan tundra, King *et al.* (1989) measured $\alpha^{C}_{soil} = 1.016$ and 1.027 at two sites. Tyler *et al.* (1994) measured α^{C}_{soil} several times throughout the year in a New Hampshire temperate forest and reported $\alpha^{C}_{soil} = 1.023 \pm 0.004$ (n=6). Reeburgh *et al.* (1997) determined $\alpha^{C}_{soil} = 1.023$ and 1.026 in Alaskan boreal forest soils. The addition of these determinations of α^{C}_{soil} to previous results indicates that α^{C}_{soil} varies within a relatively narrow range across many different ecosystem types.

The measurements of α^{C}_{soil} presented in this study imply a KIE during microbial oxidation of $\alpha^{C}_{ox} = 1.0121$ to 1.0183. These values are slightly lower than $\alpha^{C}_{ox} = 1.022$-1.025 determined from field measurements of the depth distribution of CH_4 concentration and $\delta^{13}C$ content in boreal forest soils (Reeburgh *et al.*, 1997). However, these results are within the range of determinations of α^{C}_{ox} in landfill cover soils, *i.e.*, $\alpha^{C}_{ox} = 1.008 \pm 0.004$ (Bergamaschi *et al.*; 1998) and $\alpha^{C}_{ox} = 1.022 \pm 0.008$ (Liptay *et al.*, 1998), and in laboratory culture measurements with an atmosphere of 18-30% CH_4 where $\alpha^{C}_{ox} = 1.0130 \pm 0.0002$ to 1.0248 ± 0.0008 (Coleman *et al.*, 1981).

Implications for the Global Methane Budget

Assuming that soil uptake of atmospheric CH_4 occurs with a hydrogen isotopic fractionation of $\alpha^D_{soil} \approx 1.088$, *i.e.*, ε^D_{soil} $(=(1/\alpha - 1)\cdot 1000) \approx -81‰$, the KIE associated with this sink is significantly smaller than the KIEs associated with the other CH_4 sinks. Assuming removal by tropospheric OH, soil uptake and stratospheric loss accounts for 88%, 5% and 7% of the total CH_4 sink, respectively (Houghton *et al.*, 1996), and utilizing the value of $\varepsilon^D_{OH} = -230 \pm 45‰$ (at 277 K) derived from the work of Gierczak *et al.* (1997), and $\varepsilon^D_{STRAT} = -160 \pm 20‰$ from Irion *et al.* (1996), the overall KIE for CH_4 loss would be $\varepsilon^D_{TOTAL} = -220 \pm 40‰$.

Because the isotopic fractionation associated with soil uptake of atmospheric CH_4 is significantly different from the fractionations associated with the other CH_4 removal processes, the soil sink is an important contributor to the isotopic budget of atmospheric CH_4. The smaller KIE associated with soil uptake decreases the overall KIE and implies a more δD enriched source than if there were no soil sink. In addition, the latitudinal distribution of both the strength of the soil sink and its relative importance to other atmospheric CH_4 removal processes will result in zonal variations in the overall KIE of CH_4 removal. At temperate northern latitudes where the amount of CH_4 removed by soils has been estimated to be 20-70% of the OH sink (Fung *et al.*, 1991), the fractionation associated with the soil sink may be especially important. Removal by soils is the only major sink of atmospheric CH_4 with a significant interhemispheric asymmetry, resulting from the asymmetry of land mass distribution between the two hemispheres. Using

the geographic distribution of CH_4 removal by OH and soils presented by Fung *et al.* (1991) and assuming that CH_4 loss in the stratosphere is evenly distributed between the two hemispheres, the asymmetry in the soil sink strength results in a ~6‰ difference in the total KIE for CH_4 loss between the two hemispheres. This soil uptake-derived asymmetry in the total KIE partially compensates for the observed interhemispheric gradient in the δD of atmospheric CH_4 of ~10‰ with enriched CH_4 observed in the southern hemisphere (Wahlen *et al.*, 1990; Quay *et al.*, in press). Thus, CH_4 with a nearly constant δD is removed in the two hemispheres. Modeling studies of the global atmospheric CH_4 budget using deuterium as a tracer must therefore include α^D_{soil}.

CONCLUSIONS

The value of α_{soil}, the KIE associated with soil uptake of atmospheric CH_4, is well determined from static flux chamber studies and affected little by the presence of the flux chamber. Based on flux chamber studies in two areas in Washington state, *i.e.*, a native grassland and a managed forested arboretum, $\alpha^D_{soil} = 1.088 \pm 0.024$ (n=9). Local spatial variability was as important as the differences between the two ecosystems in determining α^D_{soil}. The variability in α^D_{soil} reflects differences in α^D_{ox} between study sites and/or differences in the relative rates of CH_4 oxidation and diffusion within the soil column at the different study sites. The results presented here indicate that CH_4 uptake in these areas was not limited by diffusion. The determination of $\alpha^C_{soil} = 1.0176 \pm 0.0007$ agrees well with previous determinations.

The range in α^D_{ox} was 1.094 to 1.209 at the sites in this study; overall α^D_{ox} = 1.156 ± 0.045 (n=9). The range in α^C_{ox} was 1.0121 to 1.0183, with α^C_{ox} = 1.0157 ± 0.0013 (n=9). These determinations of α_{ox}, which depend on assumed soil properties and depth distribution of CH_4 oxidation, are within the range of previous measurements of the KIE expressed by methanotrophic bacteria in other environments.

The determinations of α^D_{soil} presented here indicate that the hydrogen kinetic isotope effect associated with soil uptake of atmospheric CH_4 is significantly less than the hydrogen KIEs of the other two sinks for atmospheric CH_4: oxidation by OH and removal in the stratosphere. This will decrease the overall hydrogen KIE associated with the total CH_4 sink and implies a more δD enriched total CH_4 source than if there were no soil sink. The interhemispheric asymmetry of the soil sink strength results in an interhemispheric asymmetry of ~6‰ in the KIE of the total CH_4 sink, *i.e.*, comparable to the 10‰ difference in the δD of atmospheric CH_4 between the two hemispheres. The KIE associated with soil uptake of atmospheric CH_4 must therefore be included in models of the atmospheric CH_4 budget that use deuterium as a tracer.

The hydrogen KIE associated with soil uptake is sensitive to controls on the rate of CH_4 uptake as a result of the large difference between the hydrogen KIEs associated with CH_4 diffusion and microbial CH_4 oxidation. Thus, α^D_{soil} is likely to exhibit significantly more variability than has been observed for α^C_{soil}. Future studies elucidating the magnitude of spatial and seasonal variability in α^D_{soil}, as well as determinations of α^D_{soil} in a variety of

globally important CH_4 oxidizing ecosystems, are necessary to improve the global average value for α^D_{soil}.

CHAPTER 3: THE D/H CONTENT OF METHANE EMITTED FROM BIOMASS BURNING

INTRODUCTION

Methane is a radiatively and chemically important trace gas constituent of the atmosphere. Its concentration has more than doubled since pre-industrial times to a current atmospheric mixing ratio of ~1.72 ppm (Blunier *et al.*, 1993; Dlugokencky *et al.*, 1998), causing ~20% of the estimated increase in radiative forcing due to anthropogenic greenhouse gas emissions (Houghton *et al.*, 1996). Atmospheric oxidation of CH_4 affects the concentrations of hydroxyl radicals (OH), CO and O_3 in the troposphere and O_3 chemistry in the stratosphere (Wayne, 1993). The atmospheric growth rate of CH_4 has slowed since 1984, perhaps indicating stabilization of global CH_4 emissions (Dlugokencky *et al.*, 1998). The global CH_4 source strength is currently estimated at ~580 Tg yr^{-1} (Hein *et al.*, 1997), derived from the atmospheric burden and estimates of the CH_4 sink, primarily oxidation by OH. Estimating the contribution of individual CH_4 sources (wetlands, rice paddies, ruminants, landfills, natural gas losses, and biomass burning) to the global budget often relies on extrapolation of local flux measurements to the global scale, resulting in significant (20-75%; Crutzen, 1995) uncertainties in the individual source terms.

The $^{13}C/^{12}C$ content of atmospheric CH_4 has been used to examine the budget of atmospheric CH_4 on both regional (Thom *et al.*, 1993; Lassey *et al.*,

1993; Bergamaschi *et al.*, 1998a) and global scales (Stevens, 1988; Quay *et al.*, 1991, in press; Fung *et al.*, 1991; Gupta *et al.*, 1996; Hein *et al.*, 1997; Saeki *et al.*, 1998). These studies relied on measurements of the $^{13}C/^{12}C$ composition of atmospheric CH_4 and its sources and the carbon kinetic isotope effects (KIEs) associated with removal of CH_4 from the atmosphere.

The D/H content of CH_4 is a potentially useful tracer for the atmospheric CH_4 budget but is less well developed than $^{13}C/^{12}C$ (Wahlen *et al.*, 1990; Bergamaschi *et al.*, 1998a; Quay *et al.*, in press). There are fewer determinations of the D/H composition of atmospheric CH_4, of the hydrogen KIEs associated with the CH_4 sinks and of the D/H composition of the CH_4 sources. The δD of atmospheric CH_4 has been measured at ~-85‰, with a ~10‰ depletion in the northern versus southern hemisphere (see Chapter Four; Quay *et al.*, in press). The hydrogen kinetic isotope effects associated with loss of CH_4 from the atmosphere have been measured for the major CH_4 sinks: oxidation by OH (DeMore, 1993; Xiao *et al.*, 1993; Gierczak *et al.*, 1997), loss in the stratosphere (Irion *et al.*, 1996), and uptake by soils (Snover and Quay, in preparation). The D/H contents of CH_4 emitted from bacterial sources (wetlands, rice paddies and ruminants) and from fossil sources (natural gas losses) have also been measured (see Quay *et al.*, in press, for review). Although the D/H content of CH_4 emitted from biomass burning has been estimated (Wahlen, 1993; Whiticar, 1993), it has not been determined in field measurements of biomass fires important for CH_4 emissions on the global scale. The lack of detailed measurements of the D/H of CH_4 emitted from biomass burning limits the use of D/H as a tracer for the

atmospheric CH_4 budget. Without such measurements, for example, it is impossible to evaluate whether the D/H content of CH_4 provides an independent constraint for the atmospheric CH_4 budget.

Emissions of CH_4 from biomass burning comprise about 5-10% of the global atmospheric CH_4 source (Quay *et al.*, 1991; Hao and Ward, 1993; Hein *et al.*, 1997). Most biomass burning occurs in the tropics as a result of deforestation, shifting cultivation, savanna fires, use of fuel wood and clearing of agricultural residues (Hao and Liu, 1994); about 85% of the biomass burning source of CH_4 is emitted in this region (Hao and Ward, 1993). Methane, a product of incomplete combustion, is mostly produced during the less efficient, smoldering phase of biomass burning (Ward *et al.*, 1992; Hao and Ward, 1993). The amount of CH_4 emitted during biomass burning is therefore negatively correlated to the combustion efficiency of the fire (Hao and Ward, 1993; Hao *et al.*, 1996).

The $^{13}C/^{12}C$ content of CH_4 emitted from biomass burning has been measured to be the same as the $^{13}C/^{12}C$ of the organic material burned (Stevens and Engelkemeir, 1988; Wahlen *et al.*, 1989; Levin *et al.*, 1993). The latter is consistent across plant species, depending only on the broader category of plant photosynthetic pathway, *i.e.*, $\delta^{13}C \approx -28‰$ for C3 plants and $\delta^{13}C \approx -14‰$ for C4 plants (Troughton *et al.*, 1974). The δD content of CH_4 emitted from biomass burning has been estimated to be -90‰ from a single laboratory experiment (Whiticar, 1993, personal communication) and -10 to -50‰, assuming no fractionation during combustion as is the case for ^{13}C (Wahlen, 1993).

This work presents the results of the first measurements of the δD of CH_4 emitted during biomass burning from both laboratory combustion experiments and biomass fires in the Brazilian Amazon. Concurrent determinations of the δD and $\delta^{13}C$ composition of CH_4 emitted from biomass burning and of the fuel biomass are presented. The hydrogen isotope fractionation during biomass combustion is estimated. The implications of these results for the global atmospheric CH_4 δD budget are discussed.

METHODS

Laboratory Combustion Experiments

Two experimental fires were conducted in the large-scale combustion laboratory at the United States Department of Agriculture Forest Service (USFS) Fire Sciences Laboratory in Missoula, Montana during March, 1995. The combustion laboratory consisted of a large room (12 m x 12 m x 20 m; L x W x H) with a 1.5 m diameter exhaust stack opening into a 3.6 m diameter inverted funnel above the fuel bed. Sampling ports in the exhaust stack were located at an observation platform 15 m above the fuel bed (Griffith *et al.*, 1991; Yokelson *et al.*, 1996). The fuel for both fires was dried pine needles (*Pinus ponderosa*) collected near Missoula. Concentrations of CO_2, CO and total hydrocarbons were continuously monitored during combustion experiments via infrared spectroscopy and thermal detection. Grab samples of smoke were collected for isotopic analysis of CH_4 through 1/4" OD copper tubing and a 15 μm filter (Nupro Company, Willoughby, OH) and

compressed to 40-60 psig into ~33 L stainless-steel canisters (General Container Corp., Somerset, NJ) using an aluminum/neoprene diaphragm pump (KNF Neuberger, Trenton, NJ). Smoke samples were collected from flaming and smoldering phases of both fires, determined both visually and by smoke total hydrocarbon (THC) content. The flaming phase was maintained for the twenty minutes required for sample collection by frequent re-supply of pine needles to the fuel bed. Samples were collected from the smoldering phase when THC concentration exceeded 9 ppm. A background air sample was collected through the exhaust stack sampling ports before the first burning experiment. During sample collection from the flaming phase of the second burning experiment, a duplicate large volume (~900 L) smoke sample was cryogenically collected into a 30 L high pressure aluminum cylinder (Airco, City of Industry, CA) frozen in liquid nitrogen. This sample was dried using silica gel. A 25 minute collection resulted in a final sample pressure of ~400 psig.

Field Studies

The isotopic characterization of CH_4 emissions reported here were part of a large scale investigation of biomass burning in the Amazon region, a NASA-funded study entitled Smoke Clouds Aerosols and Radiation - Brazil (SCAR-B) (*J. Geophys. Res.*, special issue, in press). Three Brazilian fires were sampled in early September, 1995. The field sites were located near the small town of Jamari (~9°12′ S, 60°3′W) in the state of Rondônia, a Amazonian region that is undergoing rapid deforestation (Skole and Tucker, 1993;

Fearnside, 1992). The study sites were located on small farms where subsistence landowners had planned fires to clear their land and are representative of the land use in Rondônia. Smoke samples were collected from one fire on a 6.9 ha cattle pasture and two on sites where primary forest was being cleared for crops. The two forest sites of 1.5 and 3.4 ha are referred to using the names of the landowners, Balteke and Sergipe, respectively, for consistency with other studies at these sites (Guild *et al.*, in press). The mean annual temperature, precipitation and relative humidity of the region (determined at Porto Velho, Rondônia, ~100 km to the NW) are 25.2°C, 2354 mm and 85%, respectively. A distinct dry season occurs from June to September with precipitation during these months generally < 100 mm (Departamento Nacional de Meteorologia, Brasil, 1992).

The understory and trees of the forested sites had been cut at the onset of the dry season and the slash left to dry for 2-3 months until burning occurred near the end of the dry season. These sites were burned using circle-fire ignition patterns, wherein the perimeter was ignited and the fire burned towards the center. The pasture fire was ignited along the windward edge. All fires were ignited at mid-day, the time with the highest ambient temperatures and the lowest relative humidity. Fire characteristics, biomass distributions and nutrient cycling at these sites have been described in detail by Guild *et al.* (in press).

Smoke samples were collected for isotopic analysis of CH_4 by means of a computer-controlled fire atmosphere sampling system that continuously measured *in situ* temperature, wind velocity, and concentrations of CO_2 and

CO from towers located within the area burned (Susott *et al.*, 1991; Ward *et al.*, 1992; Hao *et al.*, 1996). Samples were drawn from a height of 8 m (pasture fire) and 14 m (forest fires) through a stainless-steel inlet line and two 15 μm stainless-steel filters (Nupro Company, Willoughby, OH) and compressed into ~33 L sample canisters by a pump buried below ground at the base of the sampling tower. Sample collection was timed to coincide with either the rapid initial flaming phase of combustion, for the pasture fire and sample #1 from the Balteke slash fire, or the subsequent mixed/smoldering phase, for the Sergipe slash fire and sample #2 from the Balteke fire. Ambient air samples were collected before the two forest fires.

Prior to the fires, biomass samples were collected for isotopic analysis of the fuel. Samples of dead grass were collected from the pasture site. Dead grass comprised about 40% by weight of the biomass combusted in the pasture fire with the remaining combusted biomass being residual wood debris from the forest originally occupying the site (Guild *et al.*, in press). Combustion of grass likely dominated carbon emissions during the flaming phase (Ward *et al.*, 1996) when the smoke sample was collected. At the Sergipe forest site, samples of wood were collected from downed logs > 20.5 cm in diameter, which accounted for ~42% of the mass of above-ground biomass combusted in this fire (Guild *et al.*, in press). Large diameter logs contribute more to gas emissions during the smoldering phase of a fire when most of the CH_4 is produced (Ward *et al.*, 1992). Fuel samples were air-dried for several days following collection and stored in sealed plastic bags until analysis.

Sample Analysis

Trace Gas Concentration

Concentrations of CO_2, CO, CH_4, C_2H_6, C_2H_4, C_2H_2, C_3H_8, C_3H_6 and C_3H_4 in canister samples were analyzed at the Fire Sciences Laboratory by gas chromatography (GC) as described by Hao *et al.* (1996). Detection limits were 1 ppm for CO_2, 0.2 ppm for CO and 10 ppb for hydrocarbons; analysis precision was ± 2% for CO_2, CO and CH_4, ± 5% for C2 compounds and ± 10% for C3 compounds. Storage tests on the large volume smoke sample collected during the laboratory combustion experiments showed that concentrations of identified hydrocarbons did not change for 8 months. Samples were analyzed for trace gas concentrations within two months of being collected and within four months for CH_4 isotopic composition.

Isotopic Analysis of CH_4 in Air Samples

The preparation of samples for $^{13}C/^{12}C$ and D/H analysis of CH_4 in air used during this study was identical to that described previously (Chapter Two), with the exception of the procedure for cryogenic collection of the H_2O derived from CH_4 combustion and its subsequent reduction to H_2. The complete sample preparation procedure used is described below. Although this procedure was developed for clean-air samples with near ambient concentrations of CH_4 and other trace gases, laboratory tests described below indicate that it is appropriate for the preparation of samples collected from biomass burning.

The sample preparation procedure used a high vacuum extraction system with cryogenic collection of CO_2 and H_2O from combusted CH_4, following the standard method described by Stevens and Rust (1982). The concentration procedures necessary for D/H determinations have been described by Wahlen *et al.* (1989) and Alei *et al.* (1987). The air sample was pulled through a 'Russian doll' trap at -196°C on a vacuum extraction line to remove CO_2, H_2O, N_2O and some nonmethane hydrocarbons (Brenninkmeijer, 1991), and then through a trap containing 100g charcoal (SK-4 Carbon, 40/60 mesh, Alltech Associates, Inc., Deerfield, IL) at -196°C to concentrate the CH_4. Pressure was maintained at 1/3 atmosphere or less to minimize condensation of O_2. The charcoal trap was warmed to -80°C using a dry ice/isopropanol slush while pumping to remove trapped gases such as N_2 and O_2, while retaining CH_4. The charcoal trap was then transferred to a second high vacuum extraction line where it was heated to 100°C and purged with hydrocarbon-free ultrapure air (< 0.01 ppm as methane, Scott Marrin Inc., Riverside, CA) to liberate the CH_4. The emitted gas flowed through a series of three traps at -196°C to freeze out any CO_2 and H_2O in the carrier gas and through a bed of Schütze reagent (LECO Chemical, St. Joseph, MI), quantitatively oxidizing CO to CO_2 (Smiley, 1949) which, along with the resultant H_2O, was trapped at -196°C. The CH_4 in the gas stream was then oxidized to CO_2 and H_2O, by flowing over platinized quartz wool (Shimadzu Scientific Instruments, Inc., Columbia, MD) at ~730°C, and the resultant gases trapped in a pyrex U-tube containing 150 mg zinc shot (BDH Ltd., Poole, England) at -196°C. The CO_2 was cryogenically distilled from the H_2O at -80°C

using a dry-ice/isopropanol slush transfer, and measured manometrically before mass spectrometric analysis. The U-tube containing the H_2O was flame-sealed and heated at 460°C for 36 minutes to reduce H_2O to H_2 (Tanweer *et al.*, 1988; Coleman *et al.*, 1982; Kendall and Coplen, 1985) for mass spectrometric analysis.

Measurements of $^{13}C/^{12}C$ and D/H were made on a Finnigan MAT 251 isotope-ratio mass spectrometer and results reported in customary δ notation: δ (‰) = $(R_{sample}/R_{standard} - 1)\cdot 1000$, where R = $^{13}C/^{12}C$ or D/H. Gas standards for $\delta^{13}C$ were calibrated against NBS-19, $\delta^{13}C$ = +1.95‰ vs. V-PDB. δD measurements were scale-corrected such that H_2 derived from H_2O standards V-SMOW and SLAP yielded δD values of 0‰ and -428‰, respectively. All $\delta^{13}C$ and δD measurements reported here are referenced to V-PDB and V-SMOW, respectively.

The δD analysis of CH_4 requires about 100 liters of air containing CH_4 at ambient concentrations, yielding ~400 µl H_2O and ~200 µl CO_2. For CO_2, typical extraction blanks and yields were ~0.3 µl CO_2 (n=17) and 101 ± 1% (n=6). At the time of this study, the technique for measuring H_2O blanks and yields had not been developed. Typical H_2O blanks and yields have subsequently been determined to be ~14 µl (n=15) and 102 ± 2‰ (n=20), respectively, by manometric measurement of the H_2. The precision of this method was ± 3.1‰ for δD (n=15) and ± 0.15‰ for $\delta^{13}C$ (n=18) from three laboratory standards of pure CH_4 diluted in ultrapure air analyzed during this study. The accuracy of the method has been tested by comparing the δD and $\delta^{13}C$ of laboratory standards, described above, to the δD and $\delta^{13}C$ of pure CH_4

combusted in sealed tubes. The sealed tube method yielded $\delta D = -137.8 \pm 4.0‰$ (n=4) and $\delta^{13}C = -31.74 \pm 0.13‰$ (n=10) for pure CH_4. The air sample extraction method yielded $\delta D = -135.0 \pm 2.7‰$ (n=19) and $\delta^{13}C = -31.88 \pm 0.16‰$ (n=20) for the CH_4 standards prepared in ultrapure air. All uncertainties are $\pm 1\sigma$.

The applicability of this sample preparation procedure to isotopic analysis of CH_4 in smoke samples, which contain concentrations of CO, CH_4, and nonmethane hydrocarbons (NMHCs) significantly above ambient levels, depends on its ability to efficiently extract CH_4 from samples with high CH_4 concentrations and to exclude other C- and H- containing species.

The efficiency of the sample preparation procedure at extracting CH_4 from air samples with significantly elevated CH_4 concentrations was tested using a 29.6 ppm CH_4 standard prepared by dilution of pure CH_4 in ultrapure air. The δD and $\delta^{13}C$ of this standard, $-144.7 \pm 1.3‰$ and $-32.02 \pm 0.22‰$, respectively, were indistinguishable from the δD and $\delta^{13}C$ of a 1.94 ppm standard prepared by dilution of the same pure CH_4, *i.e.*, $-142.4 \pm 0.1‰$ and $-31.51 \pm 0.02‰$, respectively (n=2).

The ability of the sample extraction/combustion procedure to exclude C_2H_6, CO and H_2 from the combustion step was tested using high concentration standards which were prepared by diluting the pure gas of interest in ultrapure air. Separate extractions of a 32 ppm ethane standard and of a 123 ppm CO standard had CO_2 recoveries equal to typical CO_2 blanks and < 0.2% (n=2) and < 0.05% (n=2) of the carbon contained in the original standards, respectively. Molecular hydrogen, although not measured in the

smoke samples in this study, is another potential contaminant of the δD-CH_4 analysis. Hydrogen concentrations up to ~17 ppm have been measured in smoke from biomass burning (Cofer *et al.*, 1990), compared to typical ambient concentrations of ~0.5 ppm (Khalil and Rasmussen, 1989b). Extractions of a 2.15 ppm CH_4 standard with δD = -140.7‰ containing 43.6 ppm H_2 with δD = -351.8‰ yielded a $\delta D = -140.1 \pm 0.8$‰ (n=3). These results indicate that the sample extraction/combustion procedure excludes C_2H_6, CO and H_2 from the combustion products, even at high concentrations.

The ability of the sample preparation procedure to extract only CH_4 and exclude the full suite of NMHCs contained in the smoke samples was tested by concentration and extraction (but not combustion) of a smoke sample, followed by GC analysis of the extracted gases. Smoke from the large volume sample collected in the laboratory combustion experiment was concentrated onto charcoal as a clean-air sample, and extracted from the charcoal (by heating to 100°C and purging as usual) directly into an evacuated canister. The canister was then pressurized with ultrapure air for GC analysis. The concentration of extracted CH_4, after re-dilution, was greater than or equal to its concentration in the original sample. In contrast, the concentrations of all NMHCs were below the GC detection limit of 0.01 ppm (n=3 extractions), significantly less than the NMHC concentrations in the original sample (0.13-0.77 ppm for the C2 hydrocarbons, Table 3.1). These results indicated that the C2 and C3 compounds were excluded by the sample preparation procedure, presumably being removed by the Russian doll trap. Other typical components of smoke, such as C4-C6 hydrocarbons, aromatic compounds and

other unoxidized pyrolysis products (Hao *et al.*, 1996; Yokelson *et al.*, 1996) have lower vapor pressures than the compounds tested and are therefore also assumed to be removed by the Russian doll trap.

These tests indicate that the sample preparation procedure developed for clean-air samples is capable of extracting all of the CH_4 from smoke samples and that the CO_2 and H_2O used for isotopic analysis of CH_4 is derived exclusively from the CH_4, *i.e.*, not from any of the other C- or H-containing trace gas constituents of smoke.

Isotopic Analysis of Biomass Samples

The sample preparation procedure for $^{13}C/^{12}C$ and D/H analysis of bulk biomass involved sealed tube combustion of biomass followed by cryogenic separation of the resultant CO_2 and H_2O. Analysis of the pine needles used in the laboratory combustion experiment was performed on individual slices of needles. The wood and dead grass samples collected in Brazil were both homogenized before analysis by grinding to a fine powder using a Wiley Mill (mesh size = 0.5 mm); individual slices of wood samples were also analyzed. Biomass samples (4-6 mg) were combusted in evacuated and sealed Vycor ampoules at 900°C for 1.5 hours using ~300 mg CuO as the oxidant. The resultant CO_2 and H_2O were separated using a small high vacuum extraction system heated to ~110°C. The sample ampoule was scored and inserted into a flexible stainless-steel tube (Cajon, Macedonia, Ohio) on the extraction line, and the line heated to ~110°C for at least two hours while pumping to remove any residual H_2O. The sample ampoule was then broken and the CO_2

and H_2O collected at -196°C in an ampoule containing 150 mg zinc shot, during heating of the stainless-steel tubing and glass manifold. The ampoule containing CO_2 and H_2O was warmed to -80°C using an isopropanol/dry ice slush and the CO_2 was transferred to a sample bottle for mass spectrometric analysis. The ampoule containing the H_2O was refrozen at -196°C, flame-sealed, and prepared for mass spectrometric analysis as described above.

The Brazilian biomass samples were analyzed using a different batch of zinc reagent (Biogeochemical Laboratories, Indiana University) which required slightly different preparation. Before use, 40 ± 1 mg zinc reagent (turnings) were activated in the evacuated ampoule by heating at 350°C for 5 minutes under vacuum. Flame-sealed ampoules containing H_2O and zinc were heated at 500°C for 30 minutes to reduce the H_2O to H_2 for mass spectrometric analysis.

The precision of the biomass combustion procedure was ± 5.7‰ for δD (n=14) and ± 0.14‰ for $\delta^{13}C$ (n=15), determined from repeat determinations of two samples of homogenized biomass. Blanks were ~21 µl H_2O and ~3 µl CO_2, *i.e.*, < 1% typical sample size (2-3 ml each H_2O and CO_2). The accuracy of the procedure was tested by analysis of NIST Intercomparison Reference Material PEF1, a polyethylene foil with a reported isotopic composition of δD = -100.3 ± 2.0‰ and $\delta^{13}C$ = -31.77 ± 0.08‰ (n=6 laboratories; Hut, 1987). Sealed tube combustion of PEF1 yielded δD = -86.9 ± 4.1‰ and $\delta^{13}C$ = -31.86 ± 0.17‰ (n=7). The values reported here for the δD of bulk biomass have been adjusted by -13.4‰ to account for this offset.

RESULTS

The ambient air samples collected prior to the laboratory combustion experiments and the Sergipe fire in Brazil had typical background-air concentrations for CO_2, CO and CH_4, of ~380 ppm, < 1 ppm and ~1.8 ppm, respectively (Table 3.1). The δD and $\delta^{13}C$ of CH_4 in these two samples, *i.e.*, -82.4‰ and -47.53‰, and -85.5‰ and -46.76‰, respectively, are also typical of background air. The global average δD and $\delta^{13}C$ for CH_4 in clean air are -88.1 ± 1.2‰ and -47.33 ± 0.04‰, respectively (see Chapter Four and Quay *et al.*, in press).

The background air sample collected before the Balteke fire in Brazil had elevated concentrations of CO_2, CO and CH_4 of 415 ppm, 3.93 ppm and 2.260 ppm, respectively. The δD and $\delta^{13}C$ of the CH_4 in this sample were -108.1‰ and -44.25‰, respectively. The elevated concentrations of C-containing compounds, coupled with the δD depletion and $\delta^{13}C$ enrichment of CH_4 in this sample, indicate the contribution of CH_4 from biomass burning emissions, as discussed below.

The smoke samples collected from the laboratory and field fires had CH_4 concentrations 2-20 times ambient levels. The concentrations of the primary combustion products, CO_2 and CO, and of the suite of NMHCs measured (C_2H_6, C_2H_4, C_2H_2, C_3H_8, C_3H_6 and C_3H_4) were all elevated above ambient concentrations in all smoke samples. The combustion efficiency associated with the smoke samples, defined here as the ratio of emitted CO_2 to the sum of emitted CO and CO_2, ranged from 93 to 99% for the samples collected during flaming phases, and from 81 to 86% for the samples collected

Table 3.1 The methane concentration and isotopic composition and trace gas composition of ambient air (background) and smoke samples collected from large-scale laboratory combustion experiments and Brazilian fires.

	δD (‰ vs. SMOW)	δ¹³C (‰ vs. PDB)	[CO_2] (ppm)	[CO] (ppm)	[CH_4] (ppm)	[C_2H_4] (ppm)	[C_2H_2] (ppm)	[C_2H_6] (ppm)	[C_3H_8] (ppm)	[C_3H_6] (ppm)	[C_4H_6] (ppm)	combustion efficiency[a]: [CO_2]/([CO]+[CO_2])
Montana Laboratory Experiments												
Fire #1												
background	-82.4	-47.53	381	0.2	1.805							
flaming[b]	-205.9	-33.49	5970	87.7	6.465	1.12	0.29	0.31	0.32	0.06	0.03	98.5%
smoldering[b]	-205.9	-31.45	1550	193.05	11.905	0.25	0.04	0.29	0.09	0.05		85.8%
Fire #2												
flaming,[b] sample 1	-208.3	-32.75	7610	92.55	7.165	1.42	0.41	0.36	0.38	0.08	0.04	98.7%
flaming,[b] sample 2[c]	-196.9	-34.39	4135	59.5	5.340	0.77	0.13	0.22		0.05		98.4%
smoldering[b]	-213.1	-31.41	1665	230	14.020	0.38	0.05	0.52	0.20	0.11		84.8%
Brazil Field Experiments												
Pasture Fire												
flaming	-161.8	-30.05	1177	65.7	4.970	0.70	0.17	0.22	0.20	0.06	0.02	92.5%
Balteke Primary Forest Slash Fire												
background	-108.1	-44.25	415	3.93	2.260	0.04	0.04	0.02				
flaming	-184.1	-31.01	2402	158.8	18.200	2.26	0.51	0.19	0.70	0.20	0.08	92.8%
smoldering	-193.4	-32.78	1047	118.2	14.190	0.96	0.16	0.87	0.42	0.18	0.03	84.7%
Sergipe Primary Forest Slash Fire												
background	-85.5	-46.76	367	0.72	1.780							
smoldering	-224.9	-27.81	1614	294.9	37.700	9.65	0.39	3.60	5.70	1.18	0.13	80.9%

a. Combustion efficiency is calculated from concentrations of emitted CO_2 and CO.

b. Fire phase was defined by visual examination of fire conditions in laboratory experiments.

c. Large volume sample collected by cryogenic concentration (see text).

during smoldering or mixed phases of combustion (Table 3.1). In the laboratory experiments, CH_4 concentrations were significantly elevated in the samples collected from the smoldering phases of combustion, at 11.91 to 14.02 ppm, versus those collected from the flaming phases, with concentrations of 5.34 to 7.17 ppm. In the Brazilian fires, the sample collected from the fire with the lowest combustion efficiency, 80.9%, exhibited the highest CH_4 concentration, *i.e.*, 37.70 ppm.

The δD and $\delta^{13}C$ of CH_4 in the biomass burning samples ranged from -196.9 to -213.1‰ and -31.41 to -34.39‰, respectively, for the laboratory experiments and from -161.8 to -224.9‰ and -27.81 to -32.78‰, respectively, for the fires in Brazil (Table 3.1). These δD and $\delta^{13}C$ values represent a 74 to 137‰ depletion in δD and 12.9 to 19.5‰ enrichment in $\delta^{13}C$ relative to the global mean isotopic composition of atmospheric CH_4.

The sealed tube combustion of the pine needles used as fuel in the laboratory combustion experiments yielded $\delta D = -127.1 \pm 17.1\%$ and $\delta^{13}C = -25.83 \pm 1.27‰$ (n=12) (Table 3.2). The dead grass and wood collected from the Brazilian field sites had $\delta D = -109.7 \pm 5.6\%$ and $-61.0 \pm 5.7‰$ and $\delta^{13}C = -12.45 \pm 0.17‰$ and $-30.42 \pm 0.12‰$, respectively. The large spread in the isotopic measurements for the pine needles, which were analyzed when a mill was unavailable, likely resulted from each determination being made using individual pieces of needles instead of a homogenized sample. This explanation was supported by a comparison of determinations of the isotopic composition of Brazilian wood using individual wood pieces, $\delta D = -55.6 \pm$

Table 3.2 The δD and $\delta^{13}C$ of fuel biomass from laboratory and field combustion studies determined from sealed tube combustion of dried samples.

Sample	δD (‰ vs. SMOW)	±1σ (‰)	n	$\delta^{13}C$ (‰ vs. PDB)	±1σ (‰)	n
Montana Biomass						
Pine Needles[a]	-127.1	17.1	12	-25.83	1.27	12
Brazilian Biomass						
Brown Grass[b]	-109.7	5.6	7	-12.45	0.17	7
Wood[b]	-61.0	5.7	7	-30.42	0.12	8
Wood[a]	-55.6	10.9	5	-29.64	1.55	5

a. Samples were not homogenized before analysis; each determination was made on an individual piece of sample.

b. Samples were homogenized using a Wiley mill prior to analysis.

10.9‰ and $\delta^{13}C$ = -29.64 ± 1.55‰, and using the ground wood, δD = -61.0 ± 5.7‰ and $\delta^{13}C$ = -30.42 ± 0.12‰ (Table 3.2).

DISCUSSION

Isotopic Signature of Methane Emitted from Biomass Burning

The isotopic composition of CH_4 produced from biomass burning ($\delta_{CH4(bb)}$) was determined from the isotopic composition of CH_4 in smoke samples by correction for background CH_4 as follows:

$$\delta_{CH_4(bb)} = \frac{C_{SM} \cdot \delta_{SM} - C_{BG} \cdot \delta_{BG}}{C_{SM} - C_{BG}} \qquad (1)$$

where δ is the δD or $\delta^{13}C$ isotopic composition, C represents CH_4 concentration and the subscripts SM, and BG refer to the smoke and background (ambient) samples, respectively.

Laboratory Combustion Experiments

The δD and $\delta^{13}C$ of the CH_4 emitted during burning in the laboratory experiments ranged from -255.3 to -228.0‰ and from -29.02 to -27.68‰, respectively (Table 3.3). The ± 1σ uncertainties in the calculated values of $\delta D_{CH4(bb)}$ and $\delta^{13}C_{CH4(bb)}$ resulting from the analytical uncertainty in the measurements of CH_4 concentration and isotopic composition in both the background air and smoke samples were 3.8-5.5‰ and 0.2-0.4‰, respectively (Table 3.3).

Table 3.3 The δD and $\delta^{13}C$ content of methane emitted from biomass burning in laboratory and field studies and the apparent kinetic isotope effects associated with combustion.

Sample	δD (‰ vs. SMOW)	±1σ[a] (‰)	ε^{D}_{burn}[b] (‰)	$\delta^{13}C$ (‰ vs. PDB)	±1σ[a] (‰)	ε^{C}_{burn}[b] (‰)
Laboratory Combustion Experiments						
Fire #1						
flaming	-253.8	4.8	-145	-28.04	0.30	-2
smoldering	-228.0	3.8	-116	-28.58	0.20	-3
Fire #2						
flaming (spl1)	-250.8	4.6	-142	-27.77	0.28	-2
flaming (spl 2)	-255.3	5.5	-147	-27.68	0.37	-2
smoldering	-232.4	3.6	-121	-29.02	0.19	-3
Brazil Field Studies						
Pasture Fire						
flaming[c]	-205.5	4.3	-127	-19.46	0.42	---[e]
Balteke Primary Forest Slash Fire						
flaming	-194.9	3.6	-143	-29.13	0.18	1
smoldering	-209.5	3.8	-158	-30.61	0.19	0
Sergipe Primary Forest Slash Fire						
smoldering	-231.8	3.3	-182	-26.87	0.16	4

a. Uncertainties (± 1σ) were calculated by propagating the analytical uncertainty in the measurements of CH_4 concentration and isotopic composition through the calculation of the isotopic content of emitted CH_4.
b. The apparent kinetic isotope effect associated with combustion = $\varepsilon_{burn} = (R_{CH4}/R_{BIO}-1)*1000$; where R = D/H or $^{13}C/^{12}C$.
c. Calculations for this fire are an average of separate calculations using the CH_4 concentration and isotopic composition of the ambient samples collected before the subsequent forest slash fires; no ambient sample was collected on the day of the pasture fire.
d. Calculated using a δD of fuel biomass of -90.2‰ derived from the 60:40 C4:C3 fuel mixture implied by the $\delta^{13}C$ results, see text.
e. Not calculated. The $\delta^{13}C$ of CH_4 emitted from this fire was used to determine the relative contribution of combustion of C3 and C4 biomass to CH_4 emissions.

The δD of CH_4 produced during the flaming phase was ~23‰ more depleted than CH_4 produced during the smoldering phase. This result may reflect either the expression of different isotopic fractionations during different combustion phases, preferential combustion of different biomass components (with different δD compositions) during different combustion phases, or a reservoir enrichment effect as combustion progressed. The similarity of the results from the same combustion phase of the two laboratory fires indicates that the isotopic content of CH_4 emitted from a homogenous fuel under similar burning conditions is reproducible.

The mean isotopic composition of CH_4 emitted during combustion can be most accurately estimated by weighting the isotopic composition of CH_4 emitted during flaming and smoldering combustion by the amount of CH_4 emitted during each combustion phase. In general, more biomass consumption occurs during flaming combustion (Ward *et al.*, 1992; Yokelson *et al.*, 1997), but more CH_4 is produced per unit biomass combusted during the smoldering phase (Hao and Ward, 1993). The average isotopic composition of CH_4 emitted from a fire can be calculated as follows:

$$\overline{\delta_{CH_4}} = \frac{\beta_f \cdot EF_f \cdot \delta_f + \beta_s \cdot EF_s \cdot \delta_s}{\beta_f \cdot EF_f + \beta_s \cdot EF_s} \qquad (2)$$

where β represents the fraction of biomass combusted during each combustion phase, EF is the amount of CH_4 emitted per unit of biomass combusted, δ represents the measured isotopic composition of emitted CH_4 and the subscripts *f* and *s* indicate the flaming and smoldering phases, respectively. Assuming that ~80% of the pine needle biomass is combusted

during flaming combustion (Yokelson *et al.*, 1998), and that 4.6 and 132 moles of CH_4 are emitted per kilogram of pine needles combusted during the flaming and smoldering phases of combustion, respectively (Yokelson *et al.*, 1998), yields an estimate for the average isotopic composition of CH_4 emitted during pine needle combustion of $\delta D = -233 \pm 2‰$ and $\delta^{13}C = -28.7 \pm 0.2‰$. The calculated uncertainties assume no uncertainty in the weighting factors.

Brazilian Fires

The CH_4 emitted during the Brazilian pasture fire had $\delta D = -205.5‰$ and $\delta^{13}C = -19.46‰$. These values were calculated using the average isotopic composition of the two background samples collected before the primary forest fires since no ambient sample was collected on the day of the pasture fire. In the Brazilian primary forest fires, the δD and $\delta^{13}C$ of emitted CH_4 ranged from -231.8 to -194.9‰ and from -30.61 to -26.87‰, respectively (Table 3.3).

Another estimate of the δD and $\delta^{13}C$ of CH_4 emitted from biomass burning in Brazil can be derived using the two background air samples. The elevated CO_2, CO and hydrocarbon concentrations, and the δD depletion and $\delta^{13}C$ enrichment of the CH_4 in the background sample collected before the Balteke fire indicates that that sample contained a significant proportion of emissions from the prevalent local burning occurring during the study period. Assuming that the difference in CH_4 concentration between the two background samples was due to CH_4 addition from biomass burning (*i.e.*, using equation (1)) yields a δD and $\delta^{13}C$ for CH_4 emitted during biomass

burning of -192.1 ± 21.7‰ and -34.94 ± 1.53‰, respectively. These results are similar to those obtained from the direct smoke measurements.

Emitted CH_4 most depleted in δD was observed during the smoldering phase of the primary forest fire. The relative enrichment observed during flaming combustion may reflect CH_4 production from combustion of fine fuels, *e.g.*, leaves, which are likely to be more enriched in δD than bulk biomass (Wershaw *et al.*, 1966; Leaney *et al.*, 1985). The total range of $\delta D_{CH4(bb)}$ observed for the fires in Brazil was ~37‰, similar to that observed in the controlled laboratory experiments. This similarity suggests that within a single tropical region, the δD of CH_4 emitted from different fires, each with a complex combination of fire processes (flaming/smoldering) and fuel types, is fairly invariant.

The mean isotopic composition of CH_4 emitted in the Brazilian fires was therefore estimated by an unweighted mean of the individual measurements. The mean $\delta D_{CH4(bb)}$ was -210.4 ± 15.5‰ (n=4). The mean $\delta^{13}C_{CH4(bb)}$ was -28.87 ± 1.88‰ in the primary forest slash fires (n=3) and -19.46 ± 0.42‰ for the pasture fire (n=1). These are the first systematic experimental determinations of $\delta D_{CH4(bb)}$. They indicate that CH_4 emitted from biomass burning is significantly more depleted in δD than previously estimated (Wahlen, 1993; Whiticar, 1993).

Fractionation Occurring During Combustion

The measured biomass $\delta^{13}C$ content was consistent with the $\delta^{13}C$ predicted from the plants' photosynthetic type. The $\delta^{13}C$ of both the pine

needles used in the laboratory combustion experiments and the wood collected from the Brazilian forest sites, $\delta^{13}C_{BIO}$ = -25.83 ± 1.27‰ and -30.42 ± 0.12‰ (Table 3.2), respectively, are consistent with typical $\delta^{13}C$ values for C3 plants, *i.e.*, -27.8 ± 2.8‰ (Troughton *et al.*, 1974). The $\delta^{13}C_{BIO}$ of -12.5 ± 0.2‰ for the grass collected from the Brazilian pasture (Table 3.2) is consistent with the range of $\delta^{13}C$ = -13.6 ± 1.6‰ reported for C4 plants (Troughton *et al.*, 1974).

Little or no fractionation of the carbon isotopes occurred during combustion. For both the laboratory experiments and the Brazilian forest fires, $\delta^{13}C_{CH4(bb)} \approx \delta^{13}C_{BIO}$. This result is consistent with previous findings that CH_4 emitted from biomass burning has the same $\delta^{13}C$ content as the organic material burned (Stevens and Engelkemeir, 1988; Wahlen *et al.*, 1989; Levin *et al.*, 1993). The $\delta^{13}C$ content of CH_4 emitted from the Brazilian pasture fire (-19.5‰) implies a fuel mix of ~60% C4 grasses with $\delta^{13}C$ = -12.5‰ and ~40% woody debris with $\delta^{13}C$ = -30.4‰ (Table 3.2). Pre- and post-fire biomass measurements indicated that the total biomass combusted in the pasture fire was 43 ± 33% C4 and 57 ± 33% C3 (Guild *et al.*, in press), *i.e.*, a slightly higher proportion of C3 plants than indicated by $\delta^{13}C_{CH4(bb)}$. During the initial flaming phase of the fire when the smoke sample was collected, however, a higher than average proportion of emissions would be expected to result from the highly combustible dead grass.

Plant δD content (δD_{BIO}) is not a distinctive marker of plant photosynthetic type as is $\delta^{13}C$. Rather, δD_{BIO} is generally related to the δD of environmental water (Schiegl and Vogel, 1970; Epstein *et al.*, 1976) but is also affected by the relative proportion of plant biochemical components

(cellulose, lignins, lipids, resins) which can have very different D/H ratios (Epstein *et al.*, 1976). The measured range of δD of -56‰ to -127‰ for the biomass samples is within the range of -20‰ to -140‰ observed for terrestrial plants (*e.g.*, Schiegl and Vogel, 1970; Epstein *et al.*, 1976; Sternberg and DeNiro, 1983).

In contrast to the situation for $\delta^{13}C$, a significant fractionation of the hydrogen isotopes occurred during the production of CH_4 from biomass combustion. The $\delta D_{CH4(bb)}$ was significantly depleted, by 110 to 180‰, compared to δD_{BIO}. The apparent D/H fractionation occurring during combustion, defined as ε^D_{burn} (‰) = $[(D/H)_{CH4}/(D/H)_{BIO}-1]\cdot 1000$, ranged from -116‰ to -147‰ in the laboratory combustion study (Table 3.3). For the Brazilian forest fires, ε^D_{burn} ranged from -143‰ to -182‰ (Table 3.3), assuming that the δD content of the biomass collected at the Sergipe site was representative of the fuel burned in the primary forest slash fires. The δD of the fuel mixture at the pasture site can be estimated to be -90.2‰, using the 60:40 C4:C3 ratio implied by the $\delta^{13}C$ results, δD(C4) = -109.7‰ and δD(C3) = -61.0‰ (Table 3.2). Using this estimate, ε^D_{burn} was -127‰ for the pasture fire.

Formation of CH_4 is a high temperature pyrolysis process which is thought to involve methyl radical abstraction of hydrogen from organic material (Edwards, 1974; Tillman, 1981). The negative D/H fractionation observed during production of CH_4 from biomass combustion may reflect the kinetic isotope effect involved in this step. Assuming that the three hydrogens of the methyl radical were transferred intact from the biomass source material, *i.e.*, with no isotopic fractionation, and that oxidative loss of

CH_4 and its associated isotopic fractionation were negligible in the combustion environment, the average isotopic composition of the abstracted (fourth) hydrogen can be estimated. For the laboratory experiments, where $\delta D_{CH4(bb)} \approx$ -244‰ and δD_{BIO} = -127‰, the δD of the fourth hydrogen ($\delta D_{(+)}$) would be -595‰, *i.e.*, $\delta D_{(+)} = 4 \cdot (-244‰) - 3 \cdot (-127‰)$, which represents a 468‰ depletion versus the biomass source material. For the Brazilian forest fires, the $\delta D_{CH4(bb)}$ of -210‰ and δD_{BIO} of -61‰ yield a $\delta D_{(+)}$ of -659‰, which is depleted by 598‰ compared to the biomass material. These calculated fractionations are comparable to fractionations observed during experimental studies of hydrocarbon production via pyrolysis of organic material (Sackett, 1978). Sackett (1978) estimated the hydrogen isotope fractionation during H loss from n-octadecane to be 560‰ and 680‰ during pyrolysis at 500°C and 400°C, respectively.

Application to the Global Methane Budget

Approximately 85% of the total CH_4 emitted from biomass burning is emitted in the tropics (Hao and Ward, 1993). The measurements of CH_4 emitted from burning of primary forest and a pasture in Brazil presented here, yield $\delta D_{CH4(bb)} = -210 \pm 16‰$. While these measurements were limited to a single tropical region, the relatively narrow range in $\delta D_{CH4(bb)}$ (~60‰) observed for laboratory and field fires with significantly different fire types, combustion efficiencies, fuel types and fuel δD content indicates that the global biomass burning source of CH_4 may have a relatively narrow δD range.

Assuming that biomass burning emits CH_4 with $\delta D \approx -210‰$, this CH_4 source is more enriched in δD than CH_4 emissions from bacterial production (in wetlands, rice paddies and ruminants) which have, on average, $\delta D = -318 \pm 18‰$, and CH_4 emissions from landfills, with $\delta D = -293 \pm 20‰$. In contrast, CH_4 release associated with fossil fuel production, with $\delta D = -175 \pm 10‰$, is more enriched in δD than the biomass burning source (Table 3.4 and references therein. See Chapter Four for a derivation of these values.). The CH_4 sources have also been shown to be categorized by $\delta^{13}C$ content. Biomass burning is the most ^{13}C enriched CH_4 source at $\delta^{13}C = -24 \pm 3‰$, followed by fossil CH_4 with $\delta^{13}C = -40 \pm 7‰$, and landfill CH_4 with $\delta^{13}C = -50 \pm 2‰$. Bacterial CH_4 is also most depleted in ^{13}C, with $\delta^{13}C = -61 \pm 3‰$ (Table 3.4).

The δD and $\delta^{13}C$ signatures of the major CH_4 sources can be combined to construct a mixing diagram for the global CH_4 source (Figure 3.1). This construct will be useful to compare the isotopic composition of the global CH_4 source estimated from the strength and isotopic composition of the individual CH_4 sources to that predicted from the measured isotopic composition of atmospheric CH_4 and the isotopic fractionations associated with removal of CH_4 from the atmosphere.

Recent CH_4 budget compilations (Hein *et al.*, 1997) indicate that approximately two-thirds of the total source of atmospheric CH_4 results from bacterial production in wetlands, ruminants and rice paddies. Methane emissions associated with fossil fuel production constitute ~18% of the total source, while biomass burning and landfills each contribute ~10%. Combining the strengths, δD and $\delta^{13}C$ of the bacterial, fossil, landfill and

Table 3.4 The mean strength and stable isotopic composition of methane sources and fractionations associated with methane sinks. Uncertainties are ± 1σ.

Source	Strength[1] ($Tg\ CH_4\ yr^{-1}$)	δD[2] (‰ vs. SMOW)	$\delta^{13}C$[3] (‰ vs. PDB)
Wetlands	232 ± 14	-321 ± 31	-60 ± 5
Rice Paddies	69 ± 12	-323 ± 19	-63 ± 5
Ruminants	90 ± 10	-305 ± 9	-60 ± 5
Landfills	40 ± 8	-293 ± 20	-50 ± 2
Fossil Fuel Prod.[a]	103 ± 8	-175 ± 10	-40 ± 7
Biomass Burning[b]	41 ± 6	-210 ± 15 [4]	-24 ± 3
Total Source	575 ± 24	-283 ± 13	-53.5 ± 2.6
Sink	**Strength[1]** ($Tg\ CH_4\ yr^{-1}$)	ε^{D} [5,c] (‰ vs. SMOW)	ε^{C} [6,c] (‰ vs. PDB)
Oxidation by OH	-469 ± 15	-160, -230, -250	-5.4, -9.9
Stratospheric Loss	-44 ± 4	-160	-12.4
Uptake by Soils	-28 ± 7	-81	-22.1
Total Sink	-541 ± 17	-158, -218, -236	-6.8, -10.7

[a] CH_4 emissions associated with fossil fuel production were assumed to be 35% coal gas and 65% natural gas, the latter with origin 80% thermogenic: 20% biogenic (Law and Nisbet, 1996; Gupta *et al.*, 1996; Hein *et al.*, 1997; Fung *et al.*, 1991; Rice and Claypool, 1981).

[b] The $\delta^{13}C$ content of CH_4 emissions from biomass burning was estimated assuming a global biomass fuel composition of 80% C3 plants: 20% C4 plants.

[c] Isotopic fractionations associated with CH_4 sinks are expressed here as ε (‰) = (*k/k - 1)·1000 where *k/k = the ratio of the rate constants for removal of isotopically heavy and light methane.

[1] Hein *et al.* (1997) (modified base scenario). [2] Wassman *et al.* (1992); Lansdown (1992); Kling *et al.* (1991); Burke *et al.* (1988, 1992); Burke and Sackett (1986); Levin *et al.* (1993); Wahlen *et al.* (1989, 1990); Woltemate *et al.* (1984); Martens *et al.* (1992); Bergamaschi (1997, 1998b); Liptay *et al.* (1998); Bergamaschi and Harris (1995); Schoell (1980); Rice and Claypool (1981); Ehhalt (1973). [3] Stevens and Engelkemeir (1988); Rust (1981); Quay *et al.* (1988); Tyler *et al.* (1988); Quay *et al.* (1991); Levin *et al.* (1993); Stevens (1993); Wahlen (1993); Tyler *et al.* (1994b); Gupta *et al.* (1996). [4] this work. [5] DeMore (1993); Gierczak *et al.* (1997); Xiao *et al.* (1993); Irion *et al.* (1996); Snover and Quay (in preparation.) [6] Cantrell *et al.* (1990); Gupta *et al.* (1997); Brennikmeijer *et al.* (1995); Sugawara *et al.* (1997); King *et al.* (1989); Tyler *et al.* (1994a); Reeburgh *et al.* (1997)

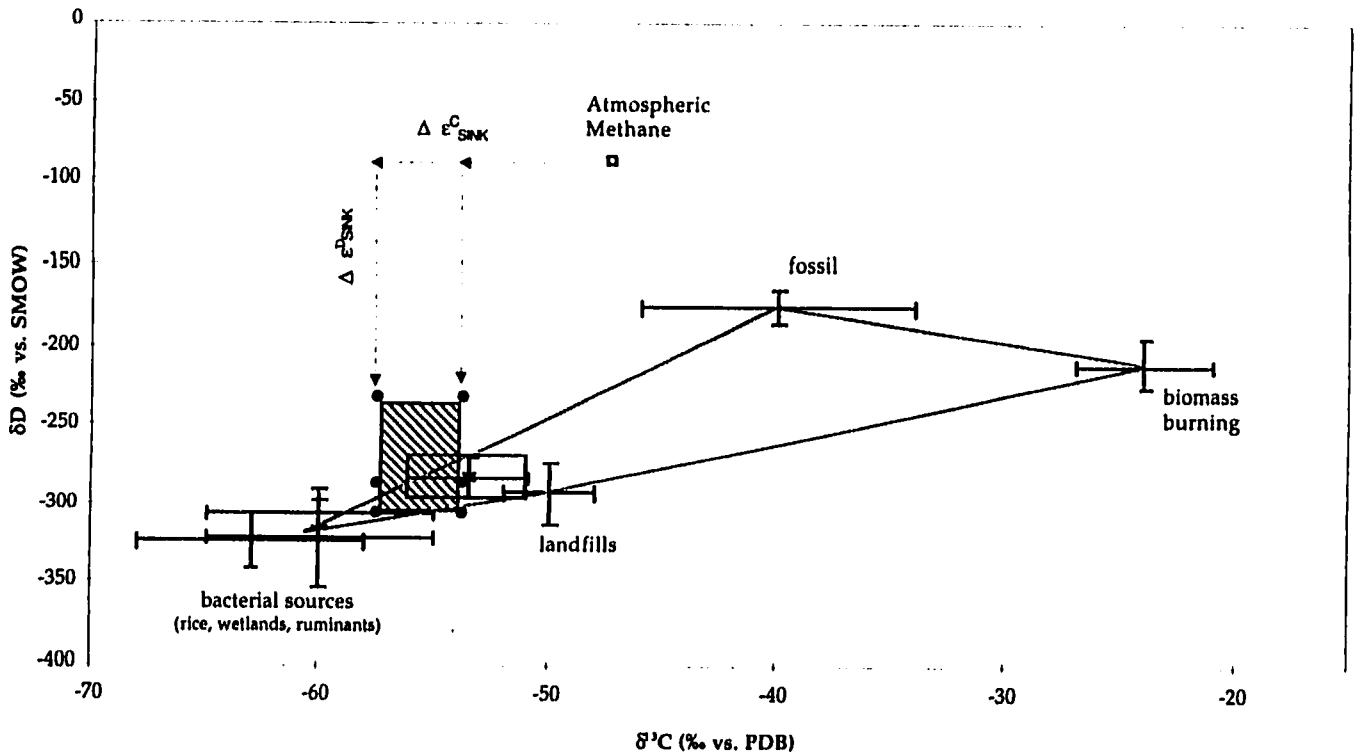

Figure 3.1 Mixing diagram for the global CH_4 source.
The δD and $\delta^{13}C$ of the major CH_4 sources define the possible combinations of δD and $\delta^{13}C$ isotopic composition for the global CH_4 source, *i.e.*, the outlined triangle (with δD = -318‰ and $\delta^{13}C$ = -61‰ for the mean biogenic source). Combining the strengths and isotopic compositions of the CH_4 sources results in a global CH_4 source with δD = -283 ± 13‰ and $\delta^{13}C$ = -53.5 ± 2.6‰ (bolded box). The δD and $\delta^{13}C$ of the global source can also be determined by adjusting the δD and $\delta^{13}C$ of atmospheric CH_4 (small rectangle) for the isotopic fractionations associated with CH_4 loss, $\Delta\varepsilon_{SINK}$, assuming steady-state. This yields the area depicted by the cross-hatched rectangle. The filled circles represent the isotopic composition of the CH_4 source derived in this manner using the hydrogen and carbon fractionations during CH_4 loss to OH determined by DeMore (1993), Gierczak *et al.* (1997) and Xiao *et al.* (1993) ($\Delta\varepsilon^D_{SINK}$ top to bottom) and Gupta *et al.* (1997) and Cantrell *et al.* (1990) ($\Delta\varepsilon^C_{SINK}$ left to right), respectively, in the calculation of $\Delta\varepsilon_{SINK}$.

biomass burning sources (Table 3.4) yields a δD of -283 ± 13‰ and $\delta^{13}C$ of -53.5 ± 2.6‰ for the global CH_4 source (Figure 3.1).

The δD and $\delta^{13}C$ of CH_4 removed from the atmosphere is equal to the δD and $\delta^{13}C$ of CH_4 inputs at steady state. Thus, the δD and $\delta^{13}C$ of the global CH_4 source can be calculated from the δD and $\delta^{13}C$ of atmospheric CH_4 by accounting for the kinetic isotope effects associated with the sinks of CH_4, assuming steady state. Given the non-steady state situation for CH_4 concentration, this balance is only approximately held.

Recent CH_4 budget compilations (Hein *et al.*, 1997) indicate that the major CH_4 sinks are oxidation by hydroxyl radicals (OH) (87%), removal in the stratosphere (8%) and oxidation by oxic soils (5%). Each sink process imparts a characteristic D/H and $^{13}C/^{12}C$ isotopic fractionation, leaving the residual atmospheric CH_4 enriched in the heavier isotope. Isotopic fractionations are expressed here in units of ‰, where ε (‰) = (*k/k - 1)·1000; *k/k is the ratio of rate constants for removal of isotopically heavy and light CH_4 by each sink process. The isotopic composition of CH_4 removed by each sink is approximately equal to the isotopic composition of atmospheric CH_4 plus the fractionation (ε) associated with that sink. The D/H fractionation occurring during reaction with OH at 277 K has been determined experimentally to be -160‰ (DeMore, 1993) and -230‰ (Gierczak *et al.*, 1997) and calculated theoretically as -255‰ (Xiao *et al.*, 1993). These values have been adjusted to the tropospheric mean temperature, 277 K, using the temperature-dependence presented by each author. However, only the determination by Gierczak *et al.* (1997) was made at temperatures relevant to the troposphere,

i.e., below 298 K. The hydrogen isotope fractionation occurring during uptake of CH_4 by soils has been measured at -81‰ (Snover and Quay, in preparation) and during CH_4 loss in the stratosphere at -160‰ (Irion *et al.*, 1996). The $^{13}C/^{12}C$ fractionation occurring during reaction with OH was determined experimentally at -5.4‰ (Cantrell *et al.*, 1990) and calculated theoretically at -9.9‰ (Gupta *et al.*, 1997). The carbon isotope fractionation during removal by soils has been measured at -22‰ (King *et al.*, 1989; Tyler *et al.*, 1994; Reeburgh, 1997) and during stratospheric loss at -12.4‰ (Brenninkmeijer *et al.*, 1995; Sugawara *et al.*, 1997). The overall fractionation effect during loss of atmospheric CH_4 can be calculated by weighting the individual fractionation effects by the relative sink strengths (Table 3.4). The overall hydrogen and carbon fractionations associated with CH_4 loss are ε^D_{SINK} = -160‰ to -240‰ and ε^C_{SINK} = -6.8‰ to -10.7‰, respectively, depending on the assumed values for the fractionations during loss to OH.

The mean isotopic composition of atmospheric CH_4 was δD = -88‰ and $\delta^{13}C$ = -47.3‰ during 1989-1995 (see Chapter 4 and Quay *et al.*, in press). Combining the δD and $\delta^{13}C$ of atmospheric CH_4 with the fractionation effects associated with CH_4 loss yields a δD and $\delta^{13}C$ for the CH_4 sink of -230 to -306‰ and -53.8 to -57.5‰, respectively. These values yield an estimate of the δD and $\delta^{13}C$ of the global CH_4 source, assuming steady state (Figure 3.1).

This estimate for the isotopic composition of the global CH_4 source, derived from the isotopic composition of atmospheric CH_4 and the fractionation effects during CH_4 loss, agrees well with that estimated from the individual source strengths and isotopic composition (Figure 3.1). This

simple comparison only approximates the global CH_4 budget as it does not account for the non-steady state situation for CH_4 concentration, nor any possible non-steady state conditions for atmospheric δD or $\delta^{13}C$. Nor does this analysis account for other factors, such as the spatial distribution of CH_4 sinks and sources, which also affect the isotopic composition of atmospheric CH_4 (Gupta *et al.*, 1996). This analysis is useful to illustrate that, within uncertainties, there is good agreement between the isotopic composition of the global CH_4 source derived from (1) the flux-weighted sum of the isotopic compositions of the individual CH_4 sources, using current estimates of relative source strengths and the experimental determination of $\delta D_{CH4(bb)}$ presented here, and (2) the δD and $\delta^{13}C$ of atmospheric CH_4 and the fractionation effects associated with CH_4 loss.

The smaller uncertainty associated with both the δD and $\delta^{13}C$ estimates for the global CH_4 source compared to the δD and $\delta^{13}C$ of the global CH_4 sink suggests that the source δD and $\delta^{13}C$ estimates can be used to constrain ε^{D}_{SINK} and ε^{C}_{SINK} (see Figure 3.1). The D/H fractionation associated with CH_4 loss to oxidation by OH presents the largest current source of uncertainty in determining ε^{D}_{SINK}. Current estimates of the $^{13}C/^{12}C$ fractionation during loss to OH differ by a factor of two. The constraints provided by the estimated δD and $\delta^{13}C$ of the global CH_4 source suggest that the larger values determined for the hydrogen fractionation (Xiao *et al.*, 1993; Gierczak *et al.*, 1997) and the smaller value for the carbon fractionation (Cantrell *et al.*, 1990) are more consistent with current understanding of controls on the isotopic composition of atmospheric CH_4 (Figure 3.1). Improved estimates of the hydrogen and

carbon fractionations during CH_4 loss to OH are necessary in order for measurements of the δD and $\delta^{13}C$ of atmospheric CH_4 to be useful in constraining the global CH_4 source.

CONCLUSIONS

The first systematic experimental determinations of the δD content of CH_4 emitted from biomass burning ($\delta D_{CH4(bb)}$) were presented. In laboratory experiments of *Pinus ponderosa* needle combustion $\delta D_{CH4(bb)} = -233 \pm 2‰$. During field sampling of fires typical to slash burning of primary forest and pasture clearing in the Brazilian Amazon, $\delta D_{CH4(bb)} = -210 \pm 16‰$. Isotopic analysis of biomass indicated that a significant D/H fractionation occurred during combustion. For the laboratory fires, $\varepsilon^D_{burn} \approx -130‰$ and in the field studies, ε^D_{burn} ranged from -130‰ to -180‰. A significant negative fractionation, such as that observed here, would be expected to occur during methane production via methyl radical abstraction of hydrogen from other organic material. In contrast, the determinations of $\delta^{13}C_{CH4(bb)}$ were consistent with earlier studies which showed that very little carbon isotopic fractionation occurs during combustion, *i.e.*, the $\delta^{13}C$ of CH_4 emitted from biomass burning equals the $\delta^{13}C$ content of the fuel burned (Stevens and Engelkemeir, 1988; Wahlen *et al.*, 1989; Levin *et al.*, 1993).

Although the results from fires in the field were limited to Brazil, the relatively small range of $\delta D_{CH4(bb)}$ observed overall indicates that the δD of CH_4 emitted from fires in other tropical ecosystems is not likely to be significantly different than $\delta D_{CH4(bb)} = -210 \pm 16‰$. This assumption should be confirmed

with additional measurements of $\delta D_{CH4(bb)}$ from fires in other tropical regions where biomass burning contributes significantly to global CH_4 emissions.

The estimate of $\delta D \approx -210‰$ for the global biomass burning CH_4 source derived from the field studies presented here, combined with previous knowledge of the strengths and δD content of other major CH_4 sources yields a δD for the global CH_4 source that is consistent with the measured δD of atmospheric CH_4 and the hydrogen isotope fractionations associated with the CH_4 sinks.

This work indicates that the δD and $\delta^{13}C$ signatures of the major CH_4 sources are distinct (Figure 3.1). Previous work has shown that the δD and $\delta^{13}C$ signatures of the major CH_4 sinks are also distinct (Snover and Quay, in preparation). The D/H content of atmospheric CH_4 is therefore a unique tracer of the atmospheric CH_4 budget and, when combined with $^{13}C/^{12}C$ measurements, can provide additional constraints on the regional, hemispheric and global budgets of atmospheric CH_4.

CHAPTER 4: THE δD COMPOSITION OF ATMOSPHERIC METHANE

INTRODUCTION

Because the spatial and temporal distribution of an atmospheric trace gas results from the spatial and temporal distribution of its sources and sinks, knowledge of the former can be useful for constraining the latter. This approach, using observations of the atmospheric abundance of a trace gas to constrain its budget, has been successfully applied to the study of atmospheric CH_4 (Fung *et al.*, 1991; Hein *et al.*, 1997; Saeki *et al.*, 1998). Using estimates of the spatial and temporal distribution of CH_4 sources and sinks in a three-dimensional atmospheric transport model, Fung *et al.* (1991) developed a CH_4 budget consistent with the observed seasonal and meridional variations in atmospheric CH_4 concentrations. Using an inverse model approach, Hein *et al.* (1997) showed that the constraint provided by globally-distributed observations of atmospheric CH_4 concentrations reduces the uncertainty associated with individual CH_4 source strengths by ~30% from a priori estimates based on extrapolation of local flux measurements.

The isotopic composition of atmospheric CH_4, which reflects the isotopic signatures and relative importance of the individual CH_4 sources and sinks, can be used to provide additional constraints on the CH_4 budget. Seasonal variations in the $^{13}C/^{12}C$ of atmospheric CH_4 have been used to elucidate the relative importance of CH_4 source and sink processes at the

regional level, providing information additional to that inherent in observations of atmospheric CH_4 concentrations alone (Lassey *et al.*, 1993; Quay *et al.*, in press). The latitudinal gradient in $^{13}C/^{12}C$ has been used to constrain the isotopic composition of the bulk southern hemisphere CH_4 source and the proportion of that source contributed by biomass burning (Quay *et al.*, in press).

Although the global modeling studies of Fung *et al.* (1991) and Hein *et al.* (1997) included the spatial and temporal distribution of the $^{13}C/^{12}C$ content of atmospheric CH_4, in neither case did the isotopic information significantly improve the source strength constraints imposed by observations of atmospheric CH_4 concentration alone. This finding likely reflects the fact that there are significantly more measurements of atmospheric CH_4 than of its $^{13}C/^{12}C$ content.

The D/H content of CH_4 is an additional, unique tracer of the atmospheric CH_4 budget. Its application to studies of atmospheric CH_4 has been limited by the lack of measurements of the δD signature of CH_4 emitted from biomass burning and of CH_4 removed by soils, gaps filled by the research presented in this dissertation, and of the D/H content of atmospheric CH_4 in clean, *i.e.*, "background" air. There have been only a few previous measurements of the δD of CH_4 in clean air, and none during this decade. Ehhalt (1973) reported -86 and -94‰ for two air samples collected in 1970. Wahlen *et al.* (1990) reported average δD values during 1986 to 1987 for the northern and southern hemispheres of -87 ± 5‰ and -77 ± 2‰, respectively.

There are no published time series observations of the D/H of atmospheric CH_4.

In this chapter, the latitudinal trend in the D/H content of atmospheric CH_4, determined from air samples collected during oceanographic research cruises in the Pacific Ocean during 1989 to 1995, is presented. Measurements of the D/H content of atmospheric CH_4 at Cheeka Peak, Washington (48.3°N, 124.6°W) between 1991 and 1996 are also presented. These data are examined in the context of the global CH_4 budget utilizing a three-dimensional chemical transport model. The factors affecting the seasonal cycles in CH_4 concentration and D/H content at Cheeka Peak and the north-south trend in the D/H of atmospheric CH_4 are discussed.

METHODS

Sampling Sites and Collection Procedures

Air samples were collected from 1991 to 1996 for measurement of the D/H composition of atmospheric CH_4 at Cheeka Peak (48.3°N, 124.6°W, 500 m elevation) on Washington State's Olympic Peninsula, 3 km west of the Pacific Ocean. Cheeka Peak is an atmospheric clean-air monitoring station operated by the University of Washington; samples collected there during onshore flow of clean air are considered to be representative of background air at this latitude. Air samples were also collected on six oceanographic research cruises between 55°N and 65°S, along ~150°W, in the Pacific Ocean during 1989 to 1995.

On all research cruises and at Cheeka Peak from 1991 to 1993, large volume air samples for isotopic analysis were dried using silica gel and compressed into 30 L high pressure Spectra Seal aluminum cylinders (Airco, City of Industry, CA) to ~2000 psig using a scuba compressor (Purus/Utilus model, with charcoal scrubber removed, Bauer Compressors, Inc., Norfolk, VA). Samples for measurement of CH_4 concentration were collected by opening a pre-evacuated 15 or 30 L stainless steel flask (Biospherics, Inc., Beaverton, OR). In January 1994, a remotely controlled sample collection procedure was implemented at Cheeka Peak, enabling collection of most air samples via modem communication from the University under clean air conditions. Clean-air was characterized by onshore air flow, *i.e.*, wind direction between 180° and 330° from the north, wind speed > 2 m sec^{-1}, condensation particle count < 500 cm^{-3} and, during 1994 only, [Rn] ≤ 300 mBq m^{-3} (T. Anderson and D. Covert, personal communication). Air samples were drawn from an 8 m tower through a polyethylene inlet line, and compressed to ~70 psig into ~33 L stainless steel canisters (General Container Corp., Somerset, NJ) using an aluminum/neoprene diaphragm pump (KNF Neuberger, Trenton, NJ). Neither sample drying nor compression have been found to alter the δD of CH_4 in the sample. The δD of dried air samples pressurized with the scuba compressor were within 4‰ of samples collected simultaneously using the aluminum/neoprene diaphragm pump and no drying agent (n=3). Methane concentration was measured on aliquots of samples collected for isotopic analysis beginning in January, 1994.

Analytical Procedures

The concentration of CH_4 in the air samples was measured by the Climate Modeling and Diagnostics Laboratory at the National Oceanic and Atmospheric Association, Boulder, Colorado, by gas chromatography with a relative measurement precision of ~0.2% (Dlugokencky *et al.*, 1994a,b). The measurement of the D/H composition of CH_4 in air samples was based on cryogenic collection of H_2O derived from combustion of the CH_4 and subsequent reduction of H_2O to H_2 over zinc, as described in Chapter 3. The instream combustion oven for combustion of CH_4 to CO_2 and H_2O was rebuilt once during the course of the time series, on March 4, 1992. The four air samples (n=13 analyses) that were combusted using the first oven were corrected by +6.4‰ to account for the offset between the δD of laboratory standards measured before and after the oven change. The precision of the D/H measurement during this study was ± 3.9‰ based on a total of 141 replicate analyses of 11 laboratory standards of pure CH_4 diluted in ultrapure air and of 7 air samples. When replicate analyses of time series or Pacific transect samples were made, the average δD was reported, after eliminating individual determinations of δD that were outside ± 3 standard deviations (3σ) of the mean for that air sample. Unless otherwise noted, all uncertainties represent $\pm 1\sigma$.

MEASUREMENT RESULTS

TIME SERIES AT CHEEKA PEAK

The time series of the δD content and concentration of atmospheric CH_4 measured at Cheeka Peak between 1991 and 1996 are reported (Figure 4.1, Tables 4.1 and 4.2). The time series of CH_4 concentration exhibited a consistent sharp seasonal decrease during the late summer/early fall. The δD record shows consistent enrichment during the late summer/early fall, although the seasonal cycle in δD was less obvious.

The seasonal cycles in both δD and concentration of atmospheric CH_4 becomes more apparent when monthly mean values are calculated, assuming the entire time series represents a single average year, after subtraction of any interannual trend from the data set. Using this method, there were typically seven measurements per month for both δD and CH_4 concentration. The time series in CH_4 concentration was normalized by subtracting the 6 ppb yr^{-1} average global increase in CH_4 concentration observed during 1991 to 1996 (Dlugokencky *et al.*, 1998). The δD data were normalized using the increase of 2.4 ± 0.8‰ yr^{-1} (95% confidence level) observed at Cheeka Peak (Figure 4.1). Both the CH_4 concentration and δD time series were normalized to January 1, 1994.

It is unclear whether the δD increase observed in the Cheeka Peak data reflected a real increase in atmospheric δD or resulted from long-term drift in the accuracy of the laboratory analytical procedure. During 1991 to 1996, the average δD of the laboratory standards was -137.0 ± 5.6‰ (n=93) with an apparent increase of 2.1 ± 1.0‰ yr^{-1} (95% c.l.) (Figure 4.2). This apparent trend

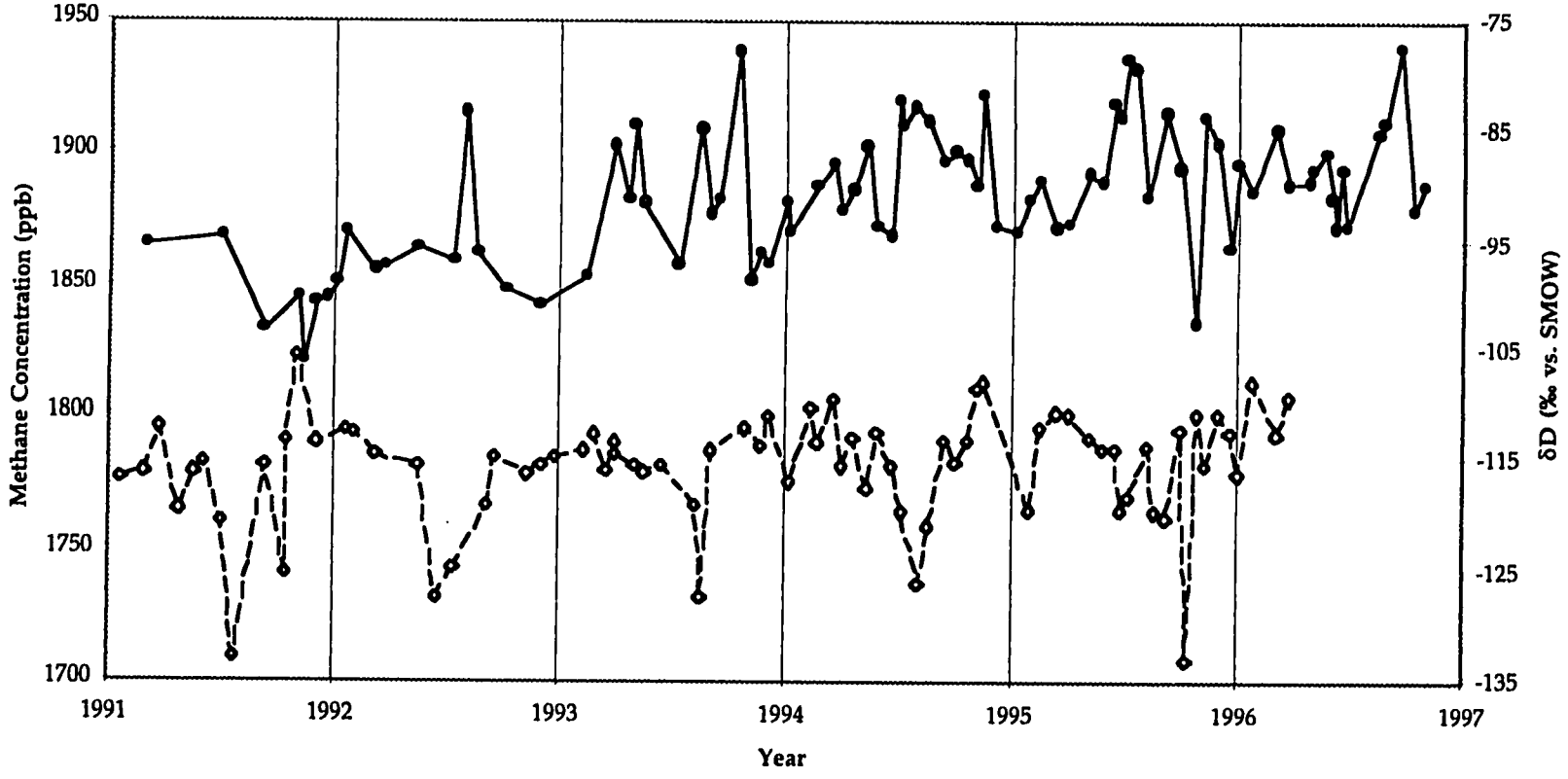

Figure 4.1 The concentration (◊) and δD (•) of atmospheric CH_4 at Cheeka Peak, Washington from 1991 to 1996.

Table 4.1 Time series of the δD of atmospheric methane measured at Cheeka Peak, Washington during 1991 to 1996.

Collection Date (month/day/year)	δD (‰ vs. SMOW)	Collection Date (month/day/year)	δD (‰ vs. SMOW)
2 / 28 / 91	-95.2	8 / 18 / 94	-84.0
6 / 26 / 91	-94.5	9 / 13 / 94	-87.7
9 / 9 / 91	-103.0	9 / 30 / 94	-86.8
11 / 2 / 91	-100.1	10 / 20 / 94	-87.6
11 / 14 / 91	-106.1	11 / 4 / 94	-89.8
12 / 2 / 91	-100.7	11 / 16 / 94	-81.6
12 / 19 / 91	-100.3	12 / 7 / 94	-93.4
1 / 3 / 92	-98.7	1 / 9 / 95	-94.0
1 / 18 / 92	-94.0	1 / 31 / 95	-91.2
3 / 5 / 92	-97.6	2 / 15 / 95	-89.2
3 / 20 / 92	-97.3	3 / 14 / 95	-93.6
5 / 15 / 92	-95.5	4 / 1 / 95	-93.3
7 / 12 / 92	-96.7	5 / 2 / 95	-88.7
7 / 30 / 92	-83.4	5 / 26 / 95	-89.4
8 / 18 / 92	-96.0	6 / 13 / 95	-82.3
10 / 4 / 92	-99.4	6 / 23 / 95	-83.7
11 / 28 / 92	-100.9	7 / 3 / 95	-78.5
2 / 15 / 93	-98.2	7 / 21 / 95	-79.3
3 / 28 / 93	-86.3	8 / 8 / 95	-90.7
4 / 18 / 93	-91.2	9 / 5 / 95	-83.3
5 / 1 / 93	-84.4	9 / 27 / 95	-88.3
5 / 15 / 93	-91.5	10 / 25 / 95	-102.5
7 / 8 / 93	-97.0	11 / 7 / 95	-83.8
8 / 17 / 93	-84.7	11 / 30 / 95	-86.0
8 / 31 / 93	-92.3	12 / 18 / 95	-95.4
9 / 14 / 93	-91.1	1 / 2 / 96	-87.8
10 / 20 / 93	-78.0	1 / 23 / 96	-90.3
11 / 6 / 93	-98.5	3 / 3 / 96	-84.8
11 / 20 / 93	-95.9	3 / 19 / 96	-89.6
12 / 1 / 93	-96.9	4 / 24 / 96	-89.5
12 / 31 / 93	-91.4	5 / 1 / 96	-88.5
1 / 10 / 94	-93.9	5 / 22 / 96	-86.9
2 / 23 / 94	-89.8	5 / 30 / 96	-90.9
3 / 17 / 94	-87.8	6 / 6 / 96	-93.6
3 / 31 / 94	-92.1	6 / 18 / 96	-88.3
4 / 19 / 94	-90.3	6 / 21 / 96	-93.5
5 / 11 / 94	-86.1	8 / 14 / 96	-85.1
5 / 26 / 94	-93.4	8 / 21 / 96	-84.3
6 / 21 / 94	-94.3	9 / 20 / 96	-77.6
6 / 30 / 94	-82.2	10 / 12 / 96	-92.0
7 / 6 / 94	-84.4	10 / 26 / 96	-89.8
7 / 25 / 94	-82.8		

Table 4.2 Time series of the concentration of atmospheric methane measured at Cheeka Peak, Washington during 1991 to 1996.

Collection Date (month/day/year)	[CH_4] (ppb)	Collection Date (month/day/year	[CH_4] (ppb)
1 / 20 / 91	1777	2 / 9 / 94	1803
2 / 24 / 91	1779	2 / 22 / 94	1790
3 / 21 / 91	1796	3 / 17 / 94	1806
4 / 24 / 91	1765	3 / 31 / 94	1781
5 / 15 / 91	1779	4 / 19 / 94	1792
5 / 31 / 91	1783	5 / 11 / 94	1773
6 / 26 / 91	1760	5 / 26 / 94	1794
7 / 21 / 91	1709	6 / 21 / 94	1781
9 / 9 / 91	1782	7 / 6 / 94	1764
10 / 11 / 91	1741	8 / 3 / 94	1737
10 / 13 / 91	1791	8 / 18 / 94	1759
10 / 31 / 91	1823	9 / 13 / 94	1791
12 / 2 / 91	1790	9 / 30 / 94	1783
1 / 18 / 92	1795	10 / 20 / 94	1791
2 / 5 / 92	1794	11 / 4 / 94	1811
3 / 5 / 92	1786	11 / 16 / 94	1813
5 / 15 / 92	1782	1 / 31 / 95	1765
6 / 14 / 92	1732	2 / 15 / 95	1796
7 / 12 / 92	1743	3 / 14 / 95	1802
9 / 2 / 92	1766	4 / 1 / 95	1801
9 / 18 / 92	1785	5 / 2 / 95	1792
11 / 8 / 92	1778	5 / 26 / 95	1788
11 / 28 / 92	1782	6 / 13 / 95	1788
12 / 20 / 92	1785	6 / 23 / 95	1765
2 / 6 / 93	1787	7 / 3 / 95	1769
2 / 27 / 93	1793	8 / 8 / 95	1789
3 / 13 / 93	1780	8 / 17 / 95	1764
3 / 28 / 93	1790	9 / 5 / 95	1762
3 / 29 / 93	1786	9 / 27 / 95	1795
5 / 1 / 93	1782	10 / 12 / 95	1708
5 / 14 / 93	1779	10 / 25 / 95	1801
6 / 13 / 93	1782	11 / 7 / 95	1782
8 / 8 / 93	1766	11 / 30 / 95	1801
8 / 17 / 93	1732	12 / 18 / 95	1794
8 / 31 / 93	1787	1 / 2 / 96	1778
10 / 28 / 93	1796	1 / 23 / 96	1813
11 / 20 / 93	1789	3 / 3 / 96	1793
12 / 1 / 93	1800	3 / 19 / 96	1807
1 / 10 / 94	1775		

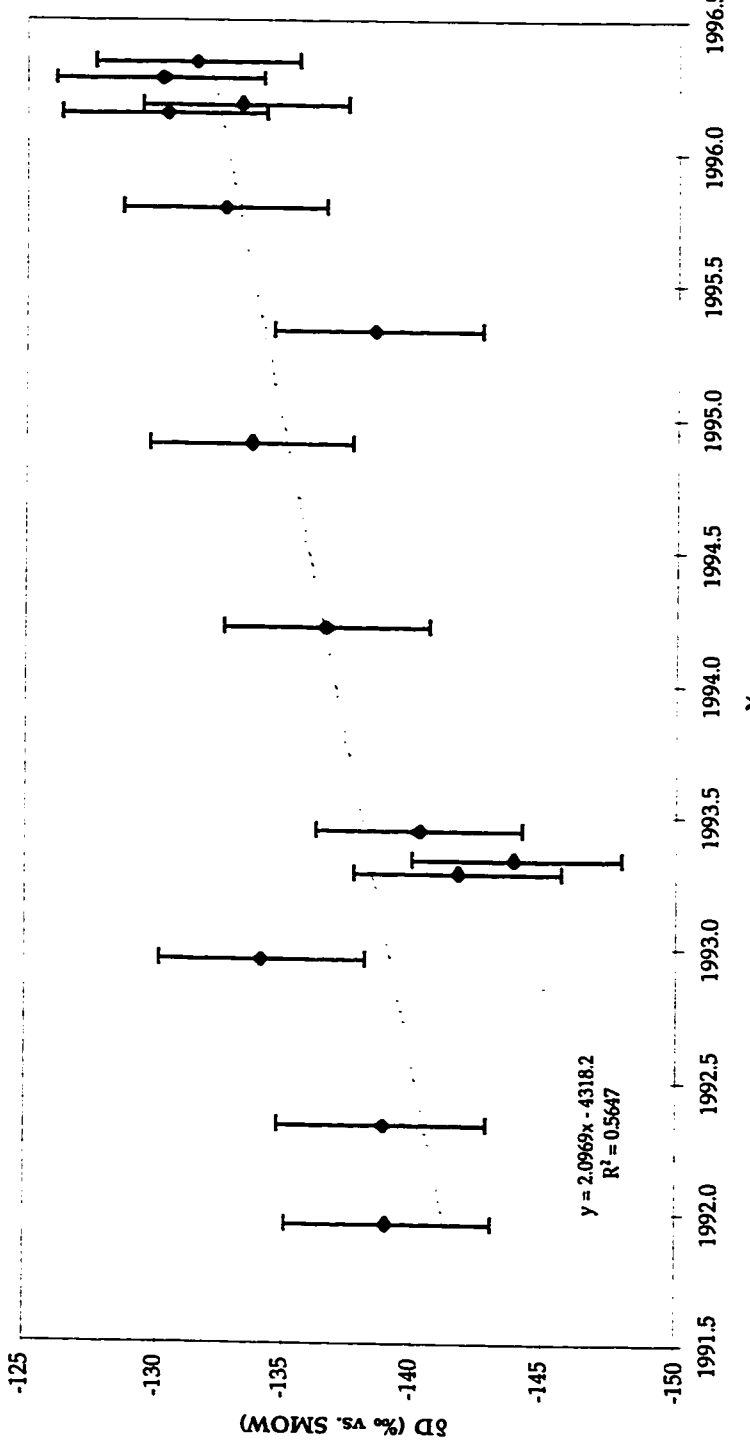

Figure 4.2 The average δD of CH_4 in laboratory standards measured during 1991 to 1996. The average δD for each laboratory standard is plotted versus the mean analysis date for all replicate analyses of that standard. Each standard was analyzed an average of seven times. The error bars shown (± 4‰) represent the mean ± 1σ precision of replicate analysis. During 1991 to 1996, the average δD of the laboratory standards was -137.0 ± 5.6‰ (total n=93) with an apparent increase of 2.1 ± 1.0‰ yr^{-1} (95% c.l.). However, the δD enrichment observed for standards measured during late 1995 and 1996 may reflect the use of δD-enriched CH_4 in the preparation of these standards rather than a drift in the accuracy of the laboratory δD analysis procedure. See text.

may have resulted from systematic errors in the standard preparation procedure. Laboratory standards containing CH_4 were prepared by dilution of aliquots of 100% CH_4 in ultrapure air. For convenience, these aliquots were generally obtained from a 500 ml glass bottle containing a subsample of 100% CH_4 from the CH_4 high pressure cylinder. Because this subsample becomes progressively enriched in δD with the removal of subsequent aliquots, it must be periodically replaced. During late 1995 and 1996, however, laboratory CH_4 standards were repeatedly prepared using aliquots from a CH_4 subsample that had been used many times without replacement. This likely caused the δD enrichment in CH_4 standards measured during this time, *i.e.*, $\delta D = -131.2 \pm 5.0‰$ (n=17), and therefore the apparent trend in the δD of the laboratory standards (Figure 4.2). This conclusion was supported by the observation that subsequent laboratory standards, prepared after the CH_4 subsample in the aliquoting volume was replaced, were significantly less enriched in δD, *i.e.*, $-136.2 \pm 3.0‰$ (n=35). This measured isotopic composition of the standard CH_4 is more consistent with that determined from sealed tube combustion of the pure CH_4, as described in Chapter Three, which yielded $\delta D = -137.8 \pm 4.0‰$ (n=4).

Replicate analyses of whole air samples, which are not affected by this standard preparation uncertainty, may provide a better evaluation of the long-term accuracy of the CH_4 sample preparation procedure. An interannual trend on the order of $+2.4‰\ yr^{-1}$, however, is difficult to detect with a δD measurement precision of $\sim\pm 4‰$. Using four air samples, each with a set of replicate analyses spanning at least three years (total n=33), the apparent drift

in the δD analysis procedure was +1.2 ± 2.3‰ yr^{-1} (95% c.l.). Given the ± 4‰ δD measurement uncertainty and the systematic errors in δD standard preparation during this study, therefore, the cause of the observed interannual increase in δD in the Cheeka Peak time series record could not be determined.

The method of correcting the δD measurements for the 2.4‰ yr^{-1} interannual trend depends on whether the trend was a real atmospheric change or a result of long-term laboratory drift. If the trend was a real atmospheric change, the δD data should be detrended based on the date of sample collection. If the trend was due to laboratory drift, the data should be trend-corrected based on the date of analysis. However, neither the seasonal cycle in δD at Cheeka Peak nor the latitudinal distribution of the δD of atmospheric CH_4 is significantly affected by the correction method used, as discussed below.

Methane concentrations at Cheeka Peak peaked during winter/spring and reached minimum values during the summertime (Figure 4.3a). The annual mean CH_4 concentration during 1991-1996 was 1781 ± 2 ppb. The annual mean was calculated by averaging monthly means calculated after subtraction of the 6 ppb yr^{-1} interannual trend (Dlugokencky *et al.*, 1998). The uncertainty in the annual mean value represents ± 1 standard error (SE) and was calculated by propagation of error from the standard error in the monthly means. The amplitude of the seasonal variation in CH_4 concentration was 47 ± 9 ppb, peak-to-trough. These observations are consistent with the 43.5 ppb

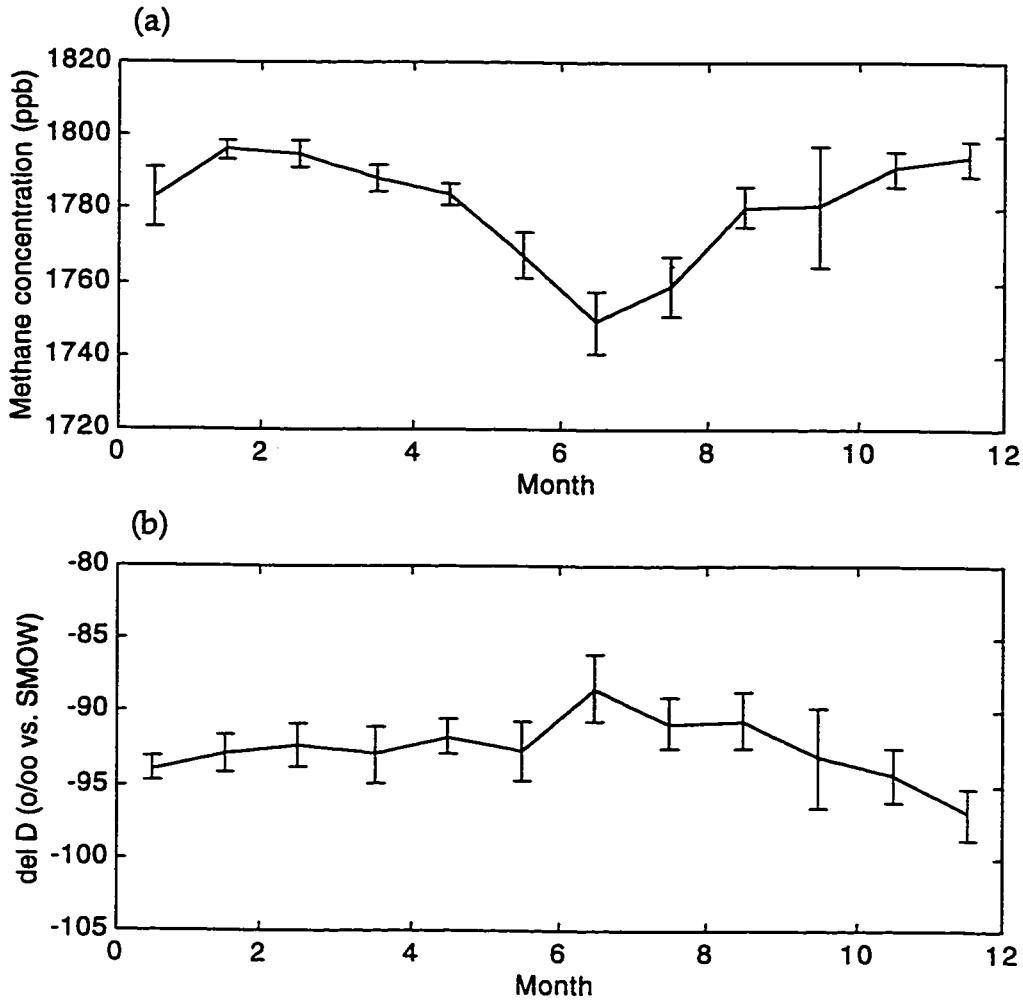

Figure 4.3 The seasonal cycle observed for CH_4 concentration and δD at Cheeka Peak, Washington from 1991 to 1996.
(a) CH_4 concentration. (b) δD. The monthly averages were calculated by assuming the entire time series shown in Figure 4.1 represented a single year, after subtraction of any interannual trend from the data set, see text. Error bars represent ± 1 SE.

seasonal cycle observed during 1991-1993 at Cape Meares, Oregon, a similar clean-air monitoring station at 45.5° N (Dlugokencky *et al.*, 1994b).

The seasonal cycle in δD is not as obvious as that for CH_4 concentration (Figure 4.3b). δD was nearly constant from February through June. δD values were most enriched in July and decreased steadily to minimum, *i.e.*, most depleted, values in December. The annual mean δD at Cheeka Peak was -92.6 ± 0.5‰ (± 1 SE), after correction for the interannual trend by date of sample analysis, with a seasonal cycle of amplitude 8.6 ± 2.9‰. Because samples collected at Cheeka Peak were generally analyzed soon after collection, the mean seasonal cycle in δD is insensitive to the correction method used. Correcting the δD measurements by date of sample collection yielded an annual mean δD of -91.9 ± 0.6‰ with a seasonal cycle of amplitude 9.5 ± 2.5‰.

Meridional Distribution

There was a clear increase in the δD of atmospheric CH_4 towards the equator in the northern hemisphere of ~13‰ from 50°N to 0° (Figure 4.4, Table 4.3). There was no evidence of a meridional trend in δD in the southern hemisphere. These measurements of the north-south trend in δD can be used to determine a global mean δD and the average interhemispheric δD gradient. The mean δD's for the northern and southern hemispheres were -93.0 ± 1.9‰ (n=47) and -83.3 ± 1.5‰ (n=48) (±1σ), respectively, after normalizing to 1994 based on date of sample analysis. Hemispheric means were determined from area-weighted means of the average δD in each 10°

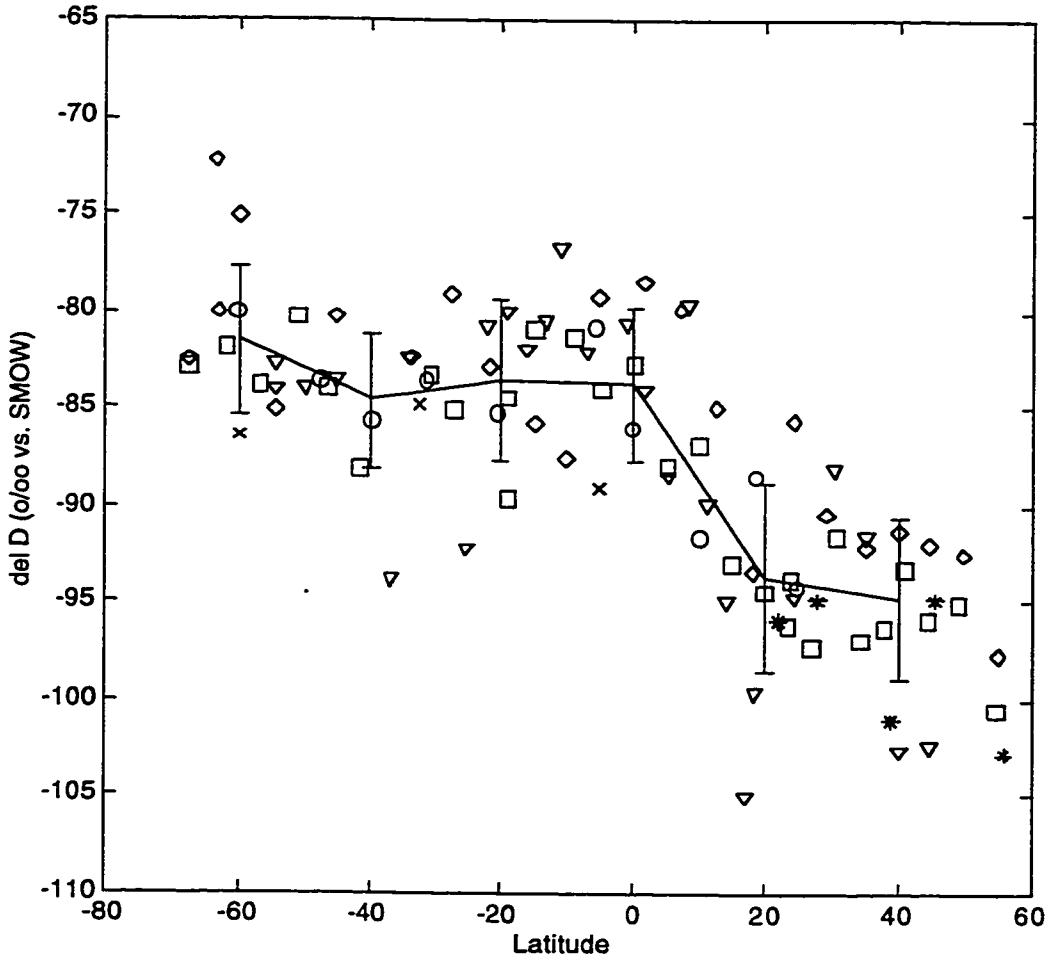

Figure 4.4 Snapshots of the meridional gradient in δD from samples collected on oceanographic research cruises in the Pacific Ocean along ~150°W. Samples were collected during March 1989 (o), March 1990 (x), March 1991 (*), April 1993 (squares), December 1993 (◊) and October 1995 (▽). Overlaid are the mean δD values for each 20° latitude band with error bars of ± 1σ. The δD data was normalized to 1994 by subtraction of an interannual trend in δD of 2.4‰ yr^{-1}, based on date of sample analysis, see text. Southern hemisphere locations are denoted by negative latitudes.

Table 4.3 The meridional trend in the δD of atmospheric methane from samples collected on oceanographic research cruises in the Pacific Ocean along ~150°W during 1989 to 1995.
These data have not been corrected for any trend in δD.

Cruise Date	Latitude[a]	δD (‰ vs. SMOW)	Cruise Date	Latitude[a]	δD (‰ vs. SMOW)
March 1989	-61	-83.9	December 1993	-67	-79.3
March 1989	-48	-87.3	December 1993	-64	-70.6
March 1989	-40	-89.7	December 1993	-63	-78.2
March 1989	-31	-88.0	December 1993	-60	-72.0
March 1989	-21	-82.8	December 1993	-55	-81.1
March 1989	-6	-84.8	December 1993	-45	-77.0
March 1989	0	-88.1	December 1993	-34	-78.4
March 1989	10	-96.1	December 1993	-27	-75.5
March 1989	18	-92.4	December 1993	-22	-79.6
March 1989	25	-97.9	December 1993	-15	-82.4
			December 1993	-10	-85.1
March 1990	-60	-88.5	December 1993	-5	-75.5
March 1990	-33	-86.8	December 1993	2	-75.6
March 1990	-5	-91.2	December 1993	7	-76.2
			December 1993	13	-81.8
March 1991	22	-99.4	December 1993	18	-90.2
March 1991	28	-97.1	December 1993	24	-83.8
March 1991	39	-103.2	December 1993	29	-87.4
March 1991	46	-97.1	December 1993	35	-88.8
March 1991	56	-105.4	December 1993	40	-89.5
			December 1993	45	-88.6
April 1993	-68	-83.3	December 1993	50	-88.6
April 1993	-62	-82.5	December 1993	55	-93.7
April 1993	-57	-84.4			
April 1993	-51	-80.9	October 1995	-54	-77.5
April 1993	-47	-84.3	October 1995	-54	-78.5
April 1993	-41	-88.6	October 1995	-50	-76.8
April 1993	-31	-83.7	October 1995	-45	-78.0
April 1993	-27	-85.6	October 1995	-37	-84.9
April 1993	-19	-90.2	October 1995	-34	-76.8
April 1993	-19	-84.7	October 1995	-25	-83.4
April 1993	-15	-81.5	October 1995	-22	-75.2
April 1993	-9	-81.7	October 1995	-19	-74.9
April 1993	-5	-84.2	October 1995	-16	-76.4
April 1993	0	-83.4	October 1995	-13	-74.9
April 1993	5	-88.4	October 1995	-11	-71.1
April 1993	10	-87.0	October 1995	-7	-76.5
April 1993	15	-93.6	October 1995	-1	-75.5
April 1993	20	-94.4	October 1995	2	-78.6
April 1993	24	-96.7	October 1995	5	-79.6
April 1993	24	-93.9	October 1995	3	-74.6
April 1993	27	-97.7	October 1995	11	-81.0
April 1993	31	-92.0	October 1995	14	-86.0
April 1993	34	-96.9	October 1995	17	-96.1
April 1993	38	-96.4	October 1995	19	-90.8
April 1993	41	-93.8	October 1995	24	-89.1
April 1993	44	-94.7	October 1995	30	-83.1
April 1993	49	-95.6	October 1995	35	-85.9
April 1993	54	-100.9	October 1995	40	-93.7
			October 1995	45	-93.5

a. Negative signs denote latitudes in the southern hemisphere.

latitude band and yield a global mean δD of -88.1 ± 1.2‰ with an interhemispheric gradient of 9.6 ± 2.5‰. The mean values are insensitive, within error, to the cause of the observed interannual trend in δD. Normalizing the δD data by date of sample collection yields a global mean δD of -84.9 ± 1.3‰ with an interhemispheric gradient of 9.9 ± 2.6‰.

DISCUSSION

THE GLOBAL METHANE BUDGET

The δD of atmospheric CH_4 depends on the average δD of the CH_4 gained from the sources and lost to the sinks and on the relative strengths of the CH_4 sources and sinks and can be expressed as follows:

$$C \cdot \frac{d(\delta D_{atm})}{dt} + \delta D_{atm} \cdot \frac{dC}{dt} = S \cdot \delta D_{src} - M \cdot \delta D_{sink} \qquad (1)$$

Here C represents atmospheric CH_4 concentration and S and M are the total annual CH_4 source and sink strengths, respectively. δD_{atm} is the global mean δD of atmospheric CH_4. δD_{src} and δD_{sink} represent the average δD of the total CH_4 source and sink, respectively. The global mean CH_4 concentration was 1715 ppb and increasing at 6 ppb yr^{-1} during 1991 to 1996 (Dlugokencky *et al.*, 1998).

Recent CH_4 budget compilations (Hein *et al.*, 1997; Fung *et al.*, 1991; Crutzen, 1995; Prather *et al.*, 1995) indicate that approximately two-thirds of the total source of atmospheric CH_4 results from bacterial production in wetlands, ruminants and rice paddies. Methane emissions associated with

fossil fuel sources (natural gas venting and transmission loss and coal mining) constitute ~18% of the total source, while biomass burning and landfills each contribute ~10%. Oxidation by tropospheric hydroxyl radicals (OH) accounts for ~87% of the total CH_4 sink and loss to soils and in the stratosphere account for 5% and 8% of the CH_4 sink, respectively. A current estimate for the strengths of the individual CH_4 sources and sinks is shown in Table 4.4. This budget was determined by Hein *et al.* (1997) using a 3-dimensional atmospheric circulation/chemistry model to predict atmospheric CH_4 concentrations with the CH_4 budget developed by Crutzen (1995) used for a priori estimates of CH_4 source strengths. The source/sink imbalance in this budget was constrained by the observed atmospheric CH_4 increase of 11.9 ppb yr^{-1} during 1983 to 1989. The sink strengths used here (Table 4.4) were increased by 3% over those of Hein *et al.* (1997) to reflect the lower atmospheric CH_4 growth rate of 6 ppb yr^{-1} observed during 1991 to 1996 (Dlugokencky *et al.*, 1998), the period during which the δD observations were made. These increases are within the uncertainties estimated by Hein *et al.* (1997) and are consistent with the observed increase in the atmospheric CH_4 burden. The total annual CH_4 source and sink strengths were 575 and 558 Tg CH_4 yr^{-1}, respectively, which translate to 208 and 202 ppb yr^{-1} using these data and the conversion factor, 1 ppb = 2.767 Tg (Fung *et al.*, 1991).

The average δD of the global CH_4 source depends on the amount and δD of CH_4 emitted from each individual source. Methane sources are generally categorized by δD content with bacterial sources most depleted and fossil sources most enriched in δD (Table 4.4). Landfills and biomass burning

Table 4.4 The mean strength and stable isotopic composition of methane sources and sinks.
Uncertainties are ± 1σ.

Source	Strength[A] ($Tg\ CH_4\ yr^{-1}$)	δD (‰ vs. SMOW)
Wetlands		
Swamps	188 ± 13	-304 ± 13 [B,a]
Bogs	39 ± 4	-340 ± 12 [B,a]
Tundra	5 ± 1	-365 ± 16 [B,a]
Ruminants	90 ± 10	-305 ± 9 [b]
Rice Paddies	69 ± 12	-323 ± 19 [c]
Landfills	40 ± 8	-293 ± 20 [d]
Biomass Burning	41 ± 6	-210 ± 15 [e]
Fossil Fuel Sources		
Gas Leakage	36 ± 12	-191 ± 15 [C,f]
Gas Venting	34 ± 7	-191 ± 15 [C,f]
Coal Mining	33 ± 5	-146 ± 8 [g]
Total CH_4 Source	575 ± 26	-279 ± 6 [D]

Sink	Strength[A] ($Tg\ CH_4/yr$)	δD[E] (‰ vs. SMOW)
Oxidation by OH	484 ± 15	-299 ± 41 [h]
Uptake by Soils	29 ± 7	-162 ± 18 [i]
Stratospheric Loss	45 ± 4	-234 ± 18 [j]
Total CH_4 Sink	558 ± 17	-286 ± 36

[A] Hein *et al.* (1997). The bog source strength was decreased by 5 Tg to account for the tundra source of 5 Tg (Whalen and Reeburgh, 1998; Bartlett and Harriss 1993). The sink strengths shown here were increased by 3% to account for the decreased growth rate of atmospheric CH_4 during 1991 to 1996, see text.

Table 4.4, continued.

[B] The global average δD signatures for emissions from swamps, bogs and tundra were calculated using the estimated latitudinal distribution of wetland types (Fung *et al.*, 1991) and literature values for δD (wetland) averaged by 10° latitude band, see text.

[C] CH_4 emissions associated with natural gas production and transmission was assumed to be of origin 80% thermogenic : 20% biogenic (Rice and Claypool, 1981). The categories "gas leakage" and "gas venting" refer to the geographic distribution of emissions of natural gas (Fung *et al.*, 1991).

[D] The uncertainty in the δD of the total CH_4 source was determined by propagating the error associated with both the individual source δD signatures and the individual source strengths through the calculation of the flux-weighted average δD_{src}.

[E] The δD of CH_4 removed by each sink process is δD_{sink} (‰) = (KIE · (δD_{atm}/1000 + 1) - 1) · 1000, where KIE is the kinetic isotope effect associated with that sink, *i.e.*, $k(CH_3D)/k(CH_4)$, and δD_{atm} is -88‰.

[a] Wassman *et al.* (1992); Lansdown (1992); Kling *et al.* (1991); Burke *et al.* (1988, 1992); Burke and Sackett (1986); Wahlen *et al.* (1989; as referenced in Lansdown, 1992); Levin *et al.* (1993); Woltemate *et al.* (1984); Martens *et al.* (1992). [b] Wahlen *et al.* (1989; 1990); Levin *et al.* (1993); Lansdown (1992). [c] Wahlen *et al.* (1989; 1990); Levin *et al.* (1993); Bergamaschi (1997). [d] Liptay *et al.* (1998); Bergamaschi *et al.* (1998b); Bergamaschi and Harris (1995); Levin *et al.* (1993). [e] Snover *et al.* (in preparation). [f] Schoell (1980); Rice and Claypool (1981); Ehhalt (1973); Levin *et al.* (1993). [g] Schoell (1980). [h] Gierczak *et al.* (1997). [i] Snover and Quay (in preparation). [j] Irion *et al.* (1996).

emit CH_4 with intermediate δD values. The mean global δD for each CH_4 source (Table 4.4) was estimated as follows, using the published determinations of the δD of CH_4 emitted from each source summarized in Chapter 1, Table 1.2.

The δD of CH_4 emitted from wetlands depends on the δD of environmental water (Lansdown, 1992) which has a meridional trend, becoming more depleted at high latitudes (IAEA, 1981). For example, the δD signatures of CH_4 emitted from Alaskan tundra (68°N) and from swamps in the Florida Everglades (26°N) were -391 ± 8‰ and -293 ± 14‰, respectively (Lansdown, 1992; Burke *et al.*, 1988). The global average δD of CH_4 emitted from wetlands can be determined, therefore, from the global distribution of each wetland type and the observed latitudinal trend in the δD of CH_4 emitted from wetlands. Literature values for the δD of CH_4 emitted from wetlands (Table 1.2) were used to construct the average δD of CH_4 emitted from this source in each 10° latitude band. This was combined with the global distribution of natural wetlands, *i.e.*, predominantly tropical swamps (30°S to 10°N), temperate bogs (40°N to 70°N) and high latitude tundra (50°N to 80°N) estimated by Fung *et al.* (1991), to yield an average δD for CH_4 emitted from swamps, bogs and tundra of -304 ± 13‰, -340 ± 12‰, and -365 ± 16‰, respectively. The uncertainty (± 1σ) in each value accounts for the uncertainty in the δD of CH_4 emitted in each 10° latitude band determined from the range in reported δD values and assumes no uncertainty in the latitudinal distribution of wetland emissions.

The global average δD signatures of CH_4 emitted from rice paddies, landfills and coal mining, *i.e.*, -323 ± 19‰, -293 ± 20‰ and -146 ± 8‰, respectively, were determined by averaging the mean values reported for each source (Tables 1.2 and 4.4). The uncertainties (± 1σ) result from the range in the mean values reported in the literature for each CH_4 source. The global average δD of CH_4 emitted from ruminants, -305 ± 9‰, was calculated by weighting each mean value for δD(ruminants) reported in the literature by the number of determinations of that value (Table 1.2), in order not to overemphasize the single determination of very depleted CH_4 from this source (*i.e.*, -390‰; Lansdown, 1992). The ± 9‰ (1σ) uncertainty was determined by propagating the uncertainties in the individual estimates of δD(ruminants) through the weighted mean calculation (Bevington and Robinson, 1992). The δD of CH_4 emissions associated with natural gas production and transmission, *i.e.*, -191 ± 15‰, was determined from measurements of natural gas CH_4 (Levin *et al.*, 1993; Ehhalt, 1973) and from measurements of the δD content of biogenic and thermogenic natural gas deposits (Schoell, 1980), assuming that natural gas CH_4 is 80% thermogenic and 20% biogenic (Rice and Claypool, 1981). The uncertainty reported for the mean δD(natural gas) assumes no uncertainty in the 80:20 ratio (Table 4.4).

Combined with the individual source strengths, the δD of the CH_4 sources result in an average δD for the total CH_4 source, δD_{src}, of -279 ± 6‰. The uncertainty in δD_{src} (± 1σ) was determined by propagating the error associated with both the individual source δD signatures and the individual

source strengths (Table 4.4) through the calculation of the flux-weighted average δD_{src} (Bevington and Robinson, 1992).

Each CH_4 removal process involves a characteristic kinetic isotope effect (KIE), preferentially removing CH_4 depleted in deuterium with respect to atmospheric CH_4. The KIE, defined as the ratio of the rate constants for removal of heavy (CH_3D) and light (CH_4) methane, has been measured at 0.769 ± 0.045 for CH_4 oxidation by OH (Gierczak *et al.* 1997), 0.919 ± 0.020 for uptake by soils (Snover and Quay, in preparation) and 0.840 ± 0.020 for loss in the stratosphere (Irion *et al.*, 1996). Weighting each KIE by the individual sink strength (Table 4.4) yields an average KIE for the total CH_4 sink of 0.783 ± 0.039. The isotopic signature of CH_4 removed by each sink pathway, *i.e.*, δ_{sink} (‰) = (KIE · (δD_{atm}/1000 + 1) - 1) · 1000, is -299 ± 41‰, -162 ± 18‰ and -234 ± 18‰, for oxidation by OH, uptake by soils and stratospheric losses, respectively, using $\delta D_{atm} = -88.1 \pm 1.2$‰. The average isotopic composition of the total CH_4 sink is therefore $\delta D_{sink} = -286 \pm 36$‰, heavily weighted towards the dominant removal process, oxidation by OH.

On a global scale, the three major components of the δD budget of atmospheric CH_4, described by equation (1), are the global mean δD_{atm} and its time rate of change, the average δD of the CH_4 source and the average δD of the CH_4 sink. The δD for each term has been estimated independently here, the first from atmospheric observations, and the latter two from independent measurements of the δD signature of each CH_4 source and sink. The requirement of mass balance, quantified by equation (1), can be used to test the

consistency of these estimates of δD_{src} and δD_{sink} with the atmospheric observations.

The a priori estimates of δD_{src} (-279 ± 6‰) and δD_{sink} (-286 ± 36‰) satisfy the δD balance described by equation (1), using δD_{atm} = -88.1 ± 1.2‰ with $d(\delta D_{atm})/dt$ = 0‰ yr^{-1}, S = 208 ± 9 ppb yr^{-1} and M = 202 ± 6 ppb yr^{-1}, as described above. The uncertainty in $d(\delta D_{atm})/dt$ was assumed to be ± 1‰ yr^{-1} to account for the possibility that the increase in δD observed at Cheeka Peak reflected a real increase in the δD of atmospheric CH_4 as discussed above. Notably, the uncertainty in δD_{sink} is significantly reduced by using the a priori estimate for δD_{src} as a constraint, *i.e.*, if the better-constrained a priori estimate for δD_{src} is assumed to be correct, equation (1) yields δD_{sink} = -285 ± 11‰. This implies a nearly fourfold reduction in the uncertainty in the KIE associated with CH_4 removal by OH, if the uncertainties for the KIEs associated with stratospheric loss and soil uptake are unchanged.

If the measured interannual trend in δD_{atm} of 2.4‰ yr^{-1} was a real atmospheric increase, the a priori estimate for δD_{src} would require a slightly more depleted δD_{sink} for isotopic balance, *i.e.*, -305 ± 11‰. This depletion in δD_{sink} implies a fractionation during CH_4 loss to OH of 0.742 which is slightly larger than, but within the uncertainty of, the experimentally determined 0.769 ± 0.045 (Gierczak *et al.*, 1997). This assumes that the KIEs for stratospheric loss and soil uptake remain unchanged.

The good agreement between the three major components of the global CH_4 budget, *i.e.*, the atmospheric observations and the δD of the total CH_4 source and sink, is encouraging. It suggests that current understanding of the

controls on the δD content of atmospheric CH_4 is fairly robust on the global scale. Application of δD as a tracer to the atmospheric CH_4 budget is currently limited by the significant uncertainty in the KIE during CH_4 loss to OH.

Three-dimensional Chemical Transport Model Simulation of the Global Atmospheric Methane - δD Cycle

The simple analysis of the global δD budget, presented above, was expanded to include processes controlling the spatial and temporal distributions of δD. This was accomplished by applying a three-dimensional chemical transport model (CTM) to the global δD budget. The CTM includes realistic seasonal and geographic distributions of CH_4 emissions and of CH_4 loss to OH, as well as realistic atmospheric transport. Use of the CTM allows an evaluation of whether current understanding of the CH_4 budget and the δD isotopic composition of its sources and sinks are consistent with the observed meridional gradient in δD and the seasonal cycle in δD observed at Cheeka Peak.

The CTM was developed by Fung *et al.* (1991) for study of the global CH_4 budget. It has a resolution of 8° latitude, 10° longitude and 9 levels in the vertical. Atmospheric circulation in the model was based on wind fields generated from the 3-dimensional global general circulation model at the Goddard Institute for Space Studies (Hansen *et al.*, 1983). The tracer transport model has been applied to the study of atmospheric tracers such as methyl-chloroform, CFCs and ^{85}Kr (Spivakovsky *et al.*, 1990b; Prather *et al.*, 1987; Jacob *et al.*, 1987).

Because meridional and seasonal variations in CH_4 concentration are less than 10% of the global annual mean, a quasi-linear assumption allows simulation of CH_4 distributions and seasonal cycles to be approximated as the sum of the individual atmospheric responses to each of the CH_4 source or sink functions. This allows both the atmospheric response to a variety of CH_4 emission scenarios and the atmospheric response to individual CH_4 sources or sinks to be easily tested. For CH_4 sources, the linear approximation is exact; for CH_4 loss to OH, which depends on the actual atmospheric CH_4 concentration, the error introduced by the approximation is ~5% of the modeled signal (Fung *et al.*, 1991).

The geographic distribution and seasonal variability of CH_4 emissions from wetlands, ruminants, rice paddies, landfills, biomass burning and fossil fuel sources used in the CTM were compiled by Fung *et al.* (1991). Methane emissions from wetlands, rice paddies and biomass burning vary seasonally in the model. Emissions from all other sources are constant throughout the year. The latitudinal distribution of CH_4 emissions (Figure 4.5) results from the strengths (Table 4.4) and geographic distribution of the individual CH_4 sources (Fung *et al.*, 1991). Most (~70%) of the CH_4 emissions occur in the northern hemisphere, with maximum emissions between 20°N and 50°N, because of the location of the fossil fuel, landfill and animal CH_4 sources. Bacterial sources of CH_4 comprise at least 40% of the emissions in each latitude band. In the southern hemisphere, ~85% of emissions are of bacterial origin because emissions from fossil sources are essentially zero. Biomass burning emissions occur between 25° N and 25° S.

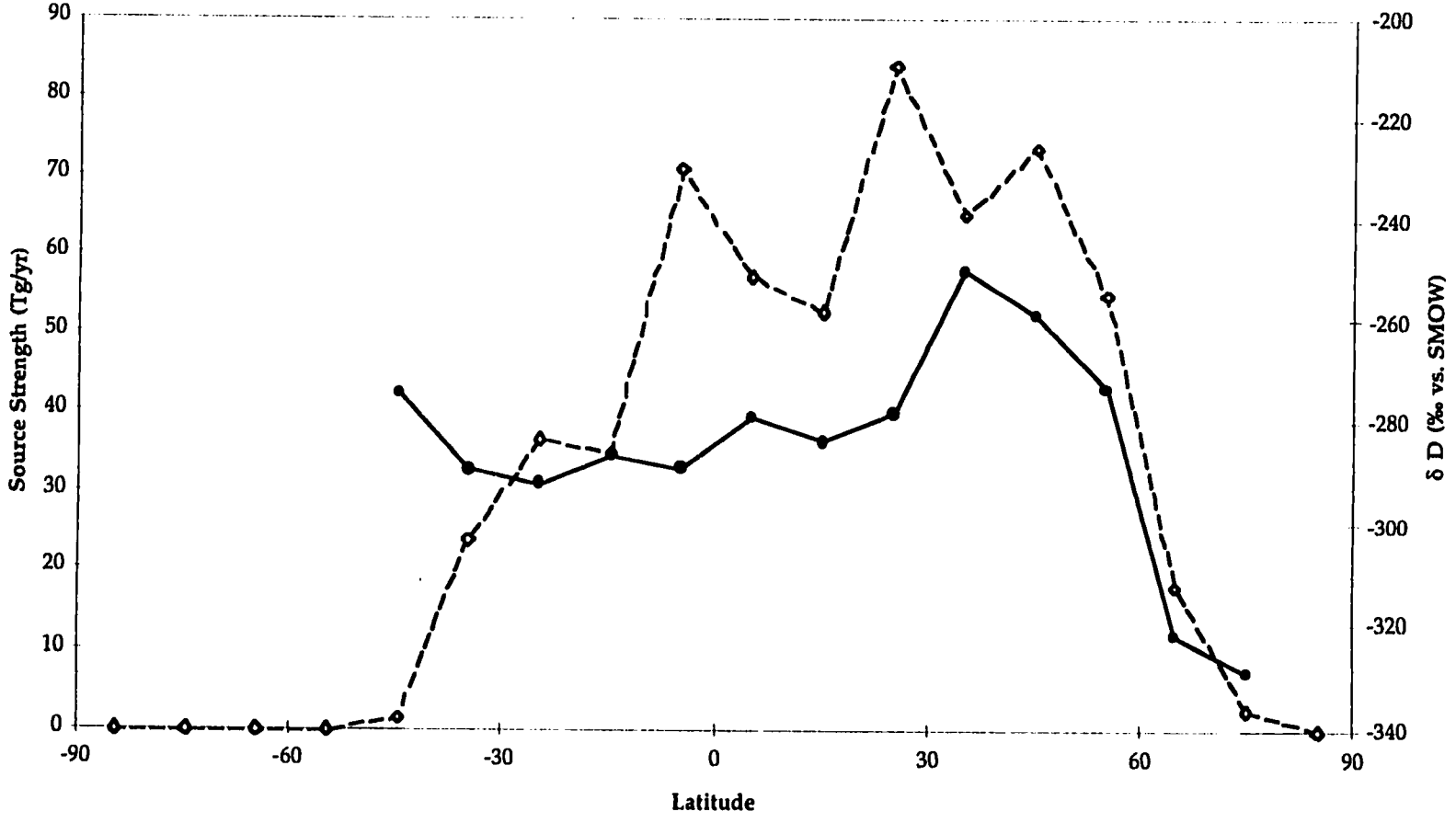

Figure 4.5 The meridional trend in the strength (◊) and δD (•) of the zonally-averaged CH_4 source determined using the strengths of the individual CH_4 sources from Hein *et al.* (1997), the geographic distribution of CH_4 sources presented by Fung *et al.* (1991), and the δD of the CH_4 sources specified in Table 4.4.

The δD of the zonally-averaged CH_4 source reflects the CH_4 source mix in each region (Figure 4.5). The average δD of CH_4 emitted in the southern hemisphere is -292 ± 14‰, reflecting a mix of CH_4 from mostly bacterial and biomass burning sources. The δD enrichment in middle latitudes of the northern hemisphere reflects the higher proportion of CH_4 emissions from the δD enriched fossil-fuel associated CH_4 (δD = -146‰ to -191‰) in this region. The δD depletion at high northern latitudes reflects the predominance of CH_4 emissions from bogs and tundra (δD = -340 to -365‰). The average δD of the northern hemisphere CH_4 source is -274 ± 6‰. The reported uncertainties for the δD of the hemispheric CH_4 sources reflect the uncertainties in the strengths and δD contents of the individual CH_4 sources calculated by assuming no uncertainty in the geographic distribution of CH_4 emissions.

Removal of CH_4 in the CTM was parameterized as oxidation by tropospheric OH, using the global OH fields developed by Spivakovsky *et al.* (1990a,b). The seasonal and geographic variation of OH mixing ratios results from variations in sunlight, water vapor content, and the atmospheric distributions of O_3, CO, CH_4, and NO_x (Spivakovsky *et al.* 1990a,b). Photolytic production of OH peaks during summer months and is highest in the tropics.

The δD of the total CH_4 sink (δD_{sink}) is set in the CTM to balance the δD of the total CH_4 source and any interannual trend in the concentration and δD of atmospheric CH_4 as described above (equation (1)), *i.e.*, δD_{sink} = -285‰ when δD_{atm} = -88.1‰, $d(\delta D_{atm})/dt$ = 0‰ yr^{-1}, and $d([CH_4])/dt$ = 6 ppb yr^{-1}. Due to the quasi-linear nature of the CTM, δD_{sink} is zonally constant. In reality, δD_{sink}

changes little between the hemispheres. The effect on δD_{sink} of the 10‰ difference in δD_{atm} between the two hemispheres is offset by the ~5‰ difference in the KIE of CH_4 loss between the two hemispheres caused by the asymmetry in the strength of the soil sink. On average, the difference between δD_{sink} in the northern and southern hemispheres is less than 3‰ and the approximation of a constant δD_{sink} in the CTM simulations is valid.

The strengths of the individual CH_4 sources and sinks from Hein *et al.* (1997) (Table 4.4), their geographic and seasonal variability compiled by Fung *et al.* (1991) and δD compositions specified in Table 4.4 were used in the CTM along with the CH_4 sink described above to simulate spatial and temporal variations in the concentration and δD of atmospheric CH_4. A global average CH_4 concentration of 1715 ppb and δD of -88.1‰ were used to facilitate comparison of model results with the atmospheric observations made during 1991 to 1996. The model-predicted seasonal cycle of CH_4 concentration at Cheeka Peak and interhemispheric gradient in CH_4 concentration compare well to observations (Figure 4.6 a,b). The predicted annual mean CH_4 concentration at Cheeka Peak was 1791 ± 3 ppb, compared to the observed annual mean of 1781 ± 2 ppb. (Uncertainties are ± 1 SE, calculated from the twelve monthly values.) The amplitude of the predicted seasonal cycle of 40 ppb compares well with the observed amplitude of 47 ± 9 ppb. Controls on this seasonality will be discussed in detail below. The model slightly overestimates the interhemispheric gradient in CH_4 concentration, predicting 103 ppb, versus the observed interhemispheric gradient of 89 ppb (CDIAC, 1998). The general agreement between the model predictions and

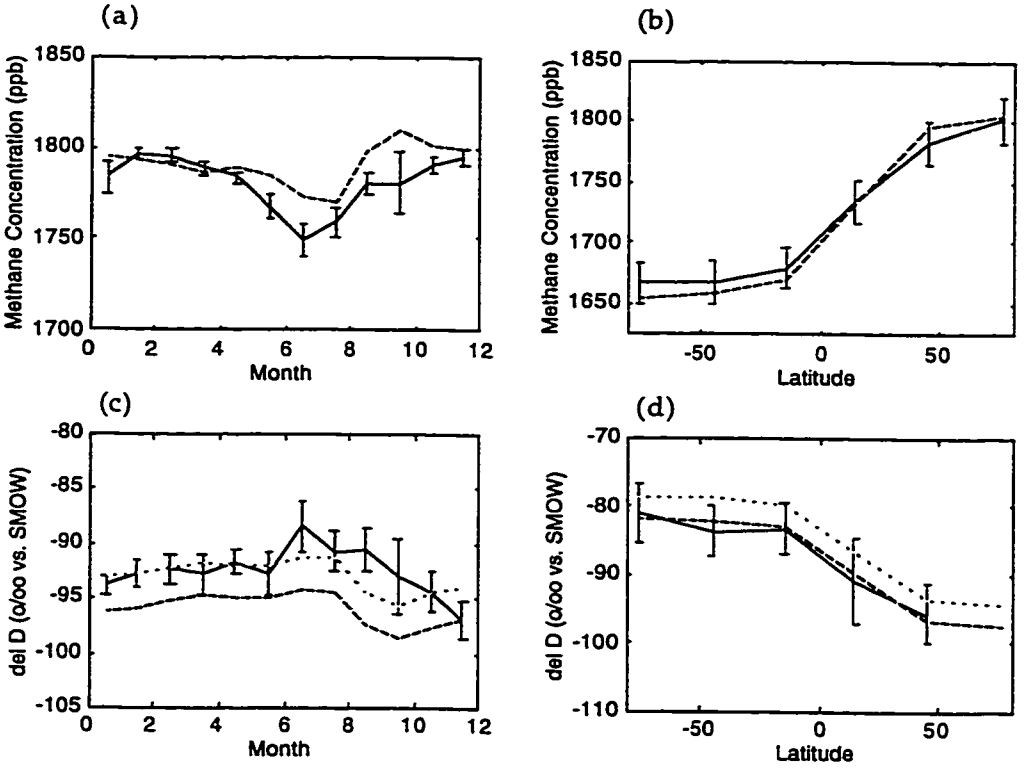

Figure 4.6 Chemical transport model predictions of the concentration and δD of atmospheric CH_4.

Model predictions are depicted by (–) for (a) the seasonal cycle in CH_4 concentration at Cheeka Peak, (b) the interhemispheric gradient in CH_4 concentration, (c) the seasonal cycle in δD at Cheeka Peak, and (d) the interhemispheric gradient in δD. The CTM used a global average CH_4 concentration of 1715 ppb and δD of -88.1‰. A better match to the observed δD at Cheeka Peak was obtained using a global average δD of -84.9‰ in the CTM (···), see text. Atmospheric observations are represented by vertical bars connected by solid lines, with an uncertainty of ± 1 SE for monthly means at Cheeka Peak and ± 1σ for the meridional trends. The observed meridional trend in CH_4 concentration is from CDIAC (1998).

observations of atmospheric CH_4 concentrations is to be expected. The CH_4 budget scenario used here (Hein *et al.*, 1997) is similar, *i.e.*, in its proportion of bacterial, landfill, biomass burning and fossil fuel sources of CH_4, to the one developed by Fung *et al.* (1991) to match observed seasonal and meridional variations in atmospheric CH_4 concentrations.

There is also good agreement between model results and atmospheric observations of the interhemispheric gradient in δD, *i.e.*, 10.9‰ and 9.6 ± 2.5‰, respectively (Figure 4.6d). At Cheeka Peak, the predicted and observed annual means were -96.0 ± 0.4‰ and -92.6 ± 0.5‰, respectively (Figure 4.6c). The model-predicted mean annual δD at Cheeka Peak is sensitive to the global mean δD used in the CTM, *i.e.*, the global mean δD the CTM is required to reproduce. As discussed above, the global mean δD of atmospheric CH_4 is expected to lie between -88.1‰ and -84.9‰, depending on the normalization procedure used for the atmospheric δD measurements. Requiring the CTM to reproduce a global mean δD of -84.9‰ results in a predicted annual mean δD of -92.9 ± 0.4‰ at Cheeka Peak, in better agreement with observations (Figure 4.6c). In this case, the model-predicted δD of atmospheric CH_4 is slightly more enriched than observations indicated in all latitudes, but within the uncertainty of the observations (Figure 4.6d). The seasonal cycle in δD is consistently underestimated by the model, at 4.6‰, versus the observed 8.6 ± 2.9‰. Possible causes of this underestimation are discussed below.

The sensitivity of the predicted distribution of atmospheric δD to uncertainty in the strengths and isotopic composition of the individual CH_4 sources and the CH_4 sink was examined as follows. The strength and δD of

each CH_4 source were randomly chosen from the means and uncertainties specified for that source (Table 4.4), assuming normal distributions, and used to calculate the average δD for the total CH_4 source. This δD_{src} then specifies a value for δD_{sink}, given the global mean CH_4 concentration (C) and δD (δD_{atm}) and their respective interannual time rates of change (dC/dt and $d(\delta D_{atm})/dt$), see equation (1). Values for C, dC/dt and $d(\delta D_{atm})/dt$ were chosen from the ranges defined by their observed means and uncertainties of 1715 ± 3 ppb, 6 ± 2 ppb yr^{-1} and 0 ± 1‰ yr^{-1}, respectively. Because the CTM is required to reproduce the global observed mean δD_{atm}, uncertainties in this value translate directly to uncertainties in model predictions. For example, a ± 1‰ uncertainty in δD_{atm} results in a ± 1‰ uncertainty in the model-predicted annual mean δD at Cheeka Peak when errors in all other parameters are assumed equal to zero. In this analysis, the model used δD_{atm} = -84.9‰ and assumed no uncertainty in this value. The range of predicted atmospheric δD responses to 500 source/sink scenarios randomly chosen in the manner described above is shown in Figure 4.7.

The seasonal cycle in δD at Cheeka Peak and the interhemispheric gradient in δD are relatively insensitive to uncertainties in the strength and δD of the individual CH_4 sources (Figure 4.7). The range of predictions for both are generally within the uncertainty of the atmospheric observations. This indicates that current understanding of the CH_4 budget and of the δD content of CH_4 sinks and sources, including the newly determined signatures of CH_4 emitted from biomass burning and removed by soils, are consistent with observations of atmospheric δD. The observed seasonal cycle in δD at

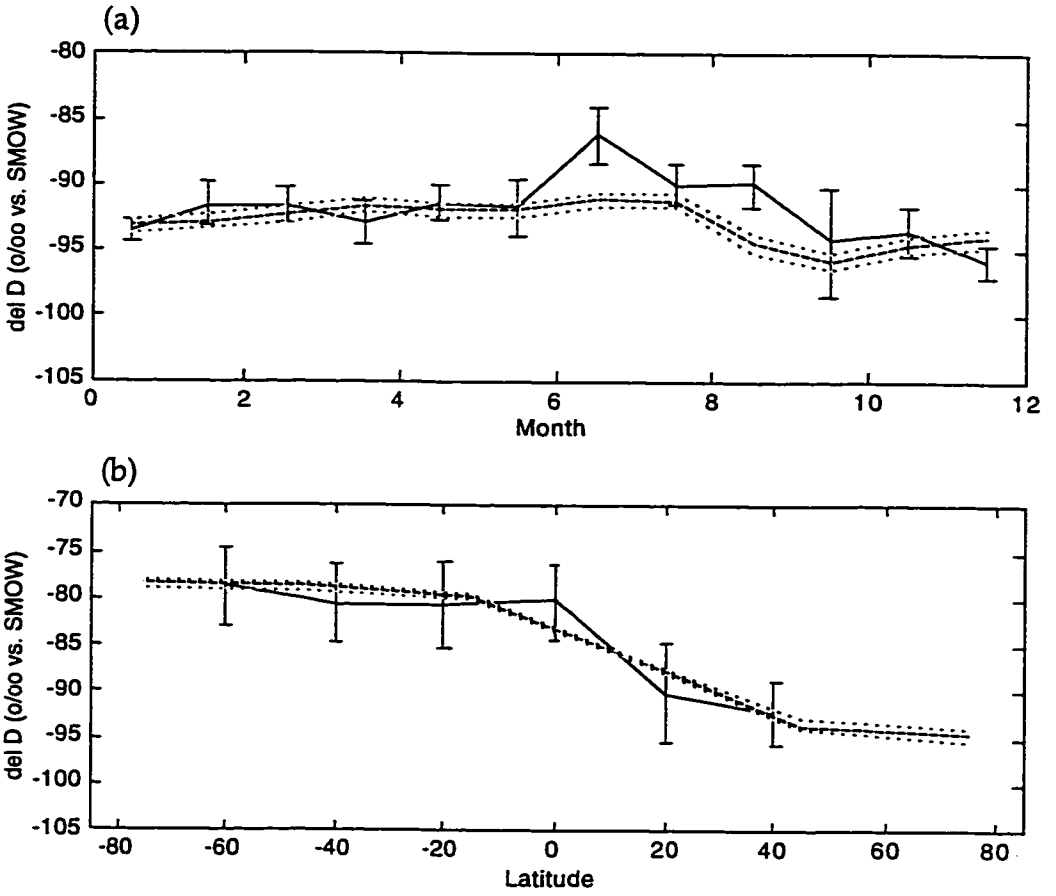

Figure 4.7 The sensitivity of the predicted distribution of atmospheric δD to uncertainty in the strengths and isotopic composition of the individual CH_4 sources and the CH_4 sink.

The mean predicted δD (–) ± 1σ (···) resulting from 500 source/sink scenarios randomly chosen to match δD_{atm} = -84.9‰, see text, is shown for (a) each month at Cheeka Peak and (b) each 20° latitude band. Atmospheric observations are represented by vertical bars connected by solid lines, with an uncertainty of ± 1 SE for monthly means at Cheeka Peak and ± 1σ for the meridional trend in δD.

Cheeka Peak and the observed north-south trend in δD do not, however, provide any additional constraints on the CH_4 budget. Controls on the interhemispheric gradient in δD, and why it is relatively insensitive to changes in the δD of the CH_4 source, will be discussed in the next section.

The Interhemispheric Gradient in the Concentration and δD of Atmospheric Methane

The existence of an interhemispheric gradient in atmospheric CH_4, with concentrations ~100 ppb higher in the northern hemisphere than in the southern hemisphere, results from the CH_4 source distribution, the lifetime of atmospheric CH_4 and the interhemispheric mixing rate. The CH_4 source is predominantly located in the northern hemisphere, with the northern hemisphere source strength ~2.5 times the southern hemisphere source strength, as discussed above. The lifetime of CH_4 of ~10 years (Prinn *et al.*, 1995) is sufficiently long, relative to the interhemispheric mixing time of ~1 year (Maiss and Levin, 1994), to allow significant mixing of CH_4 between the hemispheres. This mixing decreases the gradient in CH_4 concentration between the two hemispheres. The lifetime of CH_4 is not long enough relative to the interhemispheric mixing time, however, to eliminate the atmospheric gradient in CH_4 concentration.

Within each hemisphere, there is therefore an imbalance between CH_4 emissions and CH_4 removal by OH, soils and stratospheric losses. In the northern hemisphere, CH_4 sources exceed sinks and the concentration of atmospheric CH_4 is elevated relative to the CH_4 concentration in the southern

hemisphere where CH_4 sinks exceed sources. Mass balance is maintained in each hemisphere via atmospheric transport of CH_4 from the northern to the southern hemisphere. Atmospheric chemical/transport models have shown that 20-30% of the CH_4 released in the northern hemisphere is transported to the southern hemisphere (Hein *et al.*, 1997; Fung *et al.*, 1991).

The δD of the net CH_4 flux transported between the two hemispheres (δD_{xp}) is the ratio of the net CH_3D and CH_4 fluxes and can be expressed as follows:

$$\delta D_{xp} = \frac{X \cdot (C_N \cdot \delta D_{atm,N} - C_S \cdot \delta D_{atm,S})}{X \cdot (C_N - C_S)} \qquad (2)$$

where N and S represent the northern and southern hemispheres, respectively, and X represents the atmospheric mixing rate (Quay *et al.*, in press). δD_{xp} is thus independent of the interhemispheric mixing rate. Using northern and southern hemisphere mean CH_4 concentrations and δD compositions of 1765 ± 2 ppb and -93.0 ± 1.9‰, and 1665 ± 2 ppb and -83.3 ± 1.5‰, respectively, yields a δD for the net transport flux of -255 ± 42‰. The impact of a net north to south flux of CH_4 with this isotopic signature is examined using an example interhemispheric δD budget calculation (Figure 4.8).

Hemispheric budgets of atmospheric CH_4 were derived as follows. The total CH_4 source of 575 Tg yr^{-1} from Hein *et al.* (1997), see Table 4.4, was apportioned into northern and southern hemisphere sources of 408 Tg yr^{-1} and 168 Tg yr^{-1}, respectively, according to the geographic distribution of CH_4 sources presented by Fung *et al.* (1991) (Figure 4.5). The total CH_4 sink of 558

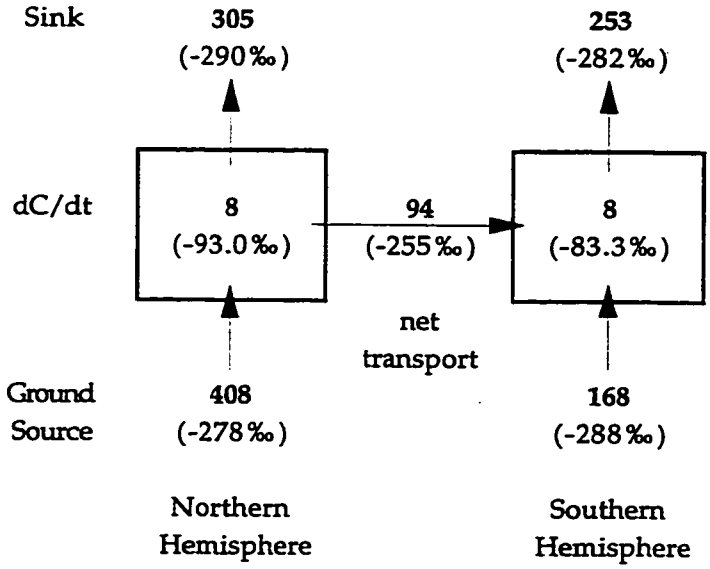

Figure 4.8 Hemispheric mass and δD budgets for atmospheric CH_4.
The methane fluxes (Tg yr^{-1}) are denoted by bold type. The δD of each flux is shown in parentheses. The CH_4 sink and ground source fluxes in each hemisphere represent the global fluxes from Hein *et al.* (1997), see Table 4.4, apportioned according to the geographic distribution of CH_4 sources and sinks presented by Fung *et al.* (1997). The δD of the net CH_4 flux transported between the two hemispheres was determined from the net CH_3D and CH_4 fluxes, see text. The δD of the CH_4 sink in each hemisphere was determined using a KIE of 0.783 and a δD of -93.0‰ and -83.3‰ for the northern and southern hemisphere, respectively. The δD of the ground sources was determined from isotopic balance. The time rate of change of δD_{atm} was assumed equal to zero. Due to rounding, mass and isotope fluxes may not appear to balance exactly.

Tg yr^{-1} (Table 4.4) was apportioned between the hemispheres according to the geographic distribution of CH_4 sinks from Fung *et al.* (1991), with 305 Tg yr^{-1} and 253 Tg yr^{-1} occurring in the northern and southern hemispheres, respectively. Thus, 94 Tg yr^{-1} is transported from the northern to southern hemisphere, equivalent to ~60% of the CH_4 emitted from ground sources within the southern hemisphere (Figure 4.8).

The δD of the net interhemispheric CH_4 flux was -255‰, as discussed above. The δD of the total CH_4 sink in the northern and southern hemispheres was -290‰ and -282‰, respectively. This corresponds to a total KIE of 0.783 acting on atmospheric CH_4 with a δD of -93.0‰ and -83.3‰, in the northern and southern hemispheres, respectively. The δD of the CH_4 ground source in each hemisphere was calculated by accounting for the δD of the CH_4 lost to the sink, the δD of the net CH_4 transport flux, and the increase in atmospheric CH_4 concentration. For this calculation, the time rate of change of δD_{atm} was assumed equal to zero. This yields a δD for the ground source in the northern and southern hemispheres of -278‰ and -288‰, respectively (Figure 4.8).

In the northern hemisphere, the CH_4 flux from the ground source is both higher (408 Tg yr^{-1}) and more enriched in δD (-278‰) than the amount (305 Tg yr^{-1}) and δD (-290‰) of CH_4 removed by the sink (Figure 4.8). To obtain δD balance in the northern hemisphere, after accounting for the increase in atmospheric CH_4 concentration with δD = -93.0‰, the excess of CH_4 emissions over CH_4 removal requires net CH_4 transport to the southern hemisphere that is relatively enriched in δD (-255‰). In the southern

hemisphere, the CH_4 sink (253 Tg yr^{-1} at -282‰) dominates over ground emissions (168 Tg yr^{-1}) of CH_4 which is relatively depleted in δD (-288‰) (Figure 4.8). This requires a net transport of δD enriched CH_4 (-255‰) from the northern hemisphere for isotopic balance.

The δD of the net interhemispheric CH_4 flux (δD_{xp}) is sensitive to small changes in the interhemispheric gradient of δD_{atm}. When the interhemispheric gradients in CH_4 concentration and δD are 100 ppb and 9.7‰, respectively, δD_{xp} is -255‰, as shown above. With an atmospheric δD gradient of 10.7‰ and the same gradient in CH_4 concentration, however, δD_{xp} would be -272‰. Thus large changes to the δD content of the CH_4 ground source in either hemisphere would result in significant changes to δD_{xp} and therefore require only slight changes to the difference in δD_{atm} between the two hemispheres to rebalance the system. This can be illustrated by determining the δD_{atm}(north), δD_{atm}(south) and δD_{xp} that result from different scenarios for the δD of the ground source (Figure 4.9), using the source, sink and transport flux strengths and KIE for CH_4 loss from the interhemispheric δD budget calculation described above and in Figure 4.8.

Emissions of CH_4 which are 38‰ more enriched in the northern than in the southern hemisphere, with δD of -270‰ and -308‰, respectively, result in an interhemispheric gradient in δD_{atm} of 7.8‰ and a δD_{xp} of -222‰ (Figure 4.9a). When the δD of CH_4 emissions is -280‰ in both hemispheres, the interhemispheric gradient in δD_{atm} is similar, *i.e.*, 10.4‰ (Figure 4.9b). Isotopic balance is maintained by a significant shift in the δD of the net interhemispheric CH_4 transport flux, from -222‰ to -265‰. The

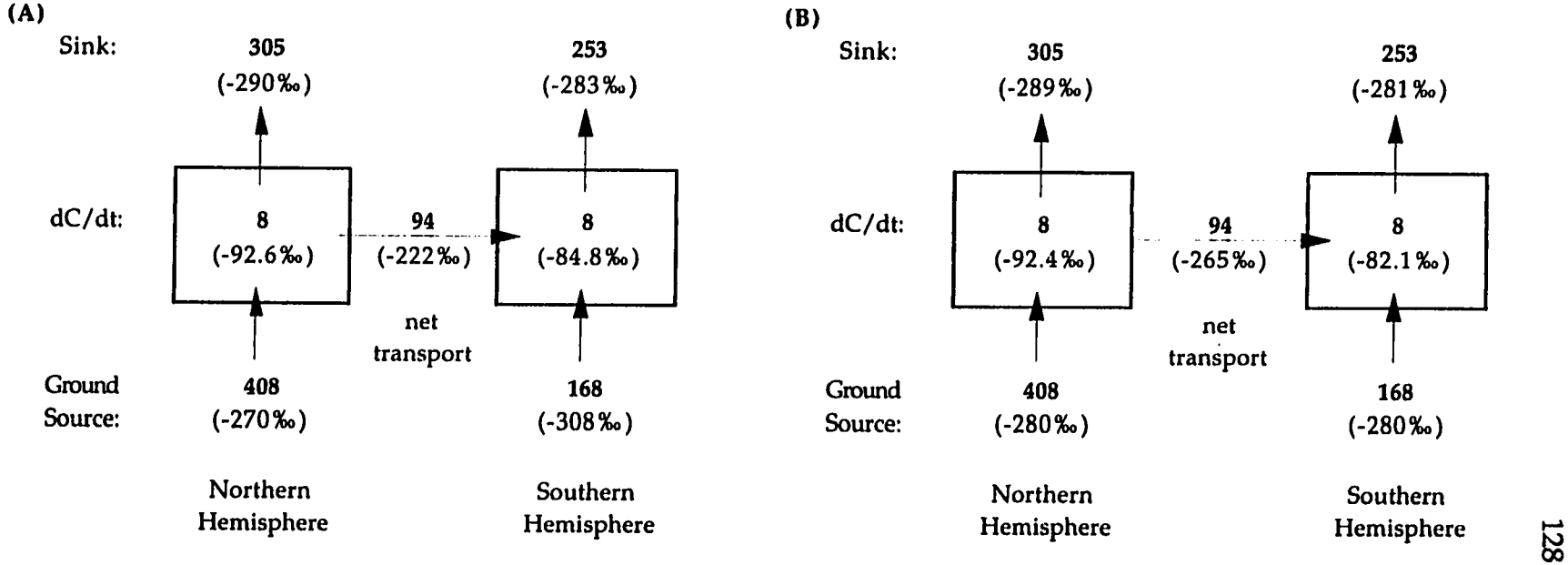

Figure 4.9 The insensitivity of the interhemispheric gradient in δD_{atm} to changes in the δD of CH_4 emissions in the northern and southern hemispheres.

A large change to the difference between the δD of CH_4 emitted in the two hemispheres has little effect on the interhemispheric gradient in δD_{atm}. (a) Emissions of CH_4 which are 38‰ more enriched in the northern than the southern hemisphere, with δD of -270‰ and -308‰, respectively, result in a interhemispheric gradient in δD_{atm} of 7.8‰ and a δD_{xp} of -222‰. (b) Emissions of CH_4 with the same δD, *i.e.* -280‰, in both hemispheres, result in a interhemispheric gradient in δD_{atm} of 10.4‰ and a δD_{xp} of -265‰. The CH_4 source, sink and transport flux strengths and the δD for CH_4 loss were derived as described in Figure 4.7. Due to rounding, mass and isotope fluxes may not appear to balance exactly.

interhemispheric gradient in δD is therefore relatively insensitive to changes in the δD of the CH_4 sinks or sources, due to the large effect these changes have on δD_{xp}.

The Seasonal Cycle of Methane Concentration and δD at Cheeka Peak

The seasonal cycles of concentration and δD content of CH_4 at any site result from the interplay between the seasonal variations of CH_4 emissions from each CH_4 source, CH_4 removal by each sink and atmospheric transport. Controls on the seasonality of CH_4 and δD at Cheeka Peak were examined using the seasonal cycles in CH_4 concentration and δD predicted by the CTM. Under the quasi-linear assumption, the total predicted CH_4 concentration or δD in the CTM is the sum of the atmospheric responses to each of the CH_4 sources and sinks. Similarly, the total predicted seasonal cycle in CH_4 concentration or δD results from the source/sink weighted sum of the individual seasonal cycles resulting from each CH_4 source and sink.

The modeled response of atmospheric CH_4 at Cheeka Peak to each CH_4 source and sink, at the strength specified in Table 4.4, is shown in Figure 4.10a. Removal of CH_4 by soil uptake and stratospheric removal processes, since they were not specified in the CTM, were assumed in the model to have the same temporal and spatial variability as CH_4 loss to OH. The primary CH_4 sink, oxidation by OH, results in the largest individual seasonal cycle, *i.e.*, a concentration change of 39 ppb peak to trough. Atmospheric OH mixing ratios peak in late July at 48°N (Spivakovsky *et al.*, 1990b) when photolytic production of OH is greatest, leading to a summertime decrease in

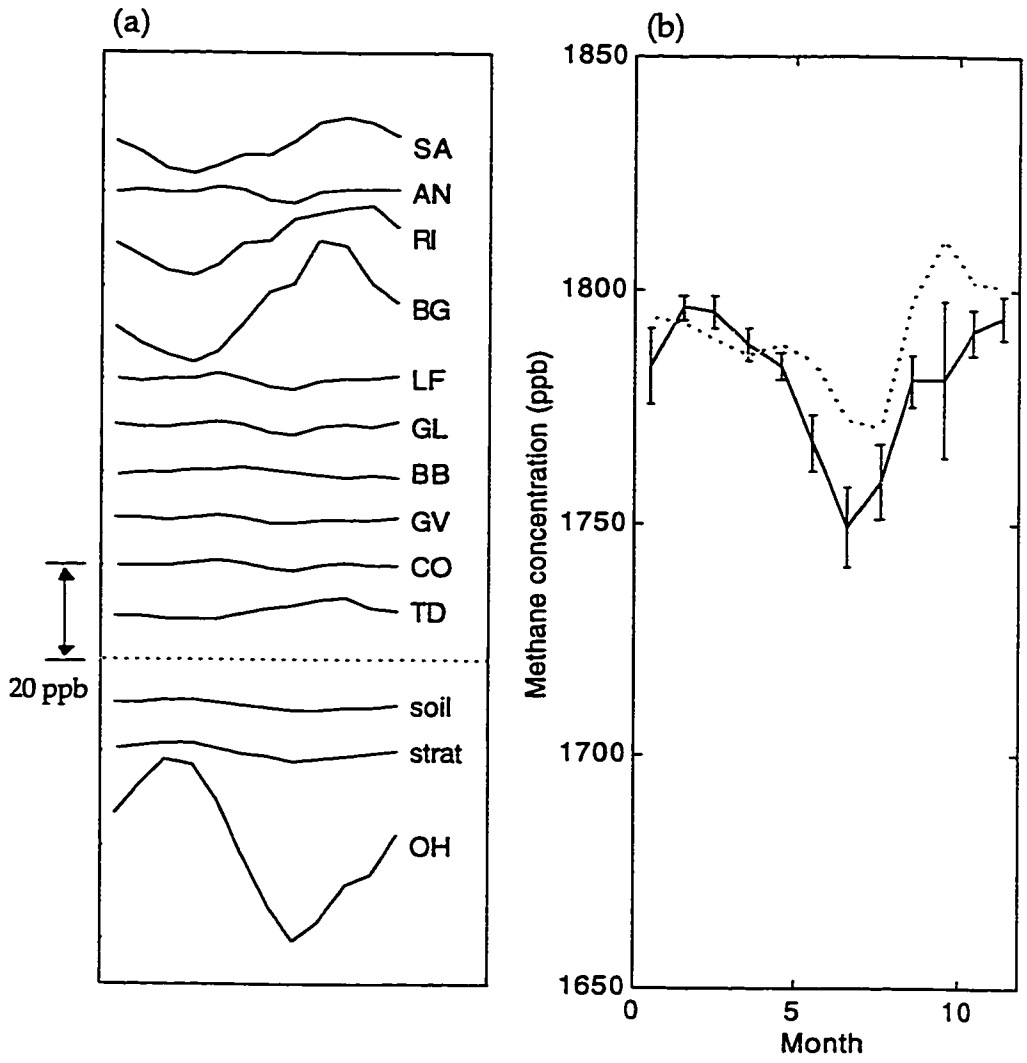

Figure 4.10 The seasonal cycle of CH_4 concentration at Cheeka Peak, Washington.

(a) The seasonal cycles in CH_4 concentration resulting from each of the individual sources and sinks of CH_4 with the strengths specified in Table 4.4. The lines are shown with an arbitrary vertical displacement to facilitate display. Methane source codes are: SA-swamps, AN-ruminants, RI-rice paddies, BG-bogs, LF-landfills, GL-gas leakage, BB-biomass burning, GV-gas venting, CO-coal mining, TD-tundra.

(b) The total model-predicted seasonal cycle in CH_4 concentration (···) compared to observations (—). The total modeled atmospheric response to CH_4 emissions is the sum of the individual responses shown in (a). The error bars on the observations represent ± 1 SE.

atmospheric CH_4 concentrations. Among the CH_4 sources, the largest seasonal cycle of 26 ppb results from CH_4 emissions from bogs which peak in August when air temperatures are at a maximum. Emissions from swamps and rice paddies result in a similar seasonal pattern with smaller amplitudes of 12 ppb and 15 ppb, respectively. The seasonal cycle in CH_4 concentration resulting from emission from bogs, swamps and rice paddies is approximately opposite in phase to that resulting from CH_4 removal by OH. The predicted seasonal cycle in CH_4 concentration at Cheeka Peak (Figure 4.10b), therefore, results primarily from the combined effect of wetland and rice paddy emission and OH oxidation.

Although there is good agreement between the pattern of model-predicted seasonality in CH_4 concentration and observations at Cheeka Peak, the model fails to reproduce the minimum CH_4 concentrations observed during July (Figure 4.10b). The predicted summertime minimum is sensitive to both the relative timing and magnitudes of CH_4 emissions from bogs and removal by OH. Therefore the model's failure to reproduce observed minimum summertime CH_4 concentrations likely results from an incorrect phasing of these two processes, overestimation of summertime CH_4 emissions from bogs, or underestimation of summertime OH levels.

The seasonal variation of CH_4 emissions from bogs in the CTM was assumed to be a function of air temperature (Fung *et al.*, 1991). Soil temperatures, which lag air temperatures, are a more important controller of emissions (Bartlett and Harriss, 1993). By parameterizing CH_4 emissions from bogs as a function of air temperature with a two-month delay, Hein *et al.*

(1997) were able to substantially improve the match between modeled and observed seasonal cycles in CH_4 concentration at high northern latitudes. In addition, the temperature dependence of CH_4 emissions from bogs may have been overestimated by Fung *et al.* (1991) who assumed that CH_4 fluxes double with a temperature increase of 10°C, *i.e.*, a Q_{10} factor of 2. More recent research indicates that a Q_{10} factor of 1.5 is more correct (Hein *et al.*, 1997), implying a smaller seasonal variation in CH_4 emissions from bogs.

The accuracy of seasonal variations in OH levels used in the CTM is difficult to evaluate. More recent calculations of OH radical concentration (Hein *et al.*, 1997) are similar in their mean monthly zonal averages to those used in the CTM (Spivakovsky *et al.*, 1990). The calculation of seasonal variations in OH at northern latitudes, however, is sensitive to effects of atmospheric transport (Spivakovsky *et al.*, 1990).

The failure of the model to reproduce observed minimum summertime CH_4 concentrations could also reflect an underestimation of the seasonal cycle due to CH_4 uptake by soils. Although CH_4 soil uptake is ~5% of the global CH_4 sink, it comprises 15-20% of the zonally-averaged CH_4 sink at 48°N (Fung *et al.*, 1991). Rates of CH_4 uptake by temperate forested soils have been shown to vary significantly throughout the year, *i.e.*, from 0 mg CH_4 m^{-2} d^{-1} during the wintertime to 5 mg CH_4 m^{-2} d^{-1} during August when soils are driest (Crill, 1991; Castro *et al.*, 1995). Thus, uptake of CH_4 by soils at ~48°N is likely stronger and more seasonally variant than was assumed in the CTM. Inclusion of a more realistic soil sink could therefore improve the predicted seasonal cycle at 48°N.

The CTM predicted a CH_4 concentration maximum in October at 48°N which was not observed in the Cheeka Peak time series measurements (Figure 4.10a). This overprediction is consistent with an overestimation in the CTM of the seasonality of CH_4 emissions from bogs, causing bogs to be a significant CH_4 source during the fall (Figure 4.10a). This overprediction could also have resulted from an underestimation in the seasonality of the soil sink.

The seasonal cycles in δD at 48°N result from the δD signatures and the seasonal patterns in the strengths of the individual CH_4 sources and sinks (Figure 4.11a). For δD, as for CH_4 concentration, the total seasonal cycle at 48°N (Figure 4.11b) depends mostly on the interplay between the competing effects of CH_4 emissions from bogs and CH_4 removal by OH. Although the seasonal pattern of the model-predicted δD generally matches observations at Cheeka Peak, the δD enrichment observed during July is underestimated. This observation is consistent with the overestimated summertime CH_4 concentration. Lower summertime CH_4 emissions from bogs, which are very depleted in δD, or increased summertime CH_4 loss to OH, which would enrich the δD of atmospheric CH_4, would improve the predictions.

CONCLUSIONS

The first time series of the δD content of atmospheric CH_4 was presented based on measurements made during 1991 to 1996 at Cheeka Peak, Washington (48.3°N, 124.6°W). The annual mean δD at this location was -92.6 ± 0.5‰. δD enrichment was observed during the summer and depletion

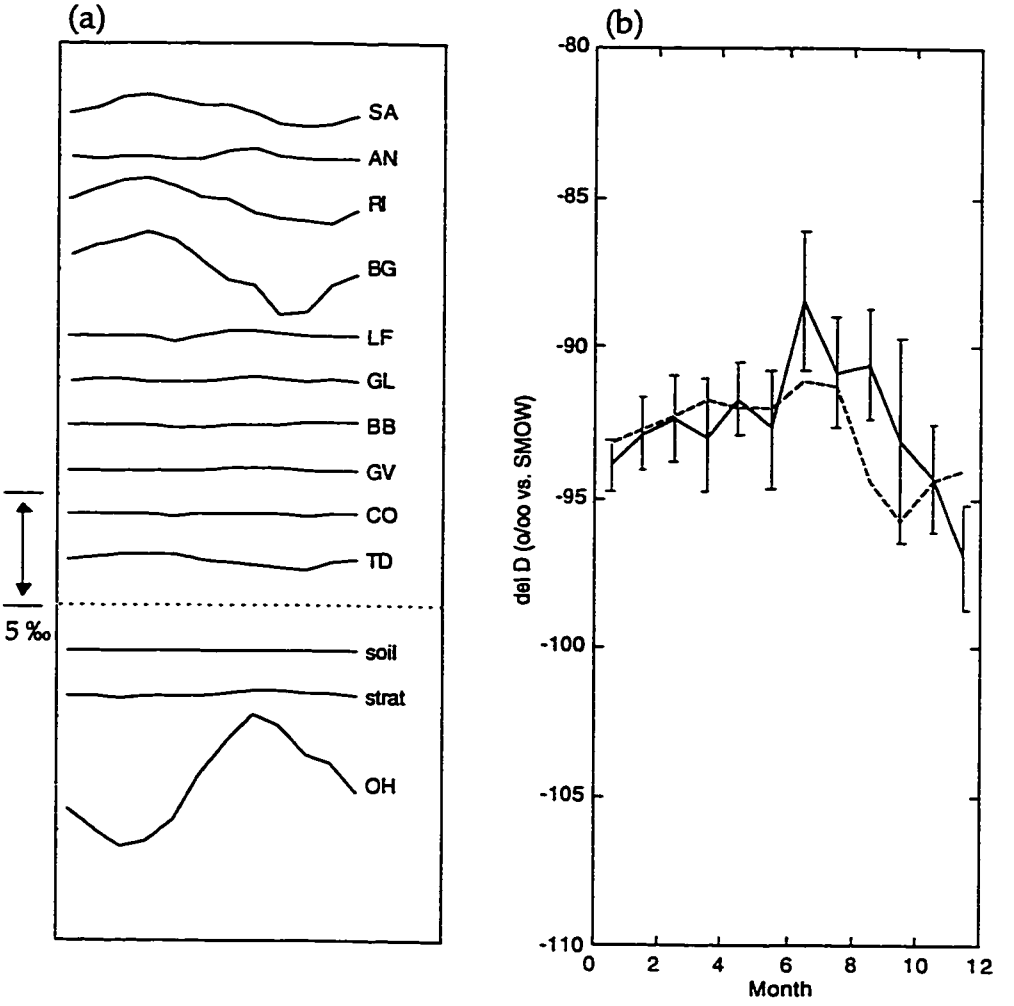

Figure 4.11 The seasonal cycle of δD at Cheeka Peak, Washington.
(a) The seasonal cycles in δD resulting from each of the individual sources and sinks of CH_4 with the strengths and δD specified in Table 4.4. The lines are shown with an arbitrary vertical displacement to facilitate display. Methane source codes are as in Figure 4.9.
(b) The total model-predicted seasonal cycle in δD (- -) compared to observations (—). The total modeled atmospheric response to CH_4 emissions is the sum of the individual responses shown in (a). The error bars on the observations represent ± 1 SE.

during the fall. The amplitude of the seasonal cycle was 8.6 ± 2.9‰. The magnitude of the seasonal cycle was primarily controlled by the balance between CH_4 emissions from bogs and CH_4 removal by OH, both of which peak during the late summer, as indicated by the predictions of an atmospheric chemical transport model.

Synoptic measurements of the meridional gradient in the δD of atmospheric CH_4 were presented based on air samples collected over the Pacific Ocean during 1989 to 1995. There was a δD decrease of ~13‰ between 50° N and the equator with approximately constant δD values in the southern hemisphere. The δD in the southern hemisphere was, on average, 9.6 ± 2.5‰ enriched versus the northern hemisphere. The southward increase in δD resulted from the higher strength and δD of the CH_4 sink versus the strength and δD of CH_4 sources in the southern hemisphere, in contrast to the situation in the northern hemisphere where the CH_4 source is stronger and more depleted in δD than the sink.

The global mean δD of atmospheric CH_4 was measured at -88.1 ± 1.2‰ during 1991 to 1996. Combining the δD of atmospheric CH_4 with the hydrogen isotopic fractionation during CH_4 loss yields an average δD for the global CH_4 sink of -286 ± 36‰. The average δD of the global CH_4 source was estimated at -279 ± 6‰ based on individual CH_4 source strengths and δD signatures. These independent estimates for the δD of CH_4 sources and sinks are in isotopic balance with observations of atmospheric CH_4, indicating that current understanding of the δD component of the CH_4 budget is robust on a global scale. The better constrained estimate for the δD of the global CH_4

source can be used to reduce the uncertainty associated with the CH_4 sink, particularly the fractionation during CH_4 loss to OH. This uncertainty currently limits the use of δD as a tracer for the global atmospheric CH_4 budget.

Current understanding of the global CH_4 budget and controls on the δD composition of atmospheric CH_4 are consistent with observations of both the interhemispheric gradient in δD and the δD seasonal cycle at Cheeka Peak. The δD observations, however, do not provide an additional constraint to the global CH_4 - δD budget.

The insensitivity of the interhemispheric gradient in δD to changes in the δD of the CH_4 source suggests that refining the meridional trend in δD via additional observations would not provide a useful constraint for the global CH_4 budget. Instead, δD will likely be most useful as a tracer for atmospheric CH_4 at temperate and high latitudes in the northern hemisphere where it can be used to constrain CH_4 emissions from bacterial sources, *i.e.*, bogs and rice paddies. Methane emissions from these sources, with δD = -320‰ to -340‰, are more depleted in δD relative to the δD lost to the sink (~-286‰) and have a seasonal variation of similar size and opposite phase compared to CH_4 removal by OH and soils. At higher latitudes, where the δD of CH_4 released from bogs and tundra is most depleted, δD will be an even more sensitive tracer of these sources. Thus mid- to high-latitude time series measurements of the δD of atmospheric CH_4 may be useful for constraining bacterial emissions from rice paddies and wetlands in these regions. Additional measurements of the δD of CH_4 emitted from bogs and tundra at high

northern latitudes are needed to better define the δD signature of these sources, and any seasonal variation therein, for use in future regional budget studies.

CHAPTER 5: CONCLUSIONS AND FUTURE DIRECTIONS

RESEARCH MOTIVATION

The importance of atmospheric CH_4 to the radiative balance of the earth and to both tropospheric and stratospheric chemistry has been well established (*e.g.*, Wayne, 1993; Houghton *et al.*, 1996). The growth rate of atmospheric CH_4 has recently slowed from ~14 ppb yr^{-1} in 1984 to ~ 3 ppb yr^{-1} in 1996 (Dlugokencky *et al.*, 1998). The CH_4 budget is not sufficiently constrained, however, to attribute observed changes in the atmospheric growth rate to changes in specific CH_4 sources or sinks or to allow prediction of future changes in the burden of atmospheric CH_4 (Khalil and Rasmussen, 1993a; Dlugokencky *et al.*, 1998).

One approach towards better understanding of the global CH_4 budget has relied on the use of isotopic tracers, in particular the $\delta^{13}C$ and the $\Delta^{14}C$ content of atmospheric CH_4. The carbon isotopic composition of atmospheric CH_4, which depends on the isotopic signatures and relative importance of the individual CH_4 sources and sinks, has been used to provide additional constraints for regional, hemispheric and global CH_4 budgets (Wahlen *et al.*, 1987, 1989, 1990; Quay *et al.*, 1988, 1991, in press; Stevens, 1993; Thom *et al.*, 1993; Lassey *et al.*, 1993; Lowe *et al.*, 1994; Gupta *et al.*, 1996; Bergamaschi *et al.*, 1998a).

The δD of atmospheric CH_4 was a potentially useful tracer for the atmospheric CH_4 budget (Wahlen *et al.*, 1990; Bergamaschi *et al.*, 1998a; Quay

et al., in press). The δD of most CH_4 sources and the hydrogen isotope effects associated with CH_4 loss to OH and removal in the stratosphere had been measured (*e.g.*, Lansdown, 1992; Levin *et al.*, 1993; Wahlen *et al.*, 1989, 1990; Schoell, 1980; DeMore, 1993; Xiao *et al.*, 1993; Gierczak *et al.*, 1997; Irion *et al.*, 1996). Use of δD as a constraint for the atmospheric CH_4 budget was precluded, however, by a lack of determinations of the δD of CH_4 emitted by biomass burning and of the hydrogen isotope effect occurring during uptake of atmospheric CH_4 by soils. In addition, few observations existed of the δD of atmospheric CH_4 in background air (Ehhalt, 1973; Wahlen *et al.*, 1990).

RESEARCH RESULTS

The research presented in this dissertation closes the knowledge gaps that prevented the use of δD as a tracer for the global CH_4 budget. With characterization of the isotopic composition of CH_4 removed by soils and of CH_4 emitted from biomass burning, the δD of each sink and source of atmospheric CH_4 have been characterized. Quantification of the latitudinal and seasonal variations in the δD of atmospheric CH_4 allows an evaluation of regional, hemispheric and global CH_4 budgets using stable hydrogen isotopic information. The utility of δD as a tracer for atmospheric CH_4 can be evaluated.

The major research findings presented in each section of this dissertation and their application to the atmospheric CH_4 budget are summarized below.

HYDROGEN KINETIC ISOTOPE EFFECT DURING SOIL UPTAKE OF ATMOSPHERIC METHANE

The hydrogen kinetic isotope effect (KIE) during soil uptake of atmospheric CH_4 was determined using *in situ* static flux chamber measurements in a native grassland and a forested soil in Washington state.

- The hydrogen KIE was $\alpha^D_{soil} = k(CH_4)/k(CH_3D) = 1.099 \pm 0.030$ (n=5) and 1.067 ± 0.007 (n=4) for the grassland and forest, respectively. The overall average, determined from two sites in the grassland and one in the forest, was 1.088 ± 0.024.

- This large KIE for soil uptake, relative to the KIE for molecular diffusion (α_{diff}) of 1.0195, indicates that CH_4 uptake at the study sites was not diffusion limited.

- The apparent hydrogen KIE associated with microbial oxidation (α^D_{ox}), determined from α_{soil} and the relative rates of CH_4 oxidation and diffusion within the soil column, ranged from 1.094 to 1.209. These are the first field measurement based results of α^D_{ox} and are in general agreement with previous lab culture measurements (Coleman *et al.*, 1981).

- Concurrent determinations of the carbon KIEs during this study yielded $\alpha^C_{soil} = 1.0176 \pm 0.0007$ and α^C_{ox} of 1.0121 to 1.0183. These results are consistent with previous determinations of these fractionation effects (King *et al.*, 1989; Tyler *et al.*, 1994; Reeburgh *et al.*, 1997; Coleman *et al.*, 1981).

- The rate of methane uptake by soils has been observed to vary between diffusion- and oxidation-limited (Crill, 1991; Castro *et al.*, 1995; Torn & Harte, 1996). Because α^{D}_{ox} is much larger than α_{diff}, the hydrogen KIE during soil uptake will be sensitive to controls on CH_4 uptake rates. This is in contrast to the situation for α^{C}_{soil} which is relatively insensitive to factors controlling the rate of CH_4 uptake, since $\alpha^{C}_{ox} \approx \alpha_{diff}$. Estimating an accurate average value for α^{D}_{soil} for application to the global atmospheric CH_4 - δD budget will therefore require additional measurements elucidating the magnitude of spatial and seasonal variability in α^{D}_{soil}.

- Future measurements of α^{D}_{soil} should be made in the boreal forest, tropical rainforest and tropical seasonal forest, *i.e.*, the ecosystems thought to contribute most significantly, after temperate forests, to the total soil sink for atmospheric CH_4 (*e.g.*, review in Potter *et al.*, 1996; Dörr *et al.*, 1993). The seasonal cycle in α^{D}_{soil} should be determined, especially at sites north of 30°N where a large seasonality exists for CH_4 uptake rates (Potter *et al.*, 1996). The large spatial variability observed for α^{D}_{soil} indicates the importance of characterizing α^{D}_{soil} by determinations at more than one location within an ecosystem.

- Assuming that soil uptake of atmospheric CH_4 occurs with a hydrogen KIE of $\alpha^{D}_{soil} \approx 1.088$, the hydrogen and carbon isotope fractionation effects of the three CH_4 sinks, *i.e.*, oxidation by OH, uptake by soils and loss in the stratosphere, are unique. The smaller hydrogen KIE associated with soil uptake, relative to those associated with CH_4 loss to

OH and in the stratosphere, decreases the overall hydrogen KIE and implies a more δD enriched source than if there were no soil sink.

- The interhemispheric asymmetry in the strength of the soil sink results in a ~5‰ difference between the overall KIE for CH_4 loss in the northern and southern hemispheres, with a larger KIE in the latter. Combined with the ~10‰ enrichment in δD of atmospheric CH_4 observed for the southern hemisphere, this implies a nearly constant δD for the total CH_4 sink in the two hemispheres.

The δD of Methane Emitted from Biomass Burning

The δD of CH_4 emitted from biomass burning was measured using smoke collected from large-scale laboratory combustion experiments and from fires typical of pasture burning and of slash burning of primary forest in the Brazilian Amazon.

- In laboratory burns of ponderosa pine needles, the mean δD of CH_4 emitted from biomass burning ($\delta D_{CH4(bb)}$) was -233 ± 2‰. In Brazilian fires, $\delta D_{CH4(bb)}$ was -210 ± 16‰.
- The measured D/H of the fuel biomass ranged from -61 to -127‰ and indicated a significant hydrogen isotope fractionation of -130‰ to -180‰ during CH_4 production from biomass combustion.

- Concurrent determinations of $\delta^{13}C_{CH4(bb)}$ and of the $^{13}C/^{12}C$ of the fuel biomass were consistent with earlier studies (Stevens and Engelkemeir, 1988; Wahlen *et al.*, 1989; Levin *et al.*, 1993)) which showed that the $\delta^{13}C$ of CH_4 emitted from biomass burning is approximately equal to the $\delta^{13}C$ of the fuel burned, *i.e.*, there is no carbon isotope fractionation during combustion.

- The relatively small range observed for $\delta D_{CH4(bb)}$ overall indicates that the δD content of CH_4 emitted from biomass burning in the tropics, *i.e.*, ~85% of the CH_4 emitted from biomass burning globally (Hao and Ward, 1993), is likely to be similar to that observed in the Brazilian fires, *i.e.*, $\delta D_{CH4(bb)} = -210 \pm 16‰$. These measurements indicate that $\delta D_{CH4(bb)}$ is significantly more depleted than previously estimated (Wahlen, 1993; Whiticar, 1993).

- This determination of $\delta D_{CH4(bb)}$ indicates that the δD and $\delta^{13}C$ signatures of the major CH_4 sources are distinct. δD is therefore an independent tracer for the atmospheric CH_4 budget.

- To improve the global average estimate for $\delta D_{CH4(bb)}$, additional measurements of $\delta D_{CH4(bb)}$ should be made in other regions important for global CH_4 emissions from biomass burning, *i.e.*, tropical Africa and Asia.

THE δD COMPOSITION OF ATMOSPHERIC METHANE

The seasonal variation in the δD composition of atmospheric CH_4 was determined from measurements of δD at Cheeka Peak, Washington (48.3°N, 124.6°W) between 1991 and 1996. The latitudinal variation in δD was determined from air samples collected during oceanographic research cruises between 55°N and 65°S, along ~150°W, in the Pacific Ocean during 1989 to 1995. These measurements were combined with the measured δD of CH_4 emitted from biomass burning and removed by soils, along with literature values of the strengths and δD signatures of the other CH_4 sources and sinks, to develop regional, hemispheric and global CH_4 budgets.

- The annual mean δD was -92.6 ± 0.5‰ at Cheeka Peak. δD enrichment was observed during the summer and depletion during the fall with an amplitude of the seasonal cycle of 8.6 ± 2.9‰. The seasonal cycle in δD was controlled by the balance between CH_4 emissions from bogs and CH_4 removal by OH, both of which peak during the late summer, as indicated by the predictions of an atmospheric chemistry transport model.

- There was a δD decrease of ~13‰ between 50° N and the equator with approximately constant δD values in the southern hemisphere. The δD in the southern hemisphere was, on average, 9.6 ± 2.5‰ enriched versus the northern hemisphere. The southward increase in δD resulted from the higher strength and δD of CH_4 loss versus the strength and δD of CH_4 sources in the southern hemisphere compared

to the excess of δD depleted sources over sinks in the northern hemisphere.

- The global mean δD of atmospheric CH_4 was -88.1 ± 1.2‰ during 1991 to 1996. The δD of the global CH_4 source derived from atmospheric observations and the hydrogen kinetic isotope effect associated with CH_4 loss (-280 ± 37‰) agrees well with the δD of the global CH_4 source estimated from the strength and δD of the individual CH_4 sources (-279 ± 6‰). This indicates that current understanding of the CH_4 - δD budget, including the new determinations of $\delta D_{CH4(bb)}$ and α^D_{soil}, is fairly robust.

- The better-constrained δD estimate for the global source derived from individual source strengths and δD contents can be used to constrain the hydrogen fractionation associated with the global CH_4 sink, in particular the hydrogen KIE during CH_4 loss to OH. This KIE presents the largest current source of uncertainty in the atmospheric CH_4 - δD budget.

FUTURE DIRECTIONS

Recent observations of the slowing growth rate of atmospheric CH_4 imply that global CH_4 emissions were approximately constant from 1984 to 1996, *i.e.*, that the global CH_4 budget may be stabilizing. If CH_4 emissions and the concentration of atmospheric OH remain at 1996 levels, atmospheric CH_4 would stabilize at a steady state concentration of ~1800 ppb in ~20 years (Dlugokencky *et al.*, 1998). If the relative strengths of the individual CH_4

sources also remain constant, the isotopic composition of atmospheric CH_4 would also stabilize, although over a significantly longer period of time (Tans, 1997). Future changes to the global CH_4 budget are highly uncertain, however (Khalil and Rasmussen, 1993a). Even if total emissions remain constant, the distribution of emissions may change in the future, with CH_4 emissions from some sources increasing while others decrease. The strengths of CH_4 sinks could also change in the future.

There are many ways in which it is postulated that the strengths of individual CH_4 sources and sinks could change in the future. For example, global climate/circulation models predict that increasing levels of atmospheric CO_2 will result in significantly elevated temperatures at high latitudes (Kattenberg *et al.*, 1996). Depending on future precipitation patterns, these warmer temperatures could cause CH_4 emissions from high latitude wetlands to significantly increase or decrease (Melillo *et al.*, 1996). Because methane emissions from fossil fuel production are linked to economic conditions (Law and Nisbet, 1996), they are unlikely to remain constant in the future, and may also be impacted by future international greenhouse gas emission agreements. The importance of soil oxidation as a sink for atmospheric CH_4 may change in the future. For example, changes in precipitation patterns could shift soils from being net sources (flooded anoxic soils) to net sinks (aerated and oxic). Land use changes in the tropics, where primary forests are being converted to secondary forests and the latter to agricultural land, will continue to affect the soil sink in that region (Keller *et al.*, 1990; Mosier and Delgado, 1997).

The key to detecting future changes in CH_4 emissions will be monitoring future trends in the concentration of atmospheric CH_4, as well as the interhemispheric gradient in CH_4 concentration (Dlugokencky *et al.*, 1998). Methane concentration is currently measured at ~35 NOAA Climate Monitoring and Diagnostics Laboratory monitoring stations and measurement of the $\delta^{13}C$ of atmospheric CH_4 is beginning in this network. Monitoring future trends in the isotopic content of atmospheric CH_4 will be useful for attribution of future changes in CH_4 emissions since a shift in the distribution and/or location of CH_4 sources or sinks would impact not only the mass distribution but the isotopic composition of atmospheric CH_4.

The insensitivity of the interhemispheric gradient in δD to changes in the δD of the CH_4 source suggests that refining the meridional trend in δD via additional observations would not provide a useful constraint for the global CH_4 budget. δD will be most useful as a tracer for atmospheric CH_4 at temperate and high latitudes in the northern hemisphere where its seasonal variations can be used to constrain CH_4 emissions from bacterial sources, *i.e.*, bogs and rice paddies. Methane emission from rice agriculture is one of the least well known of the individual CH_4 sources (Crutzen, 1995). The seasonality of emissions from rice paddies is a significant contributor to the seasonal cycle in δD at 48°N and would strongly influence the δD seasonal cycle at monitoring stations nearer to rice-growing regions. At higher latitudes, where the δD of CH_4 released from bogs and tundra is most depleted, δD will be an even more sensitive tracer of these sources. Time series measurements of δD at mid- to high-latitudes in the northern

hemisphere will therefore be useful in constraining the amount and timing of current CH_4 emissions from rice paddies, bogs and tundra and any future changes in these sources.

The use of δD as a tracer for atmospheric CH_4 could be further improved by refining the estimates for the δD signature of several sources and sinks. The first priority should be reducing the uncertainty in the hydrogen isotope fractionation occurring during CH_4 oxidation by OH. This is the largest source of uncertainty in the atmospheric CH_4 - δD budget. Methane loss to OH is the largest single flux in the atmospheric CH_4 cycle, comprising ~40% of the total annual CH_4 flux (sources plus sinks). The two laboratory experimental determinations and one theoretical calculation of the KIE during CH_4 loss to OH give widely different results, *i.e.*, -160‰ (DeMore, 1993), -230‰ (Gierczak *et al.*, 1997) and -255‰ (Xiao *et al.*, 1993) (all at 277 K). Even assuming that the most recent and widely respected experimental determination, with measurements at tropospherically-relevant temperatures (Gierczak *et al.*, 1997), is correct, the experimental uncertainty is ±40‰. Until the uncertainty in this term is reduced, measurements of the δD of atmospheric CH_4 will not provide an additional constraint for the global CH_4 source budget.

Among the CH_4 sources, the first priority should be refining the meridional trend in the δD signature of CH_4 emitted from wetlands. Additional measurements of the δD of CH_4 emitted from bogs and tundra at high northern latitudes are needed to better define the δD signature of these sources, and any seasonal variation therein, for use in future regional budget

calculations. Additional measurements of CH_4 emitted from tropical wetlands would help narrow the significant uncertainty (±13‰) in the δD signature of the largest single CH_4 source. The uncertainty in the δD signature of CH_4 emissions from rice paddies (± 19‰) should be refined through future measurements if δD is to be used as a tracer of CH_4 from this source.

Each isotopic tracer, *i.e.*, δD, $\delta^{13}C$ and $\Delta^{14}C$, provides an independent constraint for the atmospheric CH_4 budget. In addition, each tracer is sensitive to a different feature of the CH_4 budget. The δD content of atmospheric CH_4 is most sensitive to the amount and timing of bacterial CH_4 released at temperate and high latitudes in the northern hemisphere. The $\delta^{13}C$ of atmospheric CH_4 is useful for constraining the amount of CH_4 released from biomass burning, due to the significant $\delta^{13}C$ enrichment of that source (Quay *et al.*, 1991, in press; Lassey *et al.*, 1993). Because the largest carbon KIE for removal of atmospheric CH_4 is associated with the soil sink (*e.g.*, Reeburgh *et al.*, 1997; Cantrell *et al.*, 1990; Sugawara *et al.*, 1997), atmospheric $\delta^{13}C$ also responds to the hemispheric asymmetry in the strength of the soil sink. The ^{14}C composition of atmospheric CH_4 constrains CH_4 emissions associated with fossil fuel production, *i.e.*, the only CH_4 source containing no ^{14}C (Wahlen *et al.*, 1989; Quay *et al.*, in press). Future studies of atmospheric CH_4 using a combination of isotopic tracers will be most useful for constraining regional, hemispheric and global budgets of atmospheric CH_4.

BIBLIOGRAPHY

Alei, M., Cappis, J. H., Fowler, M. M., Frank, D. J., Goldblatt, M., Guthals, P. R., Mason, A. S., Mills, T. R., Mroz, E. J., Norris, T. L., Perrin, R. E., Poths, J., Rokop, D. J., & Shields, W. R. (1987). Determination of deuterated methanes for use as atmospheric tracers. *Atmos. Environ.*, 21, 909-915.

Bartlett, K. B., & Harriss, R. C. (1993). Review and assessment of methane emissions from wetlands. *Chemosphere*, 26, 261-320.

Bekki, S., Law, K. S., & Pyle, J. A. (1994). Effect of ozone depletion on atmospheric CH_4 and CO concentrations. *Nature*, 371, 595-597.

Bender, M. L. (1990). The $\delta^{18}O$ of dissolved O_2 in seawater: a unique tracer of circulation and respiration in the deep sea. *J. Geophys. Res.*, 95, 22,243-22,252.

Bergamaschi, P., & Harris, G. W. (1995). Measurements of stable isotope ratios ($^{13}CH_4/^{12}CH_4$, $^{12}CH_3D/^{12}CH_4$) in landfill methane using a tunable diode laser absorption spectrometer. *Global Biogeochem. Cycles*, 9, 439-447.

Bergamaschi, P. (1997). Seasonal variations of stable hydrogen and carbon isotope ratios in methane from a Chinese rice paddy. *J. Geophys. Res.*, 102, 25,383-25,393.

Bergamaschi, P., Brenninkmeijer, C. A. M., Hahn, M., Röckmann, T., Scharffe, D. H., Crutzen, P. J., Elansky, N. F., Belikov, I. B., Trivett, N. B. A., & Worthy, D. E. J. (1998a). Isotope analysis based source identification for atmospheric CH_4 and CO sampled across Russia using the Trans-Siberian railroad. *J. Geophys. Res.*, 103, 8227-8235.

Bergamaschi, P., Lubina, C., Königstedt, R., Fischer, H., Veltkamp, A. C., & Zwaagstra, O. (1998b). Stable isotopic signatures ($\delta^{13}C$, δD) of methane from European landfill sites. *J. Geophys. Res.*, 103, 8251-8265.

Bevington, P. R., & Robinson, D. K. (1992). *Data Reduction and Error Analysis for the Physical Sciences* (Second ed.). New York: McGraw-Hill, Inc.

Blake, D. R., & Rowland, F. S. (1988). Continuing worldwide increase in tropospheric methane, 1978 to 1987. *Science*, 239, 1129-1131.

Blunier, T., Chappellaz, J. A., Schwander, J., Barnola, J.-M., Desperts, T., Stauffer, B., & Raynaud, D. (1993). Atmospheric methane, record from a Greenland ice core over the last 1000 years. *Geophys. Res. Lett.*, 20, 2219-2222.

Brenninkmeijer, C. A. M. (1991). Robust, high efficiency, high-capacity cryogenic trap. *Anal. Chem.*, 63, 1182-1184.

Brenninkmeijer, C. A. M., Lowe, D. C., Manning, M. R., Sparks, R. J., & van Velthoven, P. F. J. (1995). The ^{13}C, ^{14}C, and ^{18}O isotopic composition of CO, CH_4, and CO_2 in the higher southern latitudes lower stratosphere. *J. Geophys. Res.*, 100, 26163-26172.

Burke, R. A., Jr., & Sackett, W. M. (1986). Stable hydrogen and carbon isotopic compositions of biogenic methanes from several shallow aquatic environments. *Org. Mar. Geochem.*, 305, 297-313.

Burke, R. A., Jr., Barber, T. R., & Sackett, W. M. (1988). Methane flux and stable hydrogen and carbon isotope composition of sedimentary methane from the Florida Everglades. *Global Biogeochem. Cycles*, 2, 329-340.

Burke, R. A., Jr., Barber, T. R., & Sackett, W. M. (1992). Seasonal variations of stable hydrogen and carbon isotope ratios of methane in subtropical freshwater sediments. *Global Biogeochem. Cycles*, 6, 125-138.

Cantrell, C. A., Shetter, R. E., McDaniel, A. H., Calvert, J. G., Davidson, J. A., Lowe, D. C., Tyler, S. C., Cicerone, R. J., & Greenberg, J. P. (1990). Carbon kinetic isotope effect in the oxidation of methane by hydroxyl radicals. *J. Geophys. Res.*, 95, 22455-22462.

Castro, M. S., Steudler, P. A., Melillo, J. M., Aber, J. D., & Bowden, R. D. (1995). Factors controlling atmospheric methane consumption by temperate forest soils. *Global Biogeochem. Cycles*, 9, 1-10.

Carbon Dioxide Information and Analysis Center (CDIAC) (1998). Trends: A compendium of data on global change (on-line), http://cdiac.esd.ornl.gov/trends/trends.htm.

Cofer, W. R., III, Levine, J. S., Winstead, E. L., & Stocks, B. J. (1990). Gaseous emissions from Canadian boreal forest fires. *Atmos. Environ.*, 24, 1653-1659.

Coleman, D. D., Risatti, J. B., & Schoell, M. (1981). Fractionation of carbon and hydrogen isotopes by methane-oxidizing bacteria. *Geochim. Cosmochim. Acta*, 45, 1033-1037.

Coleman, M. L., Shepherd, T. J., Durham, J. J., Rouse, J. E., & Moore, G. R. (1982). Reduction of water with zinc for hydrogen isotope analysis. *Anal. Chem.*, 54, 993-995.

Conrad, R. (1996). Soil microorganisms as controllers of atmospheric trace gases (H_2, CO, CH_4, OCS, N_2O, and NO). *Microbiol. Rev.*, 60, 609-640.

Craig, H., Chou, C. C., Welhan, J. A., Stevens, C. M., & Engelkemeir, A. (1988). The isotopic composition of methane in polar ice-cores. *Science*, 242, 1535-1539.

Crill, P. M. (1991). Seasonal patterns of methane uptake and carbon dioxide release by a temperate woodland soil. *Global Biogeochem. Cycles*, 5, 319-334.

Crutzen, P. J. (1995). The role of methane in atmospheric chemistry and climate. In *Ruminant Physiology: Digestion, Metabolism, Growth and Reproduction: Proceedings of the Eighth International Symposium on Ruminant Physiology*, edited by W.V. Engelhardt, S. Leonhardt-Marek, G. Breves, & D. Giesecke, pp. 291-315. Stuttgart: Ferdinand Enke Verlag.

Davidson, E. A., & Schimel, J. P. (1995). Microbial processes of production and consumption of nitric oxide, nitrous oxide and methane. In *Biogenic Trace Gases: Measuring Emissions from Soil and Water*, edited by P. A. Matson & R. C. Harriss, pp. 327-357. Oxford: Blackwell Science.

DeMore, W. B. (1993). Rate constant ratio for the reactions of OH with CH_3D and CH_4. *J. Phys. Chem.*, 97, 8564-8566.

Departmento Nacional de Meteorologia (1992). Normais climatologicas (1961-1990). Minist. da Agric. e Reforma Agraria, Brasilia, DF Brasil.

Dlugokencky, E. J., Masaire, K. A., Lang, P. M., Tans, P. P., Steele, L. P., & Nisbet, E. G. (1994a). A dramatic decrease in the growth rate of atmospheric methane in the northern hemisphere during 1992. *Geophys. Res. Lett.*, 21, 45-48.

Dlugokencky, E. J., Lang, P. M., Masarie, K. A., & Steele, L. P. (1994b). Atmospheric CH_4 records from sites in the NOAA/CMDL air sampling network. In *Trends '93: A Compendium of Data on Global Change*, edited by T. A. Boden, D. P. Kaiser, R. J. Sepanski, & F. W. Stoss, Carbon Dioxide Analysis Center ORNL/CDIAC-65. Oak Ridge, TN: Oak Ridge National Laboratory.

Dlugokencky, E. J., Masarie, K. A., Lang, P. M., & Tans, P. P. (1998). Continuing decline in the growth rate of the atmospheric methane burden. *Nature*, 393, 447-450.

Dörr, H., Katruff, L., & Levin, I. (1993). Soil texture parameterization of the methane uptake in aerated soils. *Chemosphere*, 26, 697-713.

Edwards, J. B. (1974). *Combustion: Formation and Emission of Trace Species*. Ann Arbor, Michigan: Ann Arbor Science Publishing.

Efron, B. (1991). Non-parametric estimates of the standard error: The jackknife, bootstrap and other sampling methods. *Biometrika*, 68, 589-599.

Ehhalt, D. H. (1973). Methane in the atmosphere. In *Carbon and the Biosphere, 24th Brookhaven Symposium in Biology*, edited by G. M. Woodwell & E. V. Pecan, pp. 144-157. Upton, New York: US Atomic Energy Commission.

Emery, R. (1977). Soils of the University of Washington's Arboretum. Unpublished Paper, Miller Library, Center for Urban Horticulture, University of Washington, Seattle, Washington.

Epstein, S., Yapp, C. J., & Hall, J. H. (1976). The determination of the D/H ratio of non-exchangeable hydrogen in cellulose extracted from aquatic and land plants. *Earth Planet. Sci. Lett.*, 30, 241-251.

Fletcher, C. A. J. (1988). *Computational Techniques for Fluid Dynamics*. New York: Springer-Verlag.

Fung, I., John, J., Lerner, J., Mathew, E., Prather, M., Steele, L. P., & Fraser, P. J. (1991). Three-dimensional model synthesis of the global methane cycle. *J. Geophys. Res.*, 96, 13033-13065.

Gessel, S. P. (1966). Soils of the Arboretum. *The University of Washington Arboretum Bulletin*, 29, 69-83.

Gierczak, T., Talukdar, R. K., Herndon, S. C., Vaghjiani, G. L., & Ravishankara, A. R. (1997). Rate coefficients for the reactions of hydroxyl radicals with methane and deuterated methanes. *J. Phys. Chem.*, 101, 3125-3134.

Griffith, D. W. T., Mankin, W. G., Coffey, M. T., Ward, D. E., & Riebau, A. (1991). FTIR remote sensing of biomass burning emssions of CO_2, CO, CH_4, CH_2O, NO, NO_2, NH_3, and N_2O. In *Global Biomass Burning: Atmospheric, Climatic and Biospheric Implications*, edited by J. S. Levine, pp. 230-239. Cambridge, Masssachusetts: The MIT Press.

Guild, L. S., Kauffman, J. B., Ellingson, L. J., Cummings, D. L., Castro, E. A., Babbitt, R. E., & Ward, D. E. (in press). Dynamics associated with total aboveground biomass, C, nutrient pools, and biomass burning of primary forest and pasture in Rondônia, Brazil during SCAR-B. *J. Geophys. Res.*

Gupta, M., Tyler, S., & Cicerone, R. (1996). Modeling atmospheric $\delta^{13}CH_4$ and the causes of recent changes in atmospheric CH_4 amounts. *J. Geophys. Res.*, 101, 22,923-22,932.

Gupta, M. L., McGrath, M. P., Cicerone, R. J., Rowland, F. S., & Wolfsberg, M. (1997). $^{12}C/^{13}C$ kinetic isotope effects in reactions of CH_4 with OH and Cl. *Geophys. Res. Lett.*, 24, 2761-2764.

Hansen, J., Russell, G., Rind, D., Stone, P., Lacis, A., Lebedeff, S., Ruedy, R., & Travis, L. (1983). Efficient three-dimensional global models for climate studies: Models I and II. *Mon. Weather Rev.*, 111, 609-662.

Hao, W. M., & Ward, D. E. (1993). Methane production from biomass burning. *J. Geophys. Res.*, 98, 20657-20661.

Hao, W. M., & Liu, M.-H. (1994). Spatial and temporal distribution of tropical biomass burning. *Global Biogeochem. Cycles*, 8, 495-503.

Hao, W. M., Ward, D. E., Olbu, G., & Baker, S. P. (1996). Emissions of CO_2, CO and hydrocarbons from fires in diverse African Savanna ecosystems. *J. Geophys. Res.*, 101, 23,577-23,584.

Hein, R., Crutzen, P. J., & Heimann, M. (1997). An inverse modeling approach to investigate the global atmospheric methane cycle. *Global Biogeochem. Cycles*, 11, 43-76.

Heipieper, H. J., & deBont, J. A. M. (1997). Methane oxidation by Dutch grassland and peat soil microflora. *Chemosphere*, 35, 3025-3037.

Hogan, K., & Harriss, R. (1994). Comment on "A dramatic decrease in the growth rate of atmospheric methane in the Northern Hemisphere during 1992" by E. J. Dlugokencky *et al.*, *Geophys. Res. Lett.*, 21, 2445-2446.

Houghton, J. T., Filho, L. G. M., Callander, B. A., Harris, N., Kattenberg, A., & Maskell, K. (Ed.). (1996). *Climate Change 1995: The science of climate change*. Cambridge, UK: Cambridge University Press.

Hut, G. (1987). Consultants' group meeting on stable isope reference samples for geochemical and hydrological investigations, *Report to the Director General*, International Atomic Energy Agency.

International Atomic Energy Agency (IAEA) (1981). *Stable Isotope Hydrology, Deuterium and Oxygen-18 in the Water Cycle* (Technical Reports Series No. 210), Vienna: IAEA.

Irion, F. W., Moyer, E. J., Gunson, M. R., Rinsland, C. P., Yung, Y. L., Michelsen, H. A., Salawitch, R. J., Chang, A. Y., Newchurch, M. J., Abbas,

M. M., Abrams, M. C., & Zander, R. (1996). Stratospheric observations of CH_3D and HDO from ATMOS infrared solar spectra: Enrichments of deuterium in methane and implications for HD. *Geophys. Res. Lett.*, 23, 2381-2384.

Jacob, D., Prather, M., Wofsy, S., & McElroy, M. (1987). Atmospheric distribution of ^{85}Kr simulated with a general circulation model. *J. Geophys. Res.*, 92, 6614-6626.

Jones, R. L., Pyle, J. A., Harries, J. E., Zavody, A. M., Rusell, J. M., III, & Gille, J. C. (1986). The water vapour budget of the stratosphere studies using LIMS and SAMS satellite data. *Quart. J. R. Meteorol. Soc.*, 112, 1127-1143.

Kattenberg, A., Giorgi, F., Grassl, H., Meehl, G. A., Mitchell, J. F. B., Stouffer, R. J., Tokioka, T., Weaver, A. J., & Wigley, T. M. L. (1996). Climate Models - Projections of Future Climate. In *Climate Change 1995: The science of climate change*, edited by J. T. Houghton, L. G. M. Filho, B. A. Callander, N. Harris, A. Kattenberg, & K. Maskell, pp. 285-358. Cambridge, UK: Cambridge University Press.

Keller, M., Mitre, M. E., & Stallard, R. F. (1990). Consumption of methane in soils of central Panama: Effects of agricultural development. *Global Biogeochem. Cycles*, 4, 21-27.

Kendall, C., & Coplen, T. B. (1985). Multisample conversion of water to hydrogen by zinc for stable isotope determination. *Anal. Chem.*, 57, 1437.

Khalil, M. A. K., & Rasmussen, R. A. (1985). Causes of increasing atmospheric methane: Depletion of hydroxyl radicals and the rise of emissions. *Atmos. Environ.*, 19, 397-407.

Khalil, M. A. K., & Rasmussen, R. A. (1989a). Temporal variations of trace gases in ice cores. In *The Environmental Record in Glaciers and Ice Sheets, Dahlem Konferenzen*, edited by H. Oeschger & C. C. Langway, pp. 193-205. John Wiley & Sons Limited.

Khalil, M. A. K., & Rasmussen, R. A. (1989b). Distribution and mass balance of molecular hydrogen in the earth's atmosphere. *Geophys. Monit. Clim. Change*, 17, 111-113.

Khalil, M. A. K., & Rasmussen, R. A. (1993a). Decreasing trend of methane: unpredictability of future concentrations. *Chemosphere*, 26, 803-814.

Khalil, M. A. K., Shearer, M. J., & Rasmussen, R. A. (1993b). Methane sources in China: Historical and current emissions. *Chemosphere*, 26, 127-142.

King, S. L., Quay, P. D., & Lansdown, J. M. (1989). The $^{13}C/^{12}C$ kinetic isotope effect for soil oxidation of methane at ambient atmospheric concentrations. *J. Geophys. Res.*, 94, 18273-18277.

Kling, G. W., Evans, W. C., & Tuttle, M. L. (1991). A comparative view of Lakes Nyos and Monoun, Cameroon, West Africa. *Verh. Internat. Verein. Limnol.*, 24, 1102-1105.

Krol, M., van Leeuwen, P. J., & Lelieveld, J. (1998). Global OH trend inferred from methylchloroform measurements. *J. Geophys. Res.*, 103, 10,697-10,711.

Lansdown, J. M. (1992) *The Carbon and Hydrogen Stable Isotope Composition of Methane Released from Natural Wetlands and Ruminants*. Ph.D. Dissertation, University of Washington.

Lassey, K. R., Lowe, D. C., Brenninkmeijer, C. A. M., & Gomez, A. J. (1993). Atmospheric methane and its carbon isotopes in the southern hemisphere: Their time series and an instructive model. *Chemosphere*, 26, 95-109.

Law, K. S., & Nisbet, E. G. (1996). Sensitivity of the CH_4 growth rate to changes in CH_4 emissions from natural gas and coal. *J. Geophys. Res.*, 101, 14387-14398.

Leaney, F. W., Osmond, C. B., Allison, G. B., & Ziegler, H. (1985). Hydrogen-isotope composition of leaf water in C3 and C4 plants: Its relationship to the hydrogen-isotope composition of dry matter. *Planta*, 164, 215-220.

Levin, I., Bergamaschi, P., Dorr, H., & Trapp, D. (1993). Stable isotope signatures of methane from major sources in Germany. *Chemosphere*, 26, 161-177.

Liptay, K., Chanton, J., Czepiel, P., & Mosher, B. (1998). Use of stable isotopes to determine methane oxidation in landfill cover soils. *J. Geophys. Res.*, 103, 8243-8250.

Livingston, G. P., & Hutchinson, G. L. (1995). Enclosure-based measurement of trace gas exchange: Applications and sources of error. In *Biogenic Trace Gases: Measuring emissions from soil and water*, edited by P. A. Matson & R. C. Harriss, pp. 14-51. Oxford: Blackwell Science.

Lowe, D. C., Brenninkmeijer, C. A. M., Tyler, S. C. & Dlugkencky, E. J. (1991). Determination of the isotopic composition of atmospheric methane and its application in the Antarctic. *J. Geophys. Res.*, 96, 15,455-15,467.

Lowe, D. C., Brenninkmeijer, C. A. M., Brailsford, G. W., Lassey, K. R., & Gomez, A. J. (1994). Concentration and ^{13}C records of atmospheric methane in New Zealand and Antarctica: Evidence for changes in methane sources. *J. Geophys. Res.*, 99, 16913-16925.

Maiss, M., & Levin, I. (1994). Global increase of SF_6 observed in the atmosphere. *Geophys. Res. Lett.*, 21, 569-572.

Martens, C. S., Kelley, C. A., & Chanton, J. P. (1992). Carbon and hydrogen isotopic characterization of methane from wetlands and lakes of the Yukon-Kuskokwim delta, Western Alaska. *J. Geophys. Res.*, 97, 16689-16701.

Melillo, J. M., Prentice, I. C., Farquhar, G. D., Schulze, E.-D., & Sala, O. E. (1996). Terrestrial Biotic Responses to Environmental Change and Feedbacks to Climate. In *Climate Change 1995: The science of climate change*, edited by J. T. Houghton, L. G. M. Filho, B. A. Callander, N. Harris, A. Kattenberg, & K. Maskell, pp. 445-482. Cambridge, UK: Cambridge University Press.

Mosier, A. R. (1989). Chamber and Isotope Techniques. In *Exchange of Trace Gases between Terrestrial Ecosystems and the Atmosphere*, edited by M. O. Andreae & D. S. Schimel, pp. 175-187. Chicester: John Wiley & Sons Ltd.

Mosier, A., Schimel, D., Valentine, D., Bronson, K., & Parton, W. (1991). Methane and nitrous oxide in native, fertilized and cultivated grasslands. *Nature*, 350, 330-332.

Mosier, A. R., Parton, W. J., Valentine, D. W., Ojima, D. S., Schimel, D. S., & Delgado, J. A. (1996). CH_4 and N_2O fluxes in the Colorado shortgrass steppe: 1. Impact of landscape and nitrogen addition. *Global Biogeochem. Cycles*, 10, 387-399.

Mosier, A. R., & Delgado, J. A. (1997). Methane and nitrous oxide fluxes in grasslands in western Puerto Rico. *Chemosphere*, 35, 2059-2082.

National Climatic Data Center (1998). http://www.ncdc.noaa.gov/ol/climate/climatedata.html.

Park, R., & Epstein, S. (1960). Carbon isotope fractionation during photosynthesis. *Geochim. Cosmochim. Acta*, 21, 110-126.

Potter, C. S., Davidson, E. A., & Verchot, L. V. (1996). Estimation of global biogeochemical controls and seasonality in soil methane consumption. *Chemosphere*, 32, 2219-2246.

Prather, M., McElroy, M., Wofsy, S., Russell, G., & Rind, D. (1987). Chemistry of the global troposphere: Flurocarbons as tracers of air motion. *J. Geophys. Res.*, 92, 6579-6613.

Prather, M., Derwent, R., Ehhalt, D., Fraser, P., Sanhueza, E., & Zhou, X. (1995). Other trace gases and atmospheric chemistry. In *Climate Change 1994: Radiative Forcing of Climate Change*, edited by J. T. Houghton, L. G. M. Filho, J. Bruce, H. Lee, B. A. Callander, E. Haites, N. Harris, & K. Maskell, pp. 73-126. Cambridge, UK: Cambridge University Press.

Prinn, R. G., Weiss, R. F., Miller, B. R., Huang, J., Alyea, F. N., Cunnold, D. M., Fraser, P. J., Hartley, D. E., & Simmonds, P. G. (1995). Atmospheric trends

and lifetime of CH_3CCl_3 and global OH concentrations. *Science*, 269, 187-192.

Quay, P. D., King, S. L., Lansdown, J. M., & Wilbur, D. O. (1988). Isotopic composition of methane released from wetlands: Implications for the increase in atmospheric methane. *Global Biogeochem. Cycles*, 2, 385-397.

Quay, P. D., King, S. L., Stutsman, J., Wilbur, D. O., Steele, L. P., Fung, I., Gammon, R. H., Brown, T. A., Farwell, G. W., Grootes, P. M.& Schmidt, F. H. (1991). Carbon isotopic composition of atmospheric CH_4: Fossil and biomass burning source strengths. *Global Biogeochem. Cycles*, 5, 25-47.

Quay, P. D., Stutsman, J. L., Wilbur, D. O., Snover, A. K., Dlugokencky, E. J., & Brown, T. A. (in press). The isotopic composition of atmospheric methane. *Global Biogeochem. Cycles*.

Reeburgh, W. S., Whalen, S. C., & Alperin, M. J. (1993). The Role of Methylotrophy in the Global Methane Budget. In *Microbial Growth on C1 Compounds*, edited by J. C. Murrell & D. P. Kelly, pp. 1-14. Andover: Intercept, Ltd.

Reeburgh, W. S., Hirsch, A. I., Sansone, F. J., Popp, B. N., & Rust, T. M. (1997). Carbon kinetic isotope effect accompanying microbial oxidation of methane in boreal forest soils. *Geochim. Cosmochim. Acta*, 61, 4761-4767.

Rice, D. D., & Claypool, G. E. (1981). Generation, accumulation and resource potential of biogenic gas. *Bull. Am. Assoc. Pet. Geol.*, 65, 5-25.

Sackett, W. M. (1978). Carbon and hydrogen isotope effects during the thermocatalytic production of hydrocarbons in laboratory simulation experiments. *Geochim. Cosmochim. Acta*, 42, 571-580.

Saeki, T., Nakazawa, T., Tanaka, M., & Higuchi, K. (1998). Methane emissions deduced from a two-dimensional atmospheric transport model and surface measurements. *J. Meteorol. Soc. Japan*, 76, 307-324.

Schauffler, S. M., & Daniel, J. S. (1994). On the effects of stratospheric circulation changes on trace gas trends. *J. Geophys. Res.*, 99, 257474-25754.

Schiegl, W. E., & Vogel, J. C. (1970). Deuterium content of organic matter. *Earth Planet. Sci. Lett.*, 7, 307-313.

Schimel, D., Alves, D., Enting, I., Heimann, M., Joos, F., Raynaud, D., Wigley, T., Prather, M., Derwent, R., Ehhalt, D., Fraser, P., Sanhueza, E., Zhou, X., Jonas, P., Charlson, R., Rodhe, H., Sadasivan, S., Shine, K. P., Fouquart, Y., Ramaswamy, V., Solomon, S., Srinivasan, J., Albritton, D., Derwent, R., Isaksen, I., Lala, M., & Weubbles, D. (1996). Radiative Forcing of Climate Change. In *Climate Change 1995: The science of climate change*, edited by J. T. Houghton, L. G. M. Filho, B. A. Callander, N. Harris, A. Kattenberg, & K. Maskell, pp. 65-132. Cambridge, UK: Cambridge University Press.

Schoell, M. (1980). The hydrogen and carbon isotopic composition of methane from natural gases of various origins. *Geochim. Cosmochim. Acta*, 44, 649-661.

Seiler, W., Conrad, R., & Scharffe, D. (1984). Field studies of methane emission from termite nests into the atmosphere and measurements of methane uptake by tropical soils. *J. Atmos. Chem.*, 1, 171-186.

Severson, K. J., Johnstone, D. L., Keller, C. K., & Wood, B. D. (1992). Hydrogeologic parameters affecting vadose-zone microbial distributions. *Geomicrobiol. J.*, 9, 197-216.

Skole, D., & Tucker, C. (1993). Tropical deforestation and habitat fragmentation in the Amazon: Satellite data from 1978 to 1988. *Science*, 260, 1905-1910.

Smiley, W. G. (1949). Note on reagent for oxidation of carbon monoxide. *Nucl. Sci. Abstr.*, 3, 391-392.

Snover, A. K., & Quay, P. D. (in preparation). Hydrogen and carbon kinetic isotope effects during soil uptake of atmospheric methane. Submitted to *Global Biogeochem. Cycles*.

Snover, A. K., Quay, P. D., & Hao, W. M. (in preparation). The D/H content of methane emitted from biomass burning. Submitted to *Global Biogeochem. Cycles*.

Spivakovsky, C. M., Wofsy, S. C., & Prather, M. J. (1990a). A numerical method for parameterization of atmospheric chemistry: Computation of tropospheric OH. *J. Geophys. Res.*, 95, 18,433-18,439.

Spivakovsky, C. M., Yevich, R., Logan, J. A., Wofsy, S. C., McElroy, M. B., & Prather, M. J. (1990b). Tropospheric OH in a three-dimensional chemical tracer model: An assessment based on observations of CH_3CCl_3. *J. Geophys. Res.*, 95, 18441-18471.

Sternberg, L., & DeNiro, M. J. (1983). Isotopic composition of cellulose from C3, C4 and CAM plants growing near one another. *Science*, 220, 947-949.

Steudler, P. A., Bowden, R. D., Melillo, J. M., & Aber, J. D. (1989). Influence of nitrogen fertilization on methane uptake in temperate forest soils. *Nature*, 341, 314-316.

Stevens, C. M., & Rust, F. E. (1982). The carbon isotopic composition of atmospheric methane. *J. Geophys. Res.*, 87, 4879-4882.

Stevens, C. M. (1988). Atmospheric methane. *Chem. Geol.*, 71, 11-21.

Stevens, C. M., & Engelkemeir, A. (1988). Stable carbon isotopic composition of methane from some natural and anthropogenic sources. *J. Geophys. Res.*, 93, 725-733.

Stevens, C. M. (1993). Isotopic Abundances in the Atmosphere and Sources. In *Atmospheric Methane: Sources, sinks and role in global change*, edited by M.A.K. Khalil, pp. 62-88. New York: Springer-Verlag.

Stevens, C. M. (1995). C-13 isotopic abundance and concentration of atmospheric for background air in the southern and northern hemispheres from 1978 to 1989, *Publ. 4388*, Env. Sci. Div., US Department of Energy.

Striegl, R. G., McConnaughey, T. A., Thorstenson, D. C., Weeks, E. P., & Woodward, J. C. (1992). Consumption of atmospheric methane by desert soils. *Nature*, 357, 145-147.

Striegl, R. G. (1993). Diffusional limits to the consumption of atmospheric methane by soils. *Chemosphere*, 26, 715-720.

Style and Policy Manual For Theses and Dissertations (Revised ed.) (1996) Seattle: University of Washington Graduate School.

Sugawara, S., Nakazawa, T., Shirakawa, Y., Kawamura, K., Aoki, S., Machida, T., & Honda, H. (1997). Vertical profile of the carbon isotopic ratio of stratospheric methane over Japan. *Geophys. Res. Lett.*, 24, 2989-2992.

Susott, R. A., Ward, D. E., Babbitt, R. E., & Latham, D. J. (1991). The measurement of trace emissions and combustion characteristics for a mass fire. In *Global Biomass Burning: Atmospheric, Climatic and Biospheric Implications*, edited by J. S. Levine, pp. 245-257. Cambridge, MA: The MIT Press.

Tans, P. P. (1997). A note on isotopic ratios and the global atmospheric methane budget. *Global Biogeochem. Cycles*, 11, 77-81.

Tanweer, A., Hut, G., & Burgman, J. O. (1988). Optimal conditions for the reduction of water to hydrogen by zinc for mass spectrometric analysis of the deuterium content. *Chem. Geol.*, 73, 199-203.

Thom, M., Bosinger, R., Schmidt, M., & Levin, I. (1993). The regional budget of atmospheric methane of a highly populated area. *Chemosphere*, 26, 143-160.

Tillman, D. A., Rossi, A. J., & Kitto, W. D. (1981). *Wood Combustion: Principles, processes and economics*. New York: Academic Press.

Torn, M. S., & Harte, J. (1996). Methane consumption by montane soils: implications for positive and negative feedback with climatic change. *Biogeochem.*, 32, 53-67.

Troughton, J. H., Card, K. A., & Hendy, C. H. (1974). Photosynthetic pathways and carbon isotope discrimination by plants. *Carnegie Inst. Washington Year Book*, 73, 768-780.

Tyler, S. C., Zimmerman, P. R., Cumberbatch, C., Greenberg, J. P., Westberg, C., & Darlington, J. P. E. C. (1988). Measurements and Interpretation of $\delta^{13}C$ of methane from termites, rice paddies and wetlands in Kenya. *Global Biogeochem. Cycles*, 2, 349-355.

Tyler, S. C. (1992). Kinetic isotope effects and their use in studying atmospheric trace species: Case Study, CH_4 + OH. In *ACS Symposium Series*, edited by J. A. Kaye, pp. 390-408. Washington, D.C.: American Chemical Society.

Tyler, S. C., Crill, P. M., & Brailsford, G. W. (1994a). $^{13}C/^{12}C$ fractionation of methane during oxidation in a temperate forested soil. *Geochim. Cosmochim. Acta*, 58, 1625-1633.

Tyler, S. C., Brailsford, G. W., Yagi, K., Minami, K., & Cicerone, R. (1994b). Seasonal variations in methane flux and $\delta^{13}CH_4$ values for rice paddies in Japan and their implications. *Global Biogeochem. Cycles*, 8, 1-12.

Vaghjiani, G. L., & Ravishankara, A. R. (1991). New measurement of the rate coefficient for the reaction of OH with methane. *Nature*, 350, 406-409.

Wahlen, M., Tanaka, N., Henry, R., & Yoshinari, T. (1987). ^{13}C, D and ^{14}C in methane. *EOS Transactions*, American Geophysical Union, 68, 1220.

Wahlen, M., Tanaka, N., Henry, R., Deck, B., Zeglen, J., Vogel, J. S., Southon, J., Shemesh, A., Fairbanks, R., & Broecker, W. (1989). Carbon-14 in methane sources and in atmospheric methane: The contribution from fossil carbon. *Science*, 245, 286-290.

Wahlen, M., Tanaka, N., Deck, B., Henry, R., Shemesh, A., Fairbanks, R., & Broecker, W. (1990). δD in CH_4: Additional constraints for a global CH_4 budget. *EOS Transactions*, American Geophysical Union, 71, 1249.

Wahlen, M. (1993). The global methane cycle. *Ann. Rev. Earth Plant. Sci.*, 21, 407-426.

Ward, D. E., Susott, R. A., Kauffman, J. B., Babbitt, R. E., Cummings, D. L., Dias, B., Holben, B. N., Kaufman, Y. J., Rasmussen, R. A., & Setzer, A. W.

(1992). Smoke and fire characteristics for cerrado and deforestation burns in Brazil: BASE-B experiment. *J. Geophys. Res.*, 97, 14,601-14,619.

Ward, D. E., Hao, W. M., Susott, R. A., Babbitt, R. E., Shea, R. W., Kauffman, J. B., & Justice, C. O. (1996). Effect of fuel composition on combustion efficiency and emission factors for African savanna ecosystems. *J. Geophys. Res.*, 101, 23,569-23,576.

Wassman, R., Thein, U. G., Whiticar, M. J., Rennenberg, H., Seiler, W., & Junk, W. J. (1992). Methane emissions from the Amazon floodplain: Characterization of production and transport. *Global Biogeochem. Cycles*, 6, 3-13.

Wershaw, R. L., Friedman, I., Heller, S. J., & Frank, P. A. (1966). Hydrogen isotopic fractionation of water passing through trees. In *Advances in Organic Geochemistry*, edited by G.D. Hobson & G.C. Speers, pp. 55-67. New York: Pergamon Press.

Western Regional Climate Center (1998). http://www.wrcc.dri.bin.

Wayne, R. P. (1993). *Chemistry of Atmospheres* (Second ed.). Oxford: Clarendon Press.

Whalen, S. C., & Reeburgh, W. S. (1988). A methane flux time series for tundra environments. *Global Biogeochem. Cycles*, 2, 399-409.

Whalen, S. C., & Reeburgh, W. S. (1990). Consumption of atmospheric methane by tundra soils. *Nature*, 342, 160-162.

Whalen, S. C., Reeburgh, W. S., & Kizer, K. S. (1991). Methane consumption and emission by taiga. *Global Biogeochem. Cycles*, 5, 261-273.

Whiticar, M. J., Faber, E., & Schoell, M. (1986). Biogenic methane formation in marine and freshwater environments: CO_2 reduction vs. acetate fermentation -- isotopic evidence. *Geochim. Cosmochim. Acta*, 50, 693-709.

Whiticar, M. J. (1993). Stable Isotopes and Global Budgets. In *Atmospheric Methane: Sources, Sinks and Role in Global Change*, edited by M.A.K. Khalil, Berlin: Springer-Verlag.

Willison, T. W., Webster, C. P., Goulding, K. W. T., & Powlson, D. S. (1995). Methane oxidation in temperate soils: Effects of land use and the chemical form of nitrogen fertilizer. *Chemosphere*, 30, 539-546.

Woltemate, I., Whiticar, M. J., & Schoell, M. (1984). Carbon and hydrogen isotopic composition of bacterial methane in a shallow freshwater lake. *Limnol. Oceanogr.*, 29, 985-992.

Wood, B. D., Keller, C. K., & Johnstone, D. L. (1993). In situ measurement of microbial activity and controls on microbial CO_2 production in the unsaturated zone. *Water Resour. Res.*, 29, 647-659.

Xiao, Y., Tanaka, N., & Lasaga, A. C. (1993). An evaluation of hydrogen kinetic isotope effect in the reaction of CH_4 with OH free radical. *EOS Transactions*, American Geophysical Union, 74, 71.

Yokelson, R. J., Griffith, D. W. T., & Ward, D. E. (1996). Open-path Fourier transform infrared studies of large-scale laboratory biomass fires. *J. Geophys. Res.*, 101, 21,067-21,080.

CURRICULUM VITAE

AMY KATHERINE SNOVER

1998

EDUCATION

Ph. D.	Chemistry	University of Washington. December 1998.
M.S.	Chemistry	University of Washington. March 1993.
B.A.	Chemistry	Carleton College. June 1990.
		Magna cum laude, Phi Beta Kappa

PUBLICATIONS

Refereed Journal Publications

Snover, A. K. & Quay, P. D. (1999, submitted). Hydrogen and carbon kinetic isotope effects during soil uptake of atmospheric methane. *Global Biogeochemical Cycles.*

Snover, A. K., Quay, P. D. & Hao, W. M. (1999, submitted). The D/H content of methane emitted from biomass burning. *Global Biogeochemical Cycles.*

Quay, P. D., Stutsman, J. L., Wilbur, D. O., Snover, A. K., Dlugokencky, E. J., & Brown, T. A. (in press). The isotopic composition of atmospheric methane. *Global Biogeochemical Cycles.*

Goyet, C. & Snover, A. K. (1993). High-accuracy measurements of total dissolved inorganic carbon in the ocean: Comparison of alternate detection methods. *Marine Chemistry*, 44, 235-242.

Non-refereed Publications

Snover, A. K., Miles, E., & Henry, B. (1998). *Impacts of Global Climate Change on the Pacific Northwest*, Final report of the OSTP/USGCRP Regional Workshop, NOAA Climate & Global Change Program, Special Report #11.

Miles, E., Hamlet, A., Snover, A. K., Callahan, B. & Fluharty, D. (1998, November). *The sensitivity and vulnerability of the Pacific Northwest (USA) to climate variability and change: A human dimensions*

perspective. Paper prepared for the IHDP/GECHS Workshop on Water and Human Security in Southeast Asia and Oceania, Canberra Australia National University.

Snover, A. K., (1997). *Impacts of Global Climate Change on the Pacific Northwest*. Report prepared for the OSTP/USGCRP Pacific Northwest Regional Climate Change Workshop, Seattle, Washington.

Snover, A. K. & Quay, P. D. (1996). *Time series of atmospheric CH_4 concentration and stable isotopic composition at two North American temperate sites*, EOS Transactions, 77, F107.

Miles, E., Hamlet, A. & Snover, A. K. (in preparation) *Summarizing the Integrated Assessment: Approach and Findings*. To be published by MIT Press.

PRESENTATIONS

Snover, A.K. (1998, December). *The Stable Hydrogen Isotopic Composition of Atmospheric Methane*. University of Washington, School of Oceanography, Departmental Seminar.

Snover, A. K. (1998, January). *Global climate change: A local look at a global problem*, invited keynote address, Earth on Fire Summit, Bellarmine Preparatory Academy, Tacoma, Washington.

Snover, A. K. (1997, November). *Guest Lecturer*, General Studies 197: Global Warming, University of Washington.

Snover, A. K. (1997, October). *Guest Lecturer*, Atmospheric Sciences 211A: Climate and Climate Change, University of Washington.

Snover, A. K. (1997, July). *Impacts of Global Climate Change on the Pacific Northwest*. OSTP/USGCRP Pacific Northwest Regional Climate Change Workshop, Seattle, Washington.

Snover, A. K. & Quay, P. D. (1996, October). *Stable isotope Biogeochemistry of Atmospheric Methane: North American temperate and biomass burning sources*. A forum for integrating multi-disciplinary research to advance the science of global change, Graduate Fellowships for Global Change Conference, Oak Ridge, Tennessee.

Snover, A.K. (1995, June). *The Stable Isotope Geochemistry of Atmospheric Methane*. University of Washington, School of Oceanography, Departmental Seminar.

Snover, A.K. (1993, April). *History of Shipboard Measurements of CO_2: Detecting the anthropogenic signal*. University of Washington, Department of Chemistry, Departmental Seminar.

Snover, A.K. (1992, October). *Infrared Analysis of Dissolved Inorganic Carbon in Seawater*. University of Washington, School of Oceanography, Departmental Seminar.

GRANTS AND AWARDS

Graduate Fellowship. US Department of Energy, Graduate Fellowships for Global Change. (1992-1998)

Scholarship. Achievement Rewards for College Scientists (ARCS). (1991-1993)

NASA Grant to attend NASA Earth Science Summer School: Processes of Global Change, California Institute of Technology. (1995, July)

American Meteorological Society Grant to attend NSF/AMS 5th Symposium on Global Change Studies at the 74th Annual Meeting of the AMS. (1994, January)

Summer Student Fellowship. Woods Hole Oceanographic Institution. (1992, Summer)

IMAGE EVALUATION TEST TARGET (QA-3)

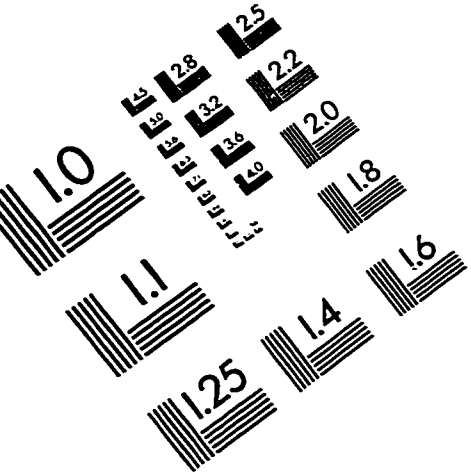

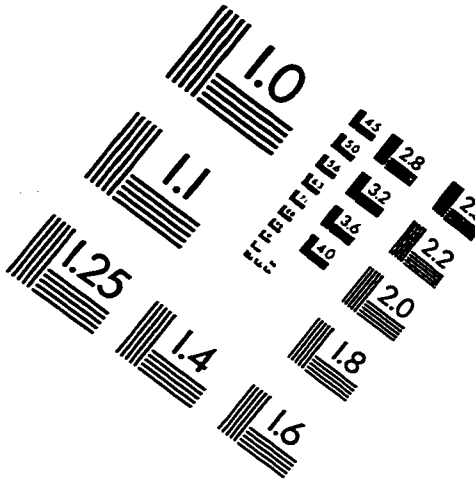

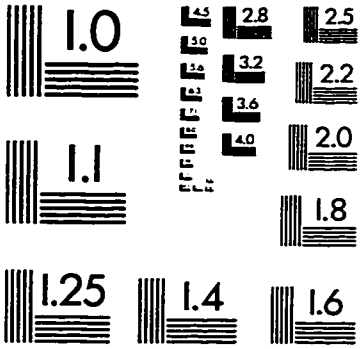

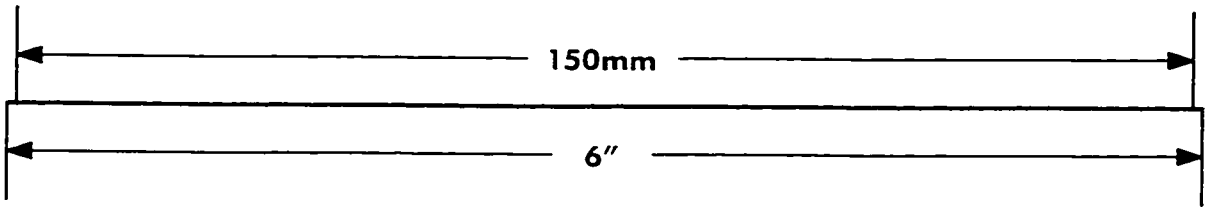

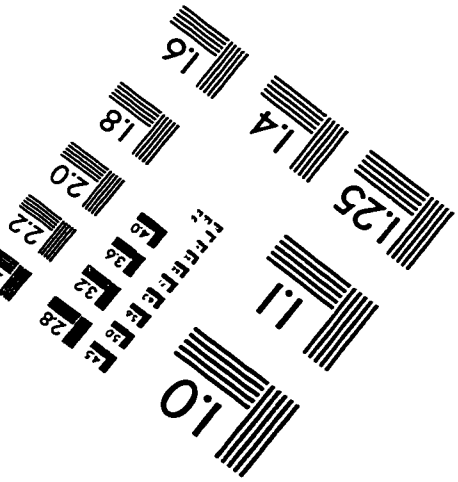

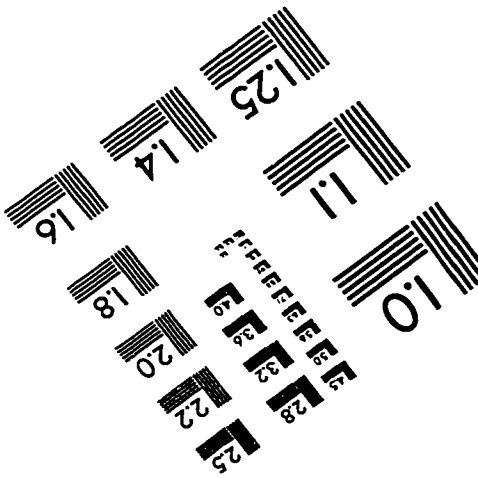

APPLIED IMAGE, Inc
1653 East Main Street
Rochester, NY 14609 USA
Phone: 716/482-0300
Fax: 716/288-5989